Supporting Information

Brønsted-Lewis dual acidic ionic liquid immobilized on mesoporous silica materials as an efficient cooperative catalyst for Mannich reaction

Hong Bo Wang,‡ Nan Yao,‡ Long Wang and Yu Lin Hu*

College of Materials and Chemical Engineering, Key laboratory of inorganic nonmetallic crystalline and energy conversion materials, China Three Gorges University, Yichang 443002, P. R. China

**Correspondence to: E-mail: huyulin1982@163.com*

Experimental Section

Chemicals and Materials. The reagents and solvents were of analytical grade. Powder X-ray diffraction (XRD) patterns were collected on a Rigaku Ultima IV diffractometer. Scanning electron microscopy (SEM) and Energy dispersive X-ray (EDX) analysis were carried out on a JSM-7500F Scanning Electron Microscope. FT-IR spectra were recorded on a Nicolet Nexus 470 Fourier transform infrared spectrometer. UV–Vis spectra were recorded on a Shimadzu UV-2450 spectrometer. Thermogravimetric analysis (TG) were measured on a Netzsch Thermoanalyzer STA 449. Nitrogen adsorption-desorption profiles were measured on an Micromeritics-2010 apparatus. LC-MS experiments were performed on a Agilent 6410 instrument. ^{1}H NMR spectra were recorded in $CDCl_3$ at room temperature on a Bruker 400 MHz spectrometer. Elemental analysis were performed on a Vario EL III instrument. Melting points were measured on an Electro-thermal IA 9100 apparatus.

Preparation of MCM-41, Ti-MCM-41, Sn-MCM-41, and Fe-MCM-41. The MCM-41 was synthesized following the procedure,[1] Ti-MCM-41 was synthesized following the procedure,[1,2] Sn-MCM-41 was synthesized following the procedure,[3] and Fe-MCM-41 was prepared according to reported process.[4]

Preparation of supported ILs. Supported ILs were prepared according to reported process[5-7] and shown in Scheme S1. Preparation **1**: Imidazole (1 mol), (3-chloropropyl) triethoxysilane (1 mol) and toluene (800 mL) were refluxed for 22 h, then triethylamine (1 mol) was added and refluxed for another 2 h. The slurry was filtrated and the toluene solution was evaporated to afford **1**. Preparation **2**: 1,4-butane sultone (0.5 mol), **1** (0.5 mol), and toluene (300 mL) were stirred at 100 °C for 10 h, and the solvent was evaporated to give **2**. Preparation **3-1**: **2** (0.1 mol), hydrochloric acid (0.1 mol), and toluene (120 mL) were stirred at 80 °C for 12 h, then the solvent was evaporated, and $CoCl_2$ or $SnCl_4$ or $TiCl_4$ (0.1 mol) in CH_3CN (150 mL) were added and the mixture was refluxed for 24 h. The resulting material was isolated and evaporated to give **3-1** $ILSO_3H$-$CoCl_3$ or $ILSO_3H$-$SnCl_5$ or $ILSO_3H$-$TiCl_5$. Preparation **3-2**: **2** (0.1 mol), trifluoromethanesulfonic acid or sulfuric acid or *p*-toluenesulfonic acid (0.1 mol), toluene (120 mL) were stirred at 80 °C for 12 h, then the solvent was evaporated to give **3-2** $ILSO_3H$-CF_3SO_3 or $ILSO_3H$-HSO_4 or $ILSO_3H$-TsO. Preparation supported ILs **4-1**: **3-1** $ILSO_3H$-$CoCl_3$ or $ILSO_3H$-$SnCl_5$ or $ILSO_3H$-$TiCl_5$ (0.01 mol), MCM-41, Ti-MCM-41, Sn-MCM-41 or Fe-MCM-41 (4 g), and toluene (500 mL) were refluxed for 24 h. The mixture was filtrated and dried under vacuum to afford the supported ILs **4-1** $ILSO_3H$-$CoCl_3$@MCM-41, $ILSO_3H$-$SnCl_5$@MCM-41, $ILSO_3H$-$TiCl_5$@MCM-41, $ILSO_3H$-$TiCl_5$@

Ti-MCM-41, $ILSO_3H$-$TiCl_5$@Sn-MCM-41, $ILSO_3H$-$TiCl_5$@Fe-MCM-41. Preparation supported ILs **4-2**: **3-2** $ILSO_3H$-CF_3SO_3 or $ILSO_3H$-HSO_4 or $ILSO_3H$-TsO (0.01 mol), MCM-41 (4 g), and toluene (500 mL) were refluxed for 24 h. The mixture was filtrated and dried under vacuum to afford the supported ILs **4-2** $ILSO_3H$-CF_3SO_3@MCM-41 or $ILSO_3H$-HSO_4@MCM-41 or $ILSO_3H$-TsO@MCM-41.

General procedure for catalytic reaction. Aromatic aldehyde (0.05 mol), aromatic amine (0.05 mol), ketone (0.05 mol), $ILSO_3H$-$TiCl_5$@Sn-MCM-41 (0.4 g), EtOH (10 mL) were added to a magnetically stirred three-neck flask. The reaction mixture was stirred at room temperature for the desired time. The reaction progress was monitored by TLC. Upon completion, the catalyst was filtered off and washed with ethanol and dried under vacuum. The filtrate was concentrated under reduced pressure and the crude product was purified by via recrystallisation from ethanol to give the corresponding pure product. The products were identified by the use of spectral data and comparison of their physical data with the literature. Fresh substrates were then recharged to the recovered catalyst and then recycled under identical reaction conditions.

Spectroscopic data for products

1,3-Diphenyl-3-(phenylamino)propan-1-one (Table S2, entry 1): White solid, mp 170-171 °C; ^{1}H NMR (400 MHz, $CDCl_3$): δ = 3.46 (dd, 2H, CH_2), 4.52 (s, 1H, NH), 5.01 (m, 1H, CH), 6.57-6.69 (m, 3H, Ar-H), 7.05-7.54 (m, 10H, Ar-H), 7.87-7.97 (m, 2H, Ar-H) ppm; LC-MS: *m/z* 302.2 [$C_{21}H_{19}NO$ (M+1) requires 302.15], 3.627 min (98%); Anal. Calcd for $C_{21}H_{19}NO$: C, 83.67; H, 6.33; N, 4.64; O, 5.28. Found: C, 83.69; H, 6.35; N, 4.65; O, 5.31.

3-((4-Isopropylphenyl)amino)-1,3-diphenylpropan-1-one (Table S2, entry 2): White solid, mp 119-120 °C; ^{1}H NMR (400 MHz, $CDCl_3$): δ = 1.23 (dd, 6H, $2CH_3$), 2.89 (m, 1H, CH), 3.48 (dd, 2H, CH_2), 4.51 (s, 1H, NH), 4.98 (m, 1H, CH), 6.51-6.87 (m, 4H, Ar-H), 7.22-7.53 (m, 8H, Ar-H), 7.89-7.98 (m, 2H, Ar-H) ppm; LC-MS: *m/z* 302.2 [$C_{24}H_{25}NO$ (M-41) requires 302.19], 3.882 min (98%); Anal. Calcd for $C_{24}H_{25}NO$: C, 83.89; H, 7.31; N, 4.05; O, 4.63. Found: C, 83.93; H, 7.34; N, 4.08; O, 4.66.

1,3-Diphenyl-3-(p-tolylamino)propan-1-one (Table S2, entry 3): White solid, mp 167-168 °C; ^{1}H NMR (400 MHz, $CDCl_3$): δ = 2.19 (s, 3H, CH_3), 3.46 (dd, 2H, CH_2), 4.50 (s, 1H, NH), 4.99 (m, 1H, CH), 6.48-6.51 (d, 2H, Ar-H), 6.88-6.92 (d, 2H, Ar-H), 7.23-7.56 (m, 8H, Ar-H), 7.88-7.97 (m, 2H, Ar-H) ppm; LC-MS: *m/z* 316.2 [$C_{22}H_{21}NO$ (M+1) requires 316.16], 3.708 min (97%); Anal. Calcd for $C_{22}H_{21}NO$: C, 83.76; H, 6.69; N, 4.41; O, 5.05. Found: C, 83.78; H, 6.71; N, 4.44; O, 5.07.

3-((4-Methoxyphenyl)amino)-1,3-diphenylpropan-1-one (Table S2, entry 4): White solid, mp 149-150 °C; ^{1}H NMR (400 MHz, $CDCl_3$): δ = 3.46 (dd, 2H, CH_2), 3.87 (s, 3H, OCH_3), 4.43 (s, 1H, NH), 4.97 (m, 1H, CH), 6.51-6.72 (m, 3H, Ar-H), 6.91-7.41 (m, 9H, Ar-H), 7.87-7.99 (m, 2H, Ar-H) ppm; LC-MS: *m/z* 332.1 [$C_{22}H_{21}NO_2$ (M+1) requires 332.16], 3.496 min (97%); Anal. Calcd for $C_{22}H_{21}NO_2$: C, 79.69; H, 6.35; N, 4.21; O, 9.63. Found: C, 79.73; H, 6.39; N, 4.23; O, 9.66.

1,3-Diphenyl-3-((4-(trifluoromethyl)phenyl)amino)propan-1-one (Table S2, entry 5): White solid, mp 141-142 °C; ^{1}H NMR (400 MHz, $CDCl_3$): δ = 3.49 (dd, 2H, CH_2), 5.02 (m, 1H, CH), 6.53-6.56 (m, 2H, Ar-H), 7.03-7.61 (m, 10H, Ar-H), 7.89-7.99 (m, 2H, Ar-H) ppm; LC-MS: *m/z* 370.1 [$C_{22}H_{18}F_3NO$ (M+1) requires 370.14], 3.754 min (97%); Anal. Calcd for $C_{22}H_{18}F_3NO$: C, 71.53; H, 4.87; F, 15.41; N, 3.76; O, 4.29. Found: C, 71.53; H, 4.91; F, 15.43; N, 3.79; O, 4.33.

3-(4-Fluorophenyl)-1-phenyl-3-((4-(trifluoromethyl)phenyl)amino)propan-1-one (Table S2, entry 6): White solid, mp 125-126 °C; ^{1}H NMR (400 MHz, $CDCl_3$): δ = 3.52 (m, 2H, CH_2), 4.74 (s, 1H, NH), 5.03 (t, 1H, CH), 6.51-6.55 (m, 2H, Ar-H), 7.33-7.61 (m, 7H, Ar-H), 7.89-8.01 (m, 4H, Ar-H) ppm; LC-MS: *m/z* 388.1 [$C_{22}H_{17}F_4NO$ (M+1) requires 388.12], 3.761 min (100%); Anal. Calcd for $C_{22}H_{17}F_4NO$: C, 68.18; H, 4.41; F, 19.60; N, 3.58; O, 4.09. Found: C, 68.21; H, 4.42; F, 19.62; N, 3.62; O, 4.13.

3-((4-Chlorophenyl)amino)-1,3-diphenylpropan-1-one (Table S2, entry 7): White solid, mp 170-172 °C; ^{1}H NMR (400 MHz, $CDCl_3$): δ = 3.48 (dd, 2H, CH_2), 4.69 (s, 1H, NH), 4.96 (m, 1H, CH), 6.48-6.51 (m, 2H, Ar-H), 7.01-7.54 (m, 10H, Ar-H), 7.88-7.96 (m, 2H, Ar-H) ppm; LC-MS: *m/z* 336.1 [$C_{21}H_{18}ClNO$ (M+1) requires 336.11], 3.736 min (100%); Anal. Calcd for $C_{21}H_{18}ClNO$: C, 75.11; H, 5.37; Cl, 10.52; N, 4.15; O, 4.73. Found: C, 75.11; H, 5.40; Cl, 10.56; N, 4.17; O, 4.76.

3-((4-Chlorophenyl)amino)-3-(4-fluorophenyl)-1-phenylpropan-1-one (Table S2, entry 8): White solid, mp 129-130 °C; ^{1}H NMR (400 MHz, $CDCl_3$): δ = 3.49 (m, 2H, CH_2), 4.71 (s, 1H, NH), 5.02 (m, 1H, CH), 6.50-6.53 (m, 2H, Ar-H), 7.29-7.55 (m, 7H, Ar-H), 7.76-7.97 (m, 4H, Ar-H) ppm; LC-MS: *m/z* 354.1 [$C_{21}H_{17}ClFNO$ (M+1) requires 354.10], 3.745 min (98%); Anal. Calcd for $C_{21}H_{17}ClFNO$: C, 71.26; H, 4.82; Cl, 10.01; F, 5.35; N, 3.94; O, 4.49. Found: C, 71.29; H, 4.84; Cl, 10.02; F, 5.37; N, 3.96; O, 4.52.

1-Phenyl-3-(phenylamino)-3-(p-tolyl)propan-1-one (Table S2, entry 9): White solid, mp 138-139 °C; ^{1}H NMR (400 MHz, $CDCl_3$): δ = 2.34 (s, 3H, CH_3), 3.46 (dd, 2H, CH_2), 4.51 (s, 1H, NH), 4.98 (m, 1H, CH), 6.56-6.68 (m, 3H, Ar-H), 7.03-7.57 (m, 9H, Ar-H), 7.90-7.97 (m, 2H, Ar-H) ppm; LC-MS: *m/z* 316.2 [$C_{22}H_{21}NO$ (M+1) requires 316.16], 3.729 min (97%); Anal. Calcd for $C_{22}H_{21}NO$: C, 83.75; H, 6.69; N,

4.41; O, 5.04. Found: C, 83.78; H, 6.71; N, 4.44; O, 5.07.

3-(4-Methoxyphenyl)-1-phenyl-3-(phenylamino)propan-1-one (Table S2, entry 10): White solid, mp 148-149 °C; ^{1}H NMR (400 MHz, $CDCl_3$): δ = 3.48 (dd, 2H, CH_2), 3.79 (s, 3H, CH_3), 4.51 (s, 1H, NH), 4.99 (m, 1H, CH), 6.57-6.73 (m, 3H, Ar-H), 6.86-7.11 (m, 4H, Ar-H), 7.34-7.56 (m, 5H, Ar-H), 7.89-7.96 (m, 2H, Ar-H), ppm; LC-MS: *m/z* 332.2 [$C_{22}H_{21}NO_2$ (M+1) requires 332.16], 3.592 min (99%); Anal. Calcd for $C_{22}H_{21}NO_2$: C, 79.71; H, 6.38; N, 4.22; O, 9.64. Found: C, 79.73; H, 6.39; N, 4.23; O, 9.66.

3-(4-Methoxyphenyl)-1-phenyl-3-((4-(trifluoromethyl)phenyl)amino)propan-1-one (Table S2, entry 11): White solid, mp 119-120 °C; ^{1}H NMR (400 MHz, $CDCl_3$): δ = 3.46 (m, 2H, CH_2), 3.84 (s, 3H, OCH_3), 5.01 (m, 1H, CH), 6.51-6.63 (m, 3H, Ar-H), 6.89-7.39 (m, 8H, Ar-H), 7.98-8.01 (m, 2H, Ar-H) ppm; LC-MS: *m/z* 400.2 [$C_{23}H_{20}F_3NO_2$ (M+1) requires 400.14], 3.725 min (100%); Anal. Calcd for $C_{23}H_{20}F_3NO_2$: C, 69.12; H, 5.03; F, 14.24; N, 3.49; O, 7.98. Found: C, 69.16; H, 5.05; F, 14.27; N, 3.51; O, 8.01.

3-(4-Methoxyphenyl)-1-phenyl-3-(p-tolylamino)propan-1-one (Table S2, entry 12): White solid, mp 157-158 °C; ^{1}H NMR (400 MHz, CDCl3): δ = 2.14 (s, 3H, CH_3), 3.47 (dd, 2H, CH_2), 3.85 (s, 3H, OCH_3), 4.37 (s, 1H, NH), 4.93 (m, 1H, CH), 6.49-6.87 (m, 6H, Ar-H), 7.35-7.54 (m, 5H, Ar-H), 7.89-7.97 (m, 2H, Ar-H) ppm; LC-MS: *m/z* 346.1 [$C_{23}H_{23}NO_2$ (M+1) requires 346.17], 3.654 min (99.8%); Anal. Calcd for $C_{23}H_{23}NO_2$: C, 79.97; H, 6.71; N, 4.05; O, 9.26. Found: C, 79.97; H, 6.71; N, 4.05; O, 9.26.

1-Phenyl-3-(p-tolyl)-3-((4-(trifluoromethyl)phenyl)amino)propan-1-one (Table S2, entry 13): White solid, mp 104-106 °C; ^{1}H NMR (400 MHz, $CDCl_3$): δ = 2.37 (s, 3H, CH_3), 3.49 (m, 2H, CH_2), 5.01 (m, 1H, CH), 6.51-6.62 (m, 3H, Ar-H), 6.87-7.35 (m, 8H, Ar-H), 7.97-7.99 (m, 2H, Ar-H) ppm; LC-MS: *m/z* 384.1 [$C_{23}H_{20}F_3NO$ (M+1) requires 384.15], 3.831 min (99%); Anal. Calcd for $C_{23}H_{20}F_3NO$: C, 72.01; H, 5.22; F, 14.86; N, 3.62; O, 4.15. Found: C, 72.05; H, 5.26; F, 14.87; N, 3.65; O, 4.17.

3-((4-Chlorophenyl)amino)-1-phenyl-3-(p-tolyl)propan-1-one (Table S2, entry 14): White solid, mp 157-158 °C; ^{1}H NMR (400 MHz, $CDCl_3$): δ = 2.29 (s, 3H, CH_3), 3.47 (dd, 2H, CH_2), 4.68 (s, 1H, NH), 4.96 (m, 1H, CH), 6.52-7.03 (m, 4H, Ar-H), 7.21-7.58 (m, 7H, Ar-H), 7.88-7.99 (m, 2H, Ar-H) ppm; LC-MS: *m/z* 350.1 [$C_{22}H_{20}ClNO$ (M+1) requires 350.12], 3.827 min (99.8%); Anal. Calcd for $C_{22}H_{20}ClNO$: C, 75.50; H, 5.72; Cl, 10.11; N, 3.97; O, 4.55. Found: C, 75.53; H, 5.76; Cl, 10.13; N, 4.00; O, 4.57.

3-(Naphthalen-1-yl)-1-phenyl-3-((4-(trifluoromethyl)phenyl)amino)propan-1-one (Table S2, entry 15): White solid, mp 160-161 °C; ^{1}H NMR (400 MHz, $CDCl_3$): δ = 3.56 (dd, 2H, CH_2), 5.07 (s, 1H, NH), 5.92

(m, 1H, CH), 6.54-6.58 (m, 2H, Ar-H), 7.32-7.62 (m, 9H, Ar-H), 7.89-8.21 (m, 5H, Ar-H) ppm; LC-MS: *m/z* 420.2 [$C_{26}H_{20}F_3NO$ (M+1) requires 420.15], 3.902 min (100%); Anal. Calcd for $C_{26}H_{20}F_3NO$: C, 74.41; H, 4.78; F, 13.55; N, 3.32; O, 3.77. Found: C, 74.45; H, 4.81; F, 13.59; N, 3.34; O, 3.81.

3-Phenyl-3-(phenylamino)-1-(p-tolyl)propan-1-one (Table S2, entry 16): White solid, mp 140-142 °C; ^{1}H NMR (400 MHz, $CDCl_3$): δ = 2.38 (s, 3H, CH_3), 3.47 (dd, 2H, CH_2), 4.76 (s, 1H, NH), 4.99 (m, 1H, CH), 6.57-7.09 (m, 5H, Ar-H), 7.19-7.46 (m, 7H, Ar-H), 7.81-7.91 (m, 2H, Ar-H) ppm; LC-MS: *m/z* 316.1 [$C_{22}H_{21}NO$ (M+1) requires 316.16], 3.722 min (97%); Anal. Calcd for $C_{22}H_{21}NO$: C, 83.73; H, 6.68; N, 4.42; O, 5.04. Found: C, 83.78; H, 6.71; N, 4.44; O, 5.07.

2-(Phenyl(phenylamino)methyl)cyclohexanone (Table S2, entry 17): White solid, mp 143-145 °C; ^{1}H NMR (400 MHz, $CDCl_3$): δ = 1.37-1.87 (m, 6H, $CH_2CH_2CH_2$), 2.36-2.52 (t, 2H, CH_2), 2.87-2.91 (m, 1H, CH), 4.69 (s, 1H, NH), 4.72 (m, 1H, CH), 6.53-6.58 (m, 3H, Ar-H), 7.01-7.23 (m, 5H, Ar-H), 7.31-7.35 (m, 2H, Ar-H) ppm; LC-MS: *m/z* 280.2 [$C_{19}H_{21}NO$ (M+1) requires 280.16], 3.579 min (98%); Anal. Calcd for $C_{19}H_{21}NO$: C, 81.66; H, 7.56; N, 4.98; O, 5.71. Found: C, 81.68; H, 7.58; N, 5.01; O, 5.73.

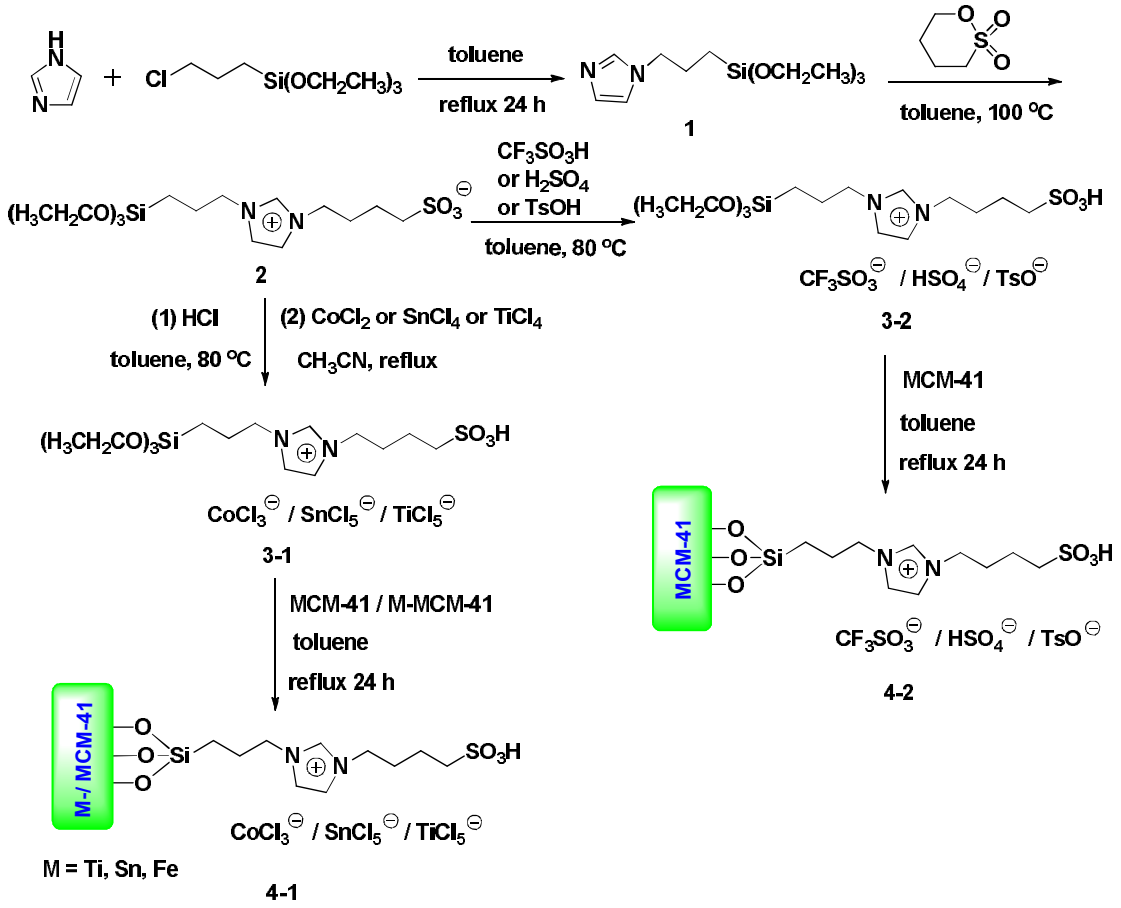

Scheme S1. Preparation of the supported ILs.

Supported ILs characterization

FT-IR spectra of the supported ILs are shown in Fig. S1. The characteristic bonds at about 1539 and 1634 cm^{-1}, which were attributed to the imidazole ring, indicating that imidazole was successfully grafted on the surface of MCM-41 and (Ti, Sn, Fe)-MCM-41. The characteristic peaks at about 3108, 2959 and 1527 cm^{-1} are due to C–H stretching and deformation vibrations of the imidazole moiety and alkyl chain.[8] The peaks observed at about 1087 and 797 cm^{-1} were belonged to the stretching vibration of Si–O–Si, which are assigned to internal asymmetric stretching vibration and identification peak for mesoporous MCM-41. The peaks at 962, 970 and 960 cm^{-1} are attributed to the absorption bands of Ti-O-Si, Sn-O-Si, Fe-O-Si, respectively.[1-4] The peaks observed at about 1474, 1267 cm^{-1} (Fig. S1b), 1028 cm^{-1} (Fig. S1c), 1713, 878 cm^{-1} (Fig. S1d), 1449 cm^{-1} (Fig. S1e), 1178, 1215 cm^{-1} (Fig. S1f) related to vibrational modes of TsO, CF_3SO_3, HSO_4, $CoCl_3$, $SnCl_5$, respectively,[9,10] characteristic peaks at about 575, 690, 822 cm^{-1} were related to the vibrational modes of $TiCl_5$.[9]

The supported ILs had characteristic peak at $2\theta \approx 25.1°$, which was the amorphous nature of the mesoporous silica support (Fig. S2). The absence of obvious characteristic peaks of anions of ILs in the XRD patterns suggests that the anion is well-dispersed on the surface and in the mesopore channels of the mesoporous silica support.[11] Fig. S3 showed the diffuse reflectance UV–Vis spectra of the supported ILs. The peak around 221-238 nm, are assigned to the O-Si transition,[1-4] another absorption region extended to about 256-758 nm, suggested that the ILs were grafted on mesoporous silica support.[12] SEM images of the supported ILs and mesoporous silica are shown in Fig. S4, it clearly observed that the morphologies of the mesoporous silica and the supported ILs are agglomerations of small spherical with uniform nanometre sized particles. Fig. S4k-m clearly showed the well-ordered arrays of the mesoporous. The morphology of this material was typical of MCM-41 materials.[1-3] Fig. S4a-i shows the aggregation of ILs particles, the clusters' sizes were slightly larger than the pore size of the mesoporous silica and led to the distortion of the channels, it implies that the TsO, CF_3SO_3-, HSO_4-, $CoCl_3$-, $SnCl_5$-, $TiCl_5$- based ILs inserted into the pores, but the mesoporous structure of support was retained after immobilized anion-based IL. Compared to mesoporous silica, the surface of the supported ILs turned smooth and soft, and the images of the supported ILs shows highly uniform particles. Fig. S5 displayed the EDX analysis of the supported ILs. EDX obtained from SEM showed the presence of the expected elements in their structure. N_2 adsorption–desorption measurements are a powerful tool for characterization of mesoporous materials. Fig.

S6 shows the isotherms and pore size distribution of supported ILs. It can be observed that the samples exhibited a type IV isotherm which was characteristic of highly ordered mesoporous materials.[2,3,5,6] No obvious change in average pore size is observed, and the surface area and pore volume decreased after immobilization of IL. The pore volumes of the materials displayed the order: Ti-MCM-41>$ILSO_3H$-$TiCl_5$@Ti-MCM-41; Sn-MCM-41>$ILSO_3H$-$TiCl_5$@Sn-MCM-41; Fe-MCM-41> $ILSO_3H$-$TiCl_5$@Fe-MCM-41. These results showed that the entrapping of the $TiCl_5$-based ionic liquid IL by Ti, Sn, Fe incorporated MCM-41 mesoporous materials had indeed occurred, and that the pore structure remained intact.

The overall thermal stability of the supported ILs were conducted through TG analysis (Fig. S7). The observed organic materials weight loss of the supported ILs showed a mass weight loss of ~59.8 % (Fig. S7a), ~60.2 % (Fig. S7b), ~54.5 % (Fig. S7c), ~51.1 % (Fig. S 7d), ~57.9 % (Fig. S7e), ~52.8 % (Fig. S7f), ~41.3 % (Fig. S7g), ~50.2 % (Fig. S7h), ~49.1 % (Fig. S7i) on heating to 800 °C. The small weight loss before 220 °C is related to the desorption of adsorbed water and solvents, indicating a considerably thermal stability up to 220 °C. There existed drastic weight loss between 220 and 500 °C is attributed to the breakdown of the organic moieties. From the curves depicted, it demonstrated that the supported ILs are thermally stable below about 220 °C.

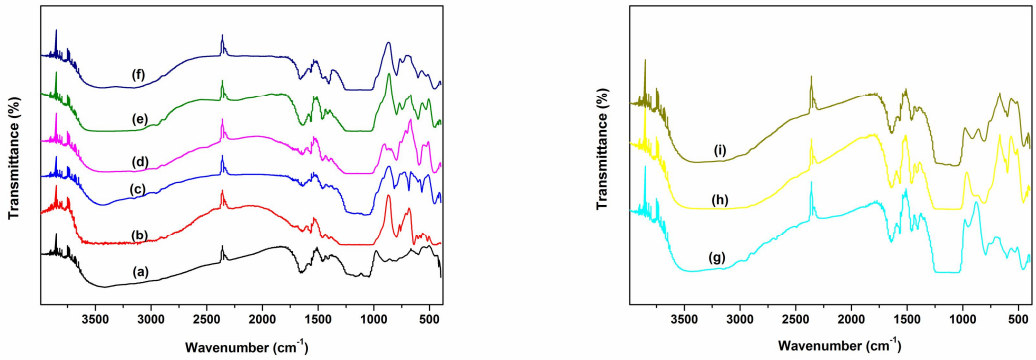

Fig. S1 FT-IR spectra of $ILSO_3H$-$TiCl_5$@MCM-41 (a), $ILSO_3H$-TsO@MCM-41 (b), $ILSO_3H$-CF_3SO_3@MCM-41 (c), $ILSO_3H$-HSO_4@MCM-41 (d), $ILSO_3H$-$CoCl_3$@MCM-41 (e), $ILSO_3H$-$SnCl_5$@MCM-41 (f), $ILSO_3H$-$TiCl_5$@Ti-MCM-41 (g), $ILSO_3H$-$TiCl_5$@Sn-MCM-41 (h), $ILSO_3H$-$TiCl_5$@Fe-MCM-41 (i).

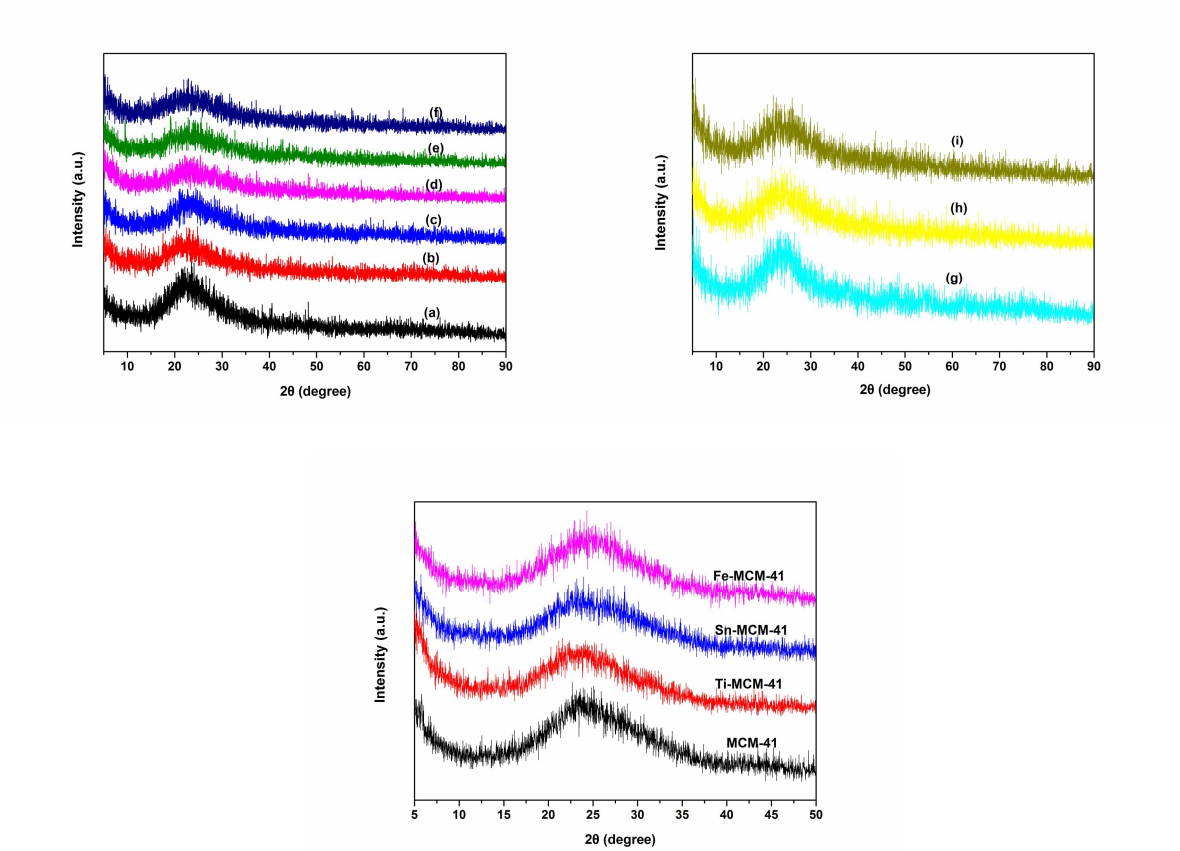

Fig. S2 XRD diffractograms $ILSO_3H$-$TiCl_5$@MCM-41 (a), $ILSO_3H$-TsO@MCM-41 (b), $ILSO_3H$-CF_3SO_3@MCM-41 (c), $ILSO_3H$-HSO_4@MCM-41 (d), $ILSO_3H$-$CoCl_3$@MCM-41 (e), $ILSO_3H$-$SnCl_5$@MCM-41 (f), $ILSO_3H$-$TiCl_5$@Ti-MCM-41 (g), $ILSO_3H$-$TiCl_5$@Sn-MCM-41 (h), $ILSO_3H$-$TiCl_5$@Fe-MCM-41 (i).

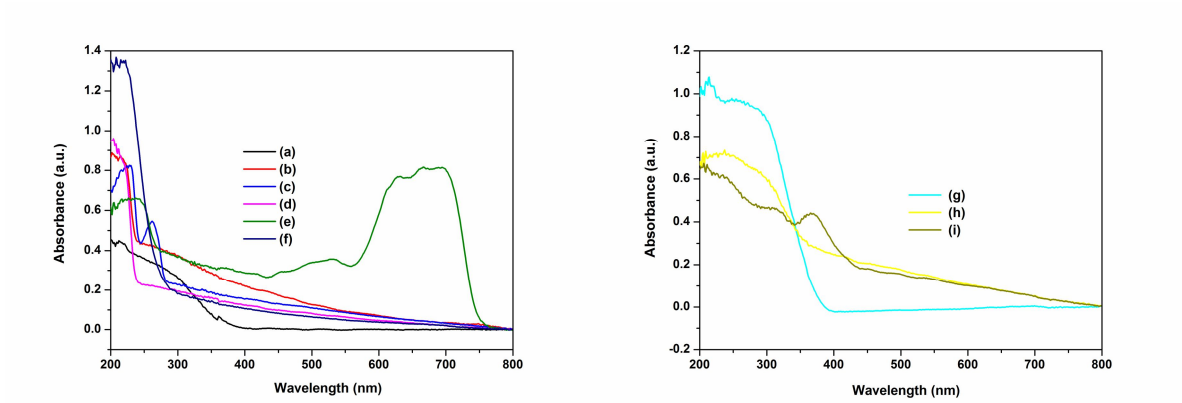

Fig. S3 UV–Vis spectra of $ILSO_3H$-$TiCl_5$@MCM-41 (a), $ILSO_3H$-TsO@MCM-41 (b), $ILSO_3H$-CF_3SO_3@MCM-41 (c), $ILSO_3H$-HSO_4@MCM-41 (d), $ILSO_3H$-$CoCl_3$@MCM-41 (e), $ILSO_3H$-$SnCl_5$@MCM-41 (f), $ILSO_3H$-$TiCl_5$@Ti-MCM-41 (g), $ILSO_3H$-$TiCl_5$@Sn-MCM-41 (h), $ILSO_3H$-$TiCl_5$@Fe-MCM-41 (i).

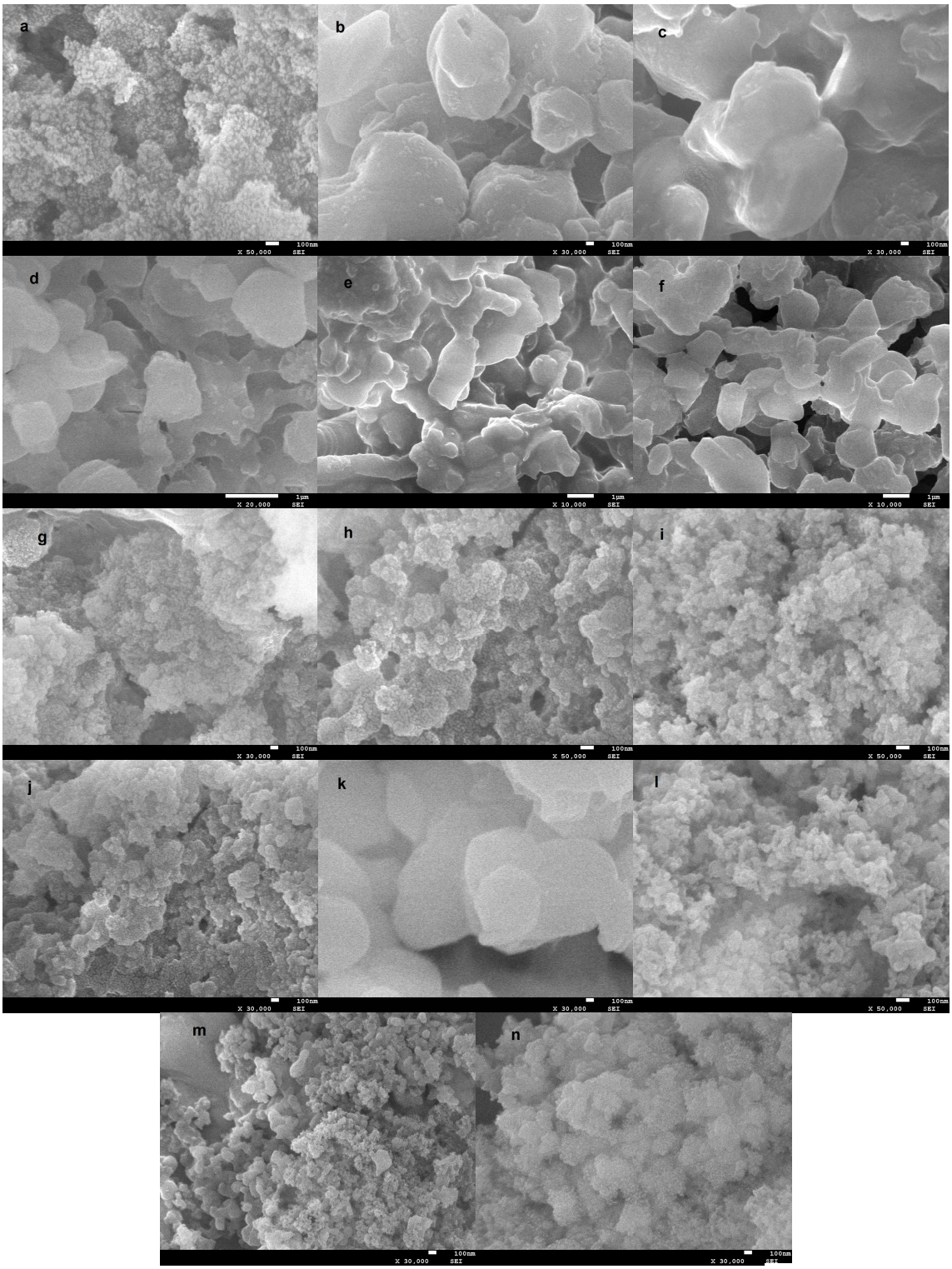

Fig. S4 SEM images of $ILSO_3H$-$TiCl_5$@MCM-41 (a), $ILSO_3H$-TsO@MCM-41 (b), $ILSO_3H$-CF_3SO_3@MCM-41 (c), $ILSO_3H$-HSO_4@MCM-41 (d), $ILSO_3H$-$CoCl_3$@MCM-41 (e), $ILSO_3H$-$SnCl_5$@MCM-41 (f), $ILSO_3H$-$TiCl_5$@Ti-MCM-41 (g), $ILSO_3H$-$TiCl_5$@Sn-MCM-41 (h), $ILSO_3H$-$TiCl_5$@Fe-MCM-41 (i), six times recycled $ILSO_3H$-$TiCl_5$@Sn-MCM-41 (j), MCM-41 (k), Ti-MCM-41 (l), Sn-MCM-41 (m), Fe-MCM-41 (n).

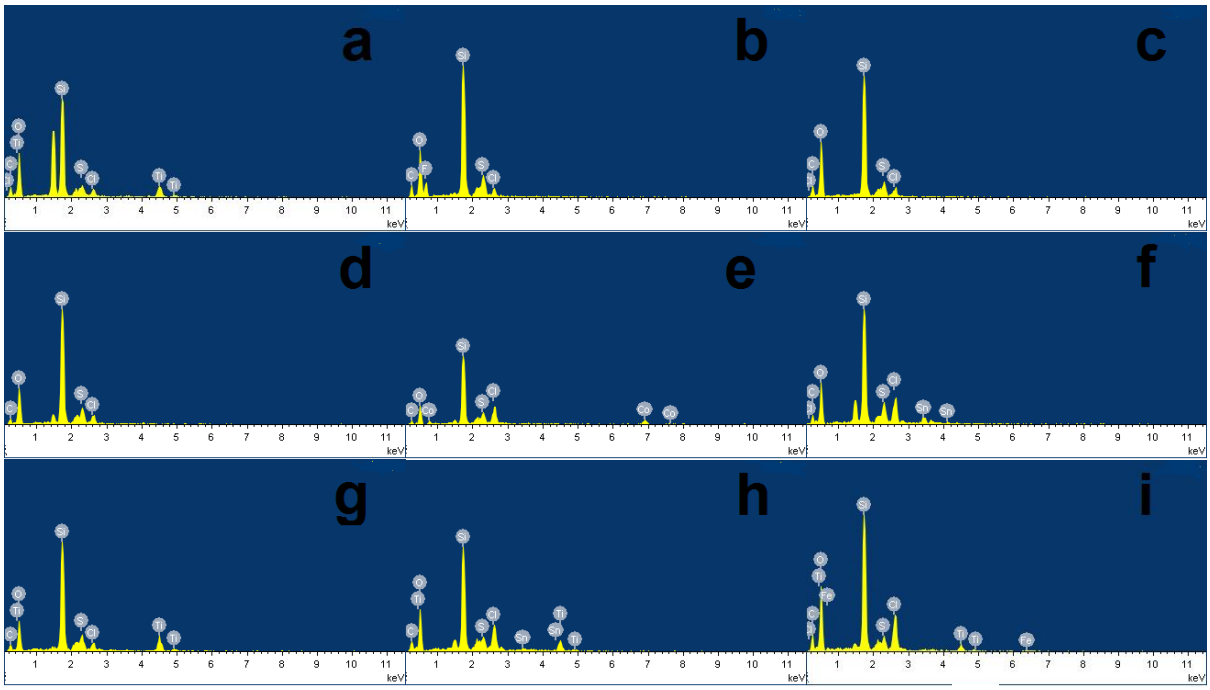

Fig. S5 EDX images of $ILSO_3H$-$TiCl_5$@MCM-41 (a), $ILSO_3H$-TsO@MCM-41 (b), $ILSO_3H$-CF_3SO_3@MCM-41 (c), $ILSO_3H$-HSO_4@MCM-41 (d), $ILSO_3H$-$CoCl_3$@MCM-41 (e), $ILSO_3H$-$SnCl_5$@MCM-41 (f), $ILSO_3H$-$TiCl_5$@Ti-MCM-41 (g), $ILSO_3H$-$TiCl_5$@Sn-MCM-41 (h), $ILSO_3H$-$TiCl_5$@Fe-MCM-41 (i).

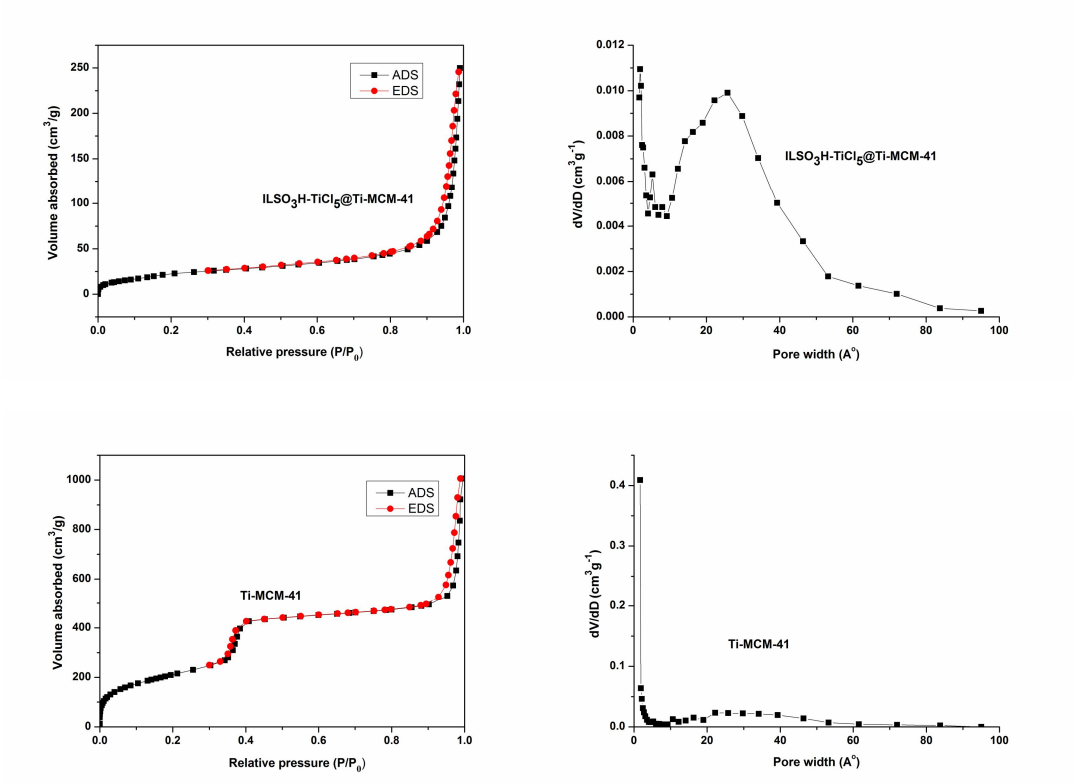

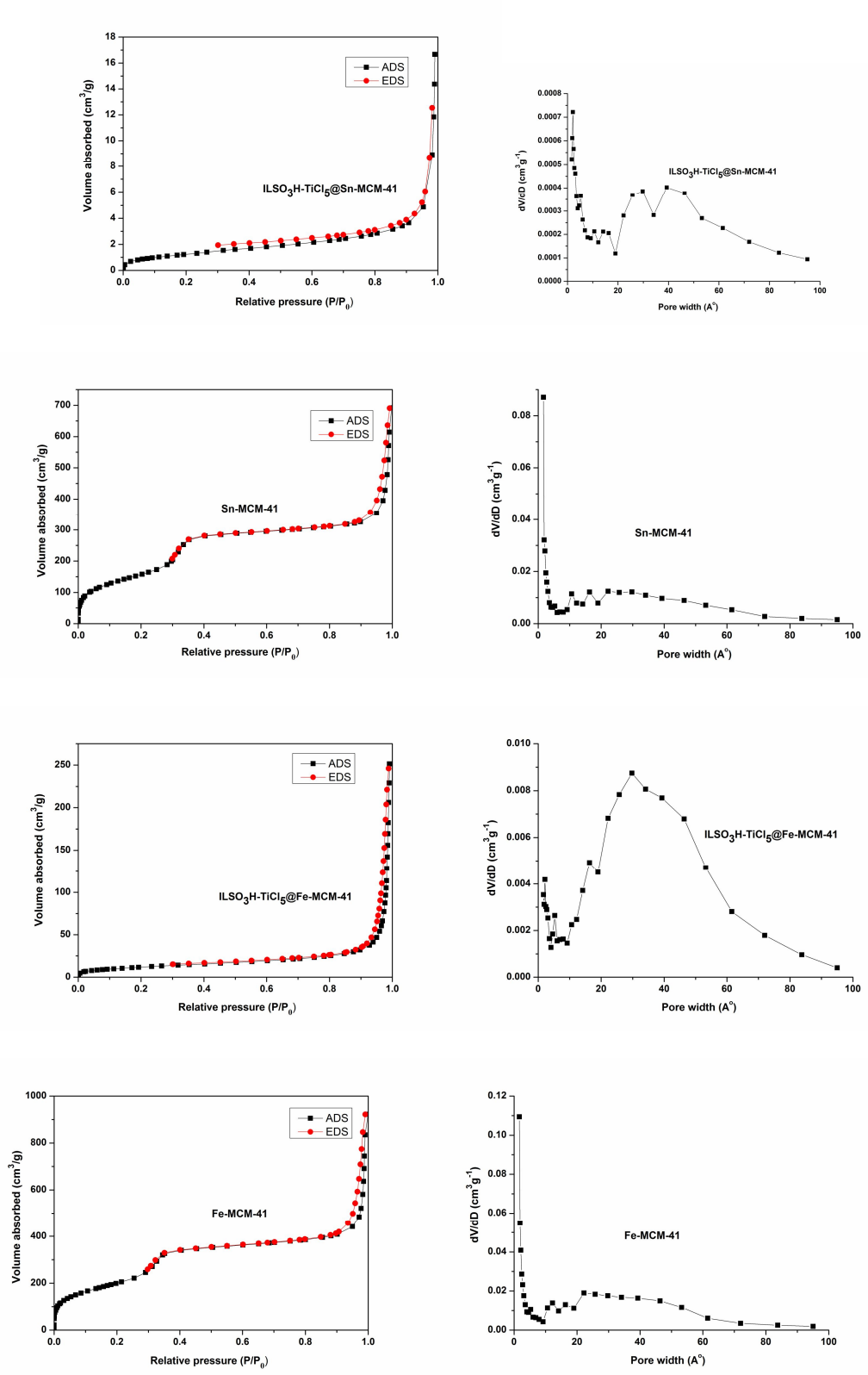

Fig. S6 N_2 adsorption–desorption isotherms and pore size distribution of $ILSO_3H$-$TiCl_5$@Ti-MCM-41/ Ti-MCM-41, $ILSO_3H$-$TiCl_5$@Sn-MCM-41 /Sn-MCM-41, and $ILSO_3H$-$TiCl_5$@Fe-MCM-41/Fe-MCM-41.

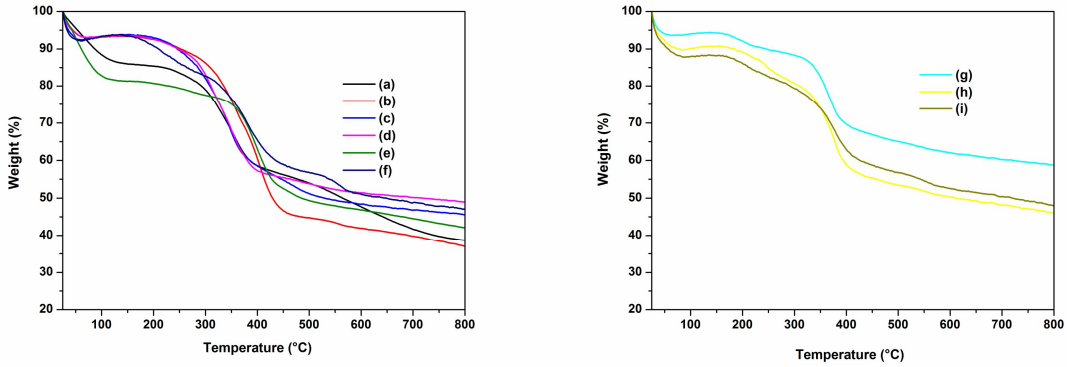

Fig. S7 TGA profiles of $ILSO_3H$-$TiCl_5$@MCM-41 (a), $ILSO_3H$-TsO@MCM-41 (b), $ILSO_3H$-CF_3SO_3@MCM-41 (c), $ILSO_3H$-HSO_4@MCM-41 (d), $ILSO_3H$-$CoCl_3$@MCM-41 (e), $ILSO_3H$-$SnCl_5$@MCM-41 (f), $ILSO_3H$-$TiCl_5$@Ti-MCM-41 (g), $ILSO_3H$-$TiCl_5$@Sn-MCM-41 (h), $ILSO_3H$-$TiCl_5$@Fe-MCM-41 (i).

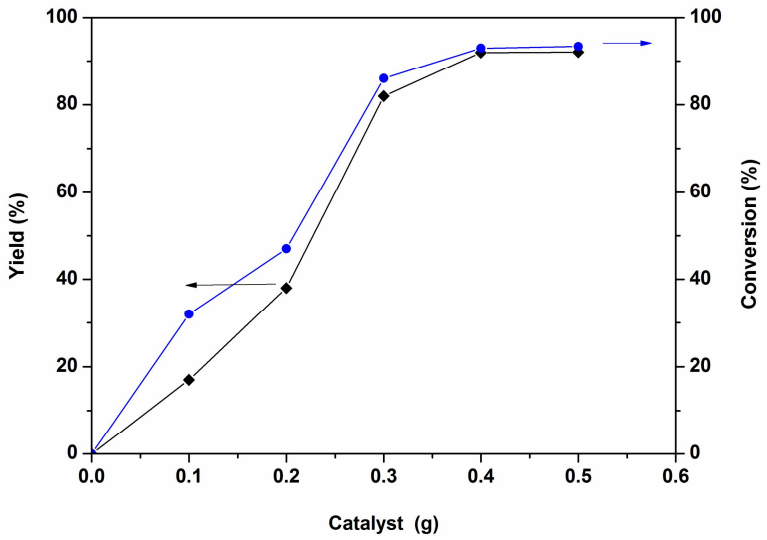

Fig. S8 Influence of catalyst amount on the three-component Mannich reaction. Reaction conditions: benzaldehyde (0.05 mol), aniline (0.05 mol), acetophenone (0.05 mol), EtOH (10 mL) were stirred in different amounts of $ILSO_3H$-$TiCl_5$@Sn-MCM-41 at room temperature for 3 h.

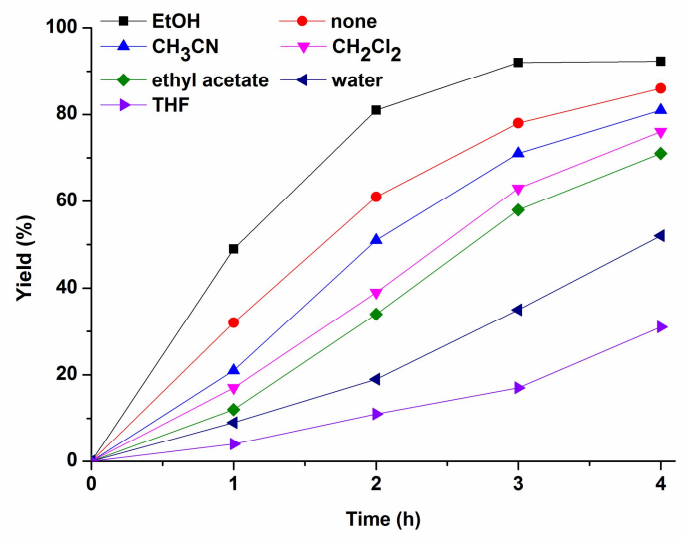

Fig. S9 Effect of solvent on the Mannich reaction. Reaction conditions: benzaldehyde (0.05 mol), aniline (0.05 mol), acetophenone (0.05 mol), solvent (10 mL), $ILSO_3H$-$TiCl_5$@Sn-MCM-41 (0.4 g) were stirred at room temperature for 3 h.

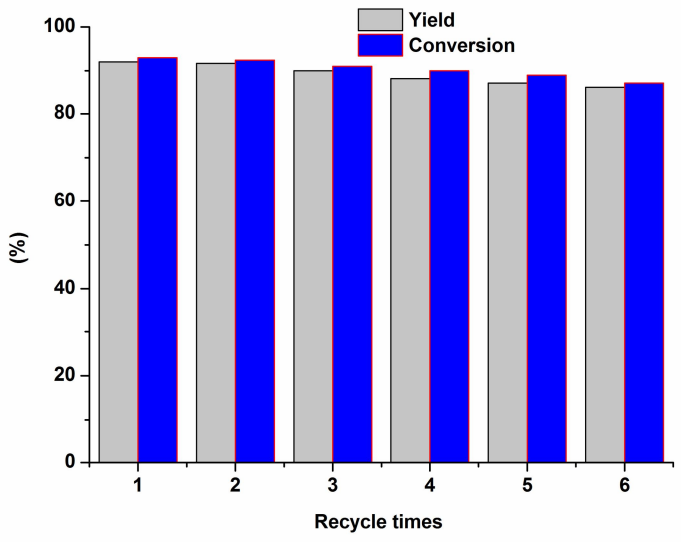

Fig. S10 Recyclability study of $ILSO_3H$-$TiCl_5$@Sn-MCM-41 on the Mannich reaction.

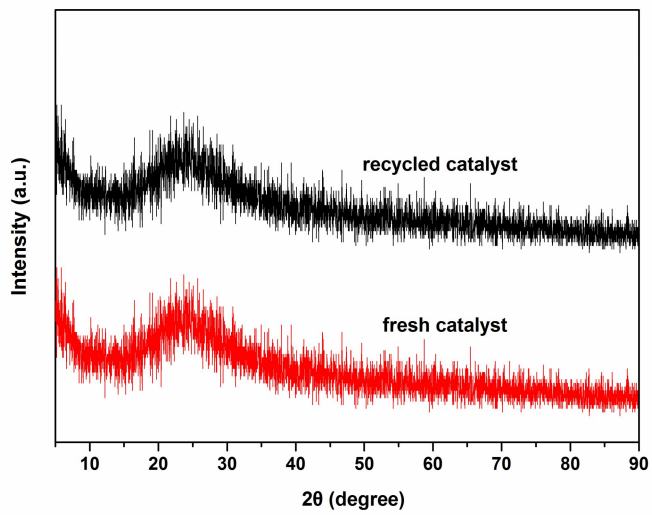

Fig. S11 XRD diffractogram of fresh and recycled $ILSO_3H$-$TiCl_5$@Sn-MCM-41.

Table S1 Elemental analysis of the fresh and reused $ILSO_3H$-$TiCl_5$@Sn-MCM-41

Catalyst	Ti (wt.%)	Sn (wt.%)	SO_3H (wt.%)
Fresh catalyst	8.736	5.183	12.317
Second reused catalyst	8.735	5.182	12.316
Fourth reused catalyst	8.734	5.181	12.315
Sixth reused catalyst	8.733	5.180	12.313

Table S2 The catalytic three-component Mannich reactions with $ILSO_3H$-$TiCl_5$@Sn-MCM-41[a]

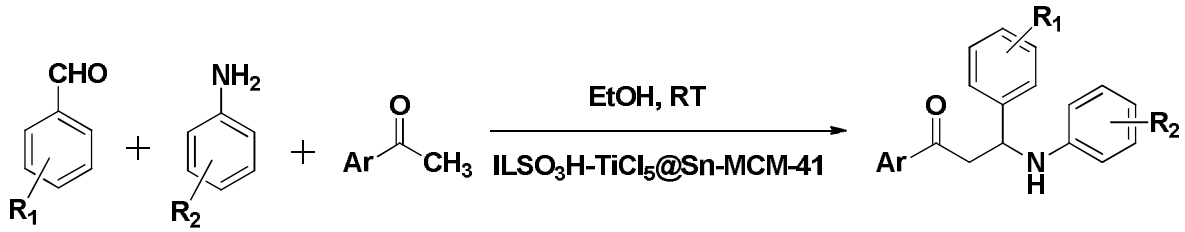

Entry	Substrates	Product	Time (h)	Yield (%)[b]
1	R_1 = H, R_2 = H 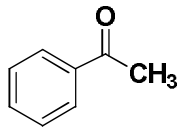	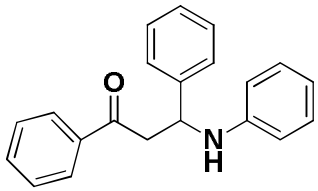	3	92
2	R_1 = H, R_2 = $CH(CH_3)_2$ 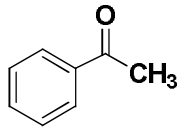	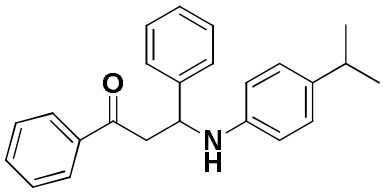	4	85
3	R_1 = H, R_2 = CH_3 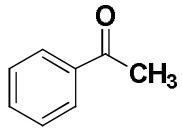	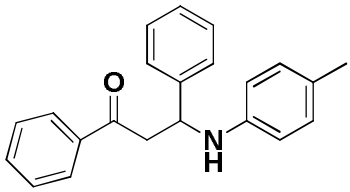	4	87
4	R_1 = H, R_2 = OCH_3 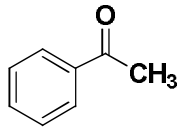	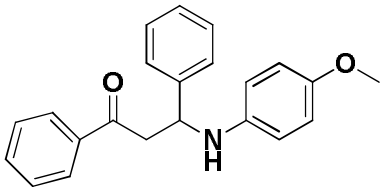	4	81

5	R_1 = H, R_2 = CF_3 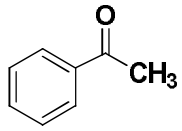	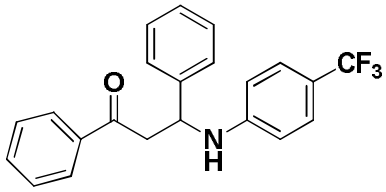	1	98
6	R_1 = F, R_2 = CF_3 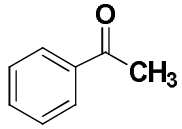	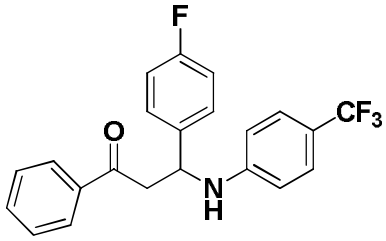	1	99
7	R_1 = H, R_2 = Cl 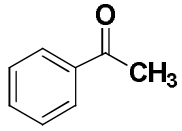	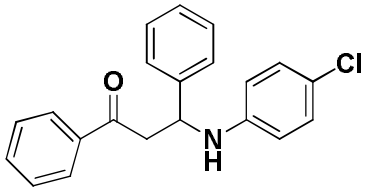	1	98
8	R_1 = F, R_2 = Cl 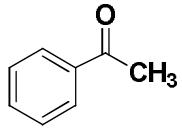	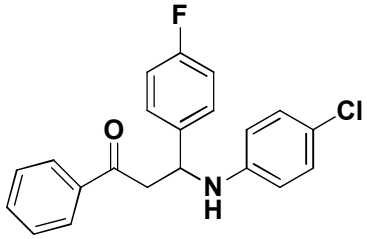	1	98
9	R_1 = CH_3, R_2 = H 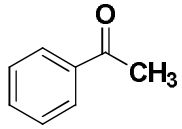	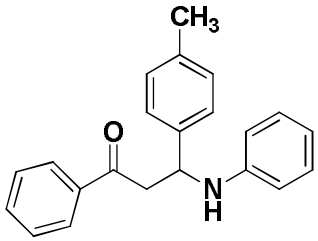	2	97
10	R_1 = OCH_3, R_2 = H 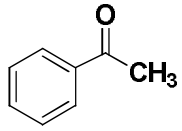	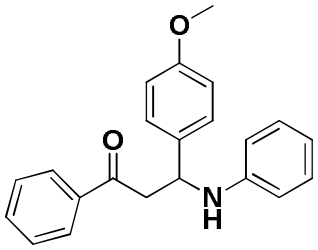	2	99
11	R_1 = OCH_3, R_2 = CF_3 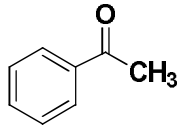	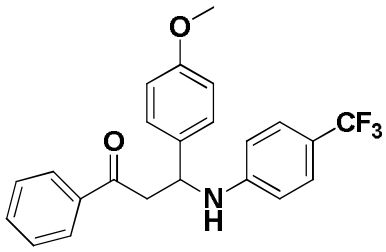	1	97

12	$R_1 = OCH_3$, $R_2 = CH_3$ 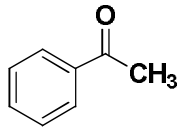	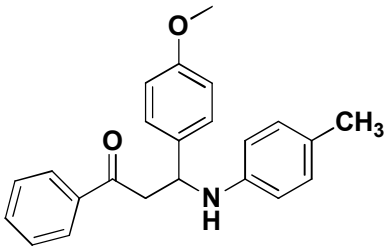	4	90
13	$R_1 = CH_3$, $R_2 = CF_3$ 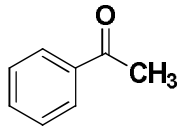	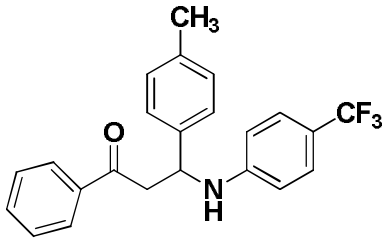	1.5	95
14	$R_1 = CH_3$, $R_2 = Cl$ 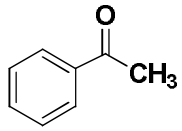	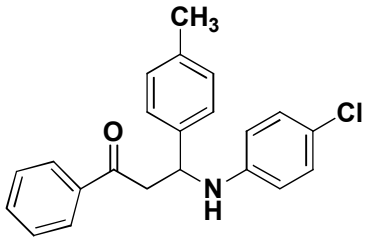	1.5	93
15	$R_1 = Ar$, $R_2 = Cl$ 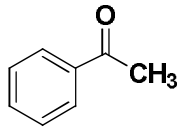	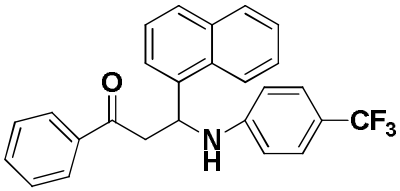	3	84
16	$R_1 = H$, $R_2 = H$ 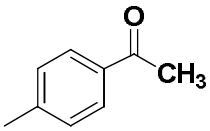	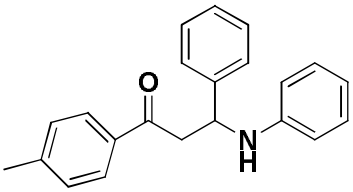	3	90
17	$R_1 = H$, $R_2 = H$ 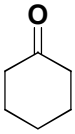	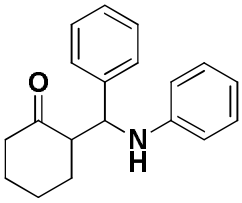	3	92

[a] Reaction conditions: aromatic aldehyde (0.05 mol), aromatic amine (0.05 mol), ketone (0.05 mol), $ILSO_3H$-$TiCl_5$@Sn-MCM-41 (0.4 g) were stirred in EtOH (10 mL) at room temperature. [b] Isolated yield.

Copies of ^{1}H NMR and LC-MS Spectra

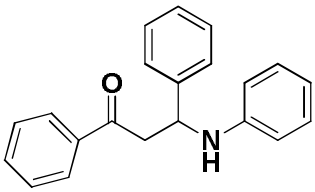

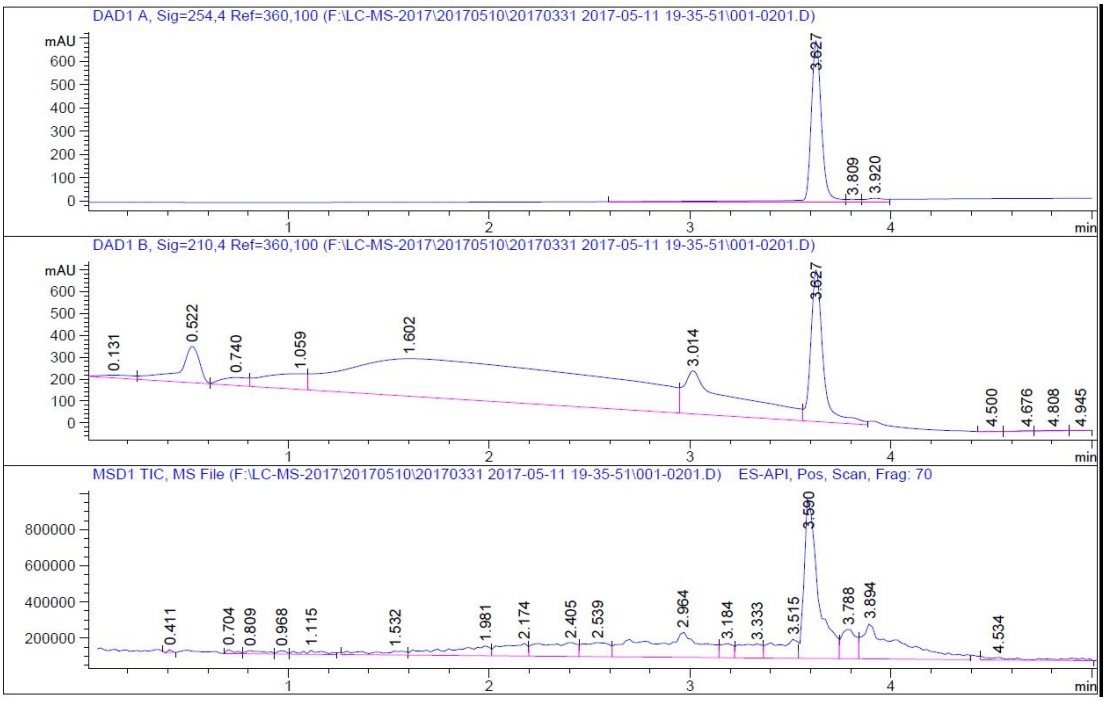

Signal 1: DAD1 A, Sig=254,4 Ref=360,100

#	Ret. [min]		Width [min]	Area [mAU*s]	Height [mAU]	Area %
1	3.627	BV	0.0573	2567.55884	691.87433	97.7071
2	3.809	VV	0.0673	48.41161	10.58913	0.7801
3	3.920	VV	0.0922	103.69799	15.46767	1.2129

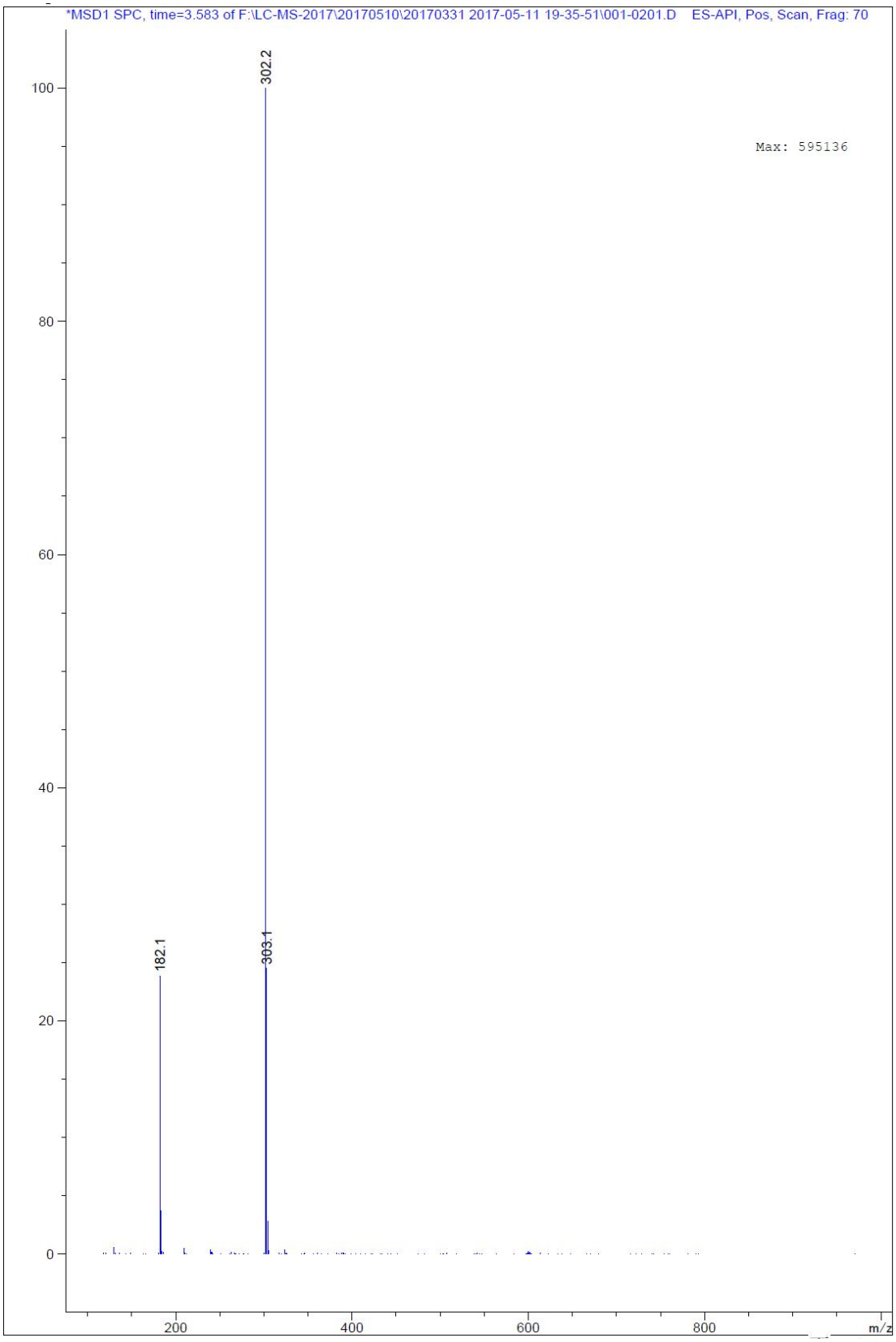
*MSD1 SPC, time=3.583 of F:\LC-MS-2017\20170510\20170331 2017-05-11 19-35-51\001-0201.D ES-API, Pos, Scan, Frag: 70
Max: 595136
302.2
182.1
303.1
100
80
60
40
20
0
200
400
600
800
m/z

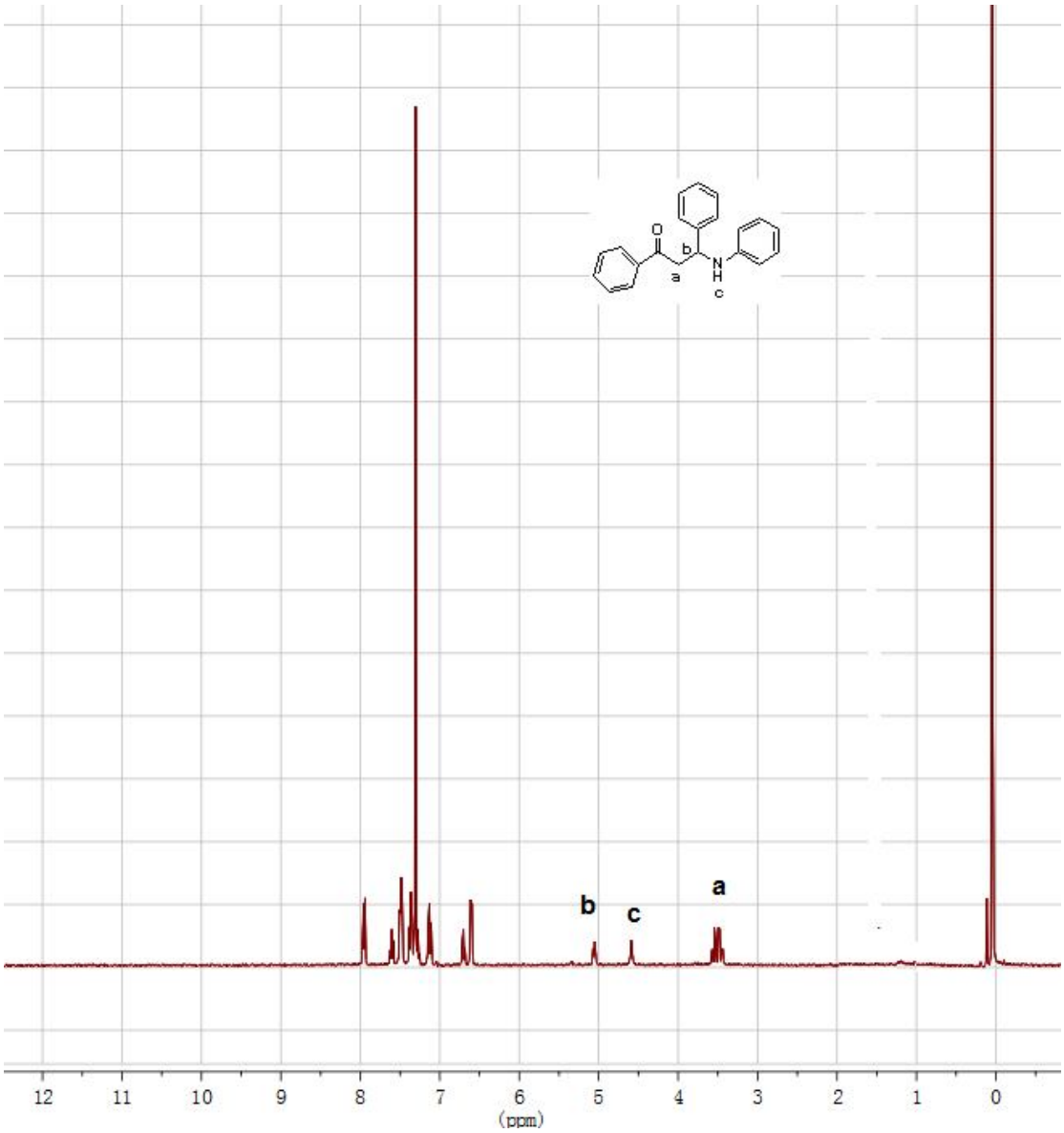
O
b
a
N
H
c
b
c
a
12
11
10
9
8
7
6
5
4
3
2
1
0
(ppm)

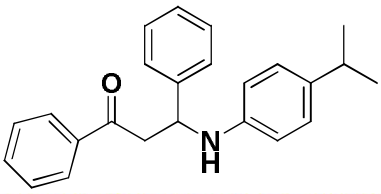

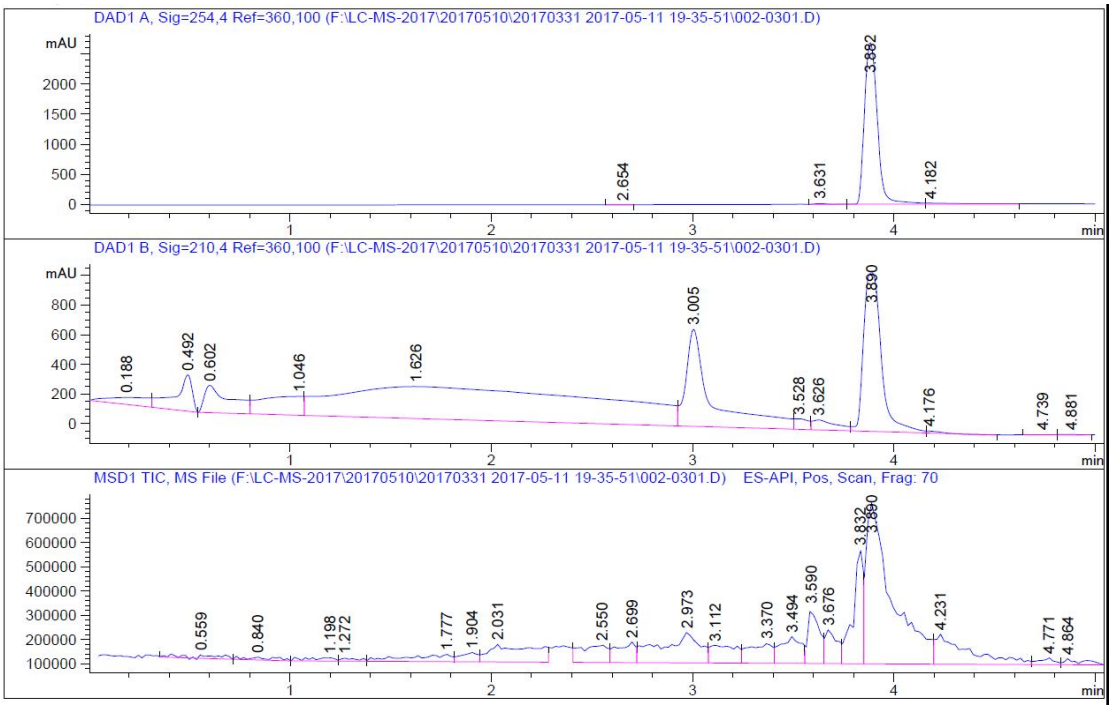

Signal 1: DAD1 A, Sig=254,4 Ref=360,100

#	Ret. [min]		Width [min]	Area [mAU*s]	Height [mAU]	Area %
1	2.654	BV	0.0652	7.13909	1.69207	0.0588
2	3.631	VV	0.0590	51.15965	13.27814	0.4217
3	3.882	VV	0.0716	1.18885e4	2686.84351	98.0001
4	4.182	VB	0.1423	184.30934	16.50471	1.5193

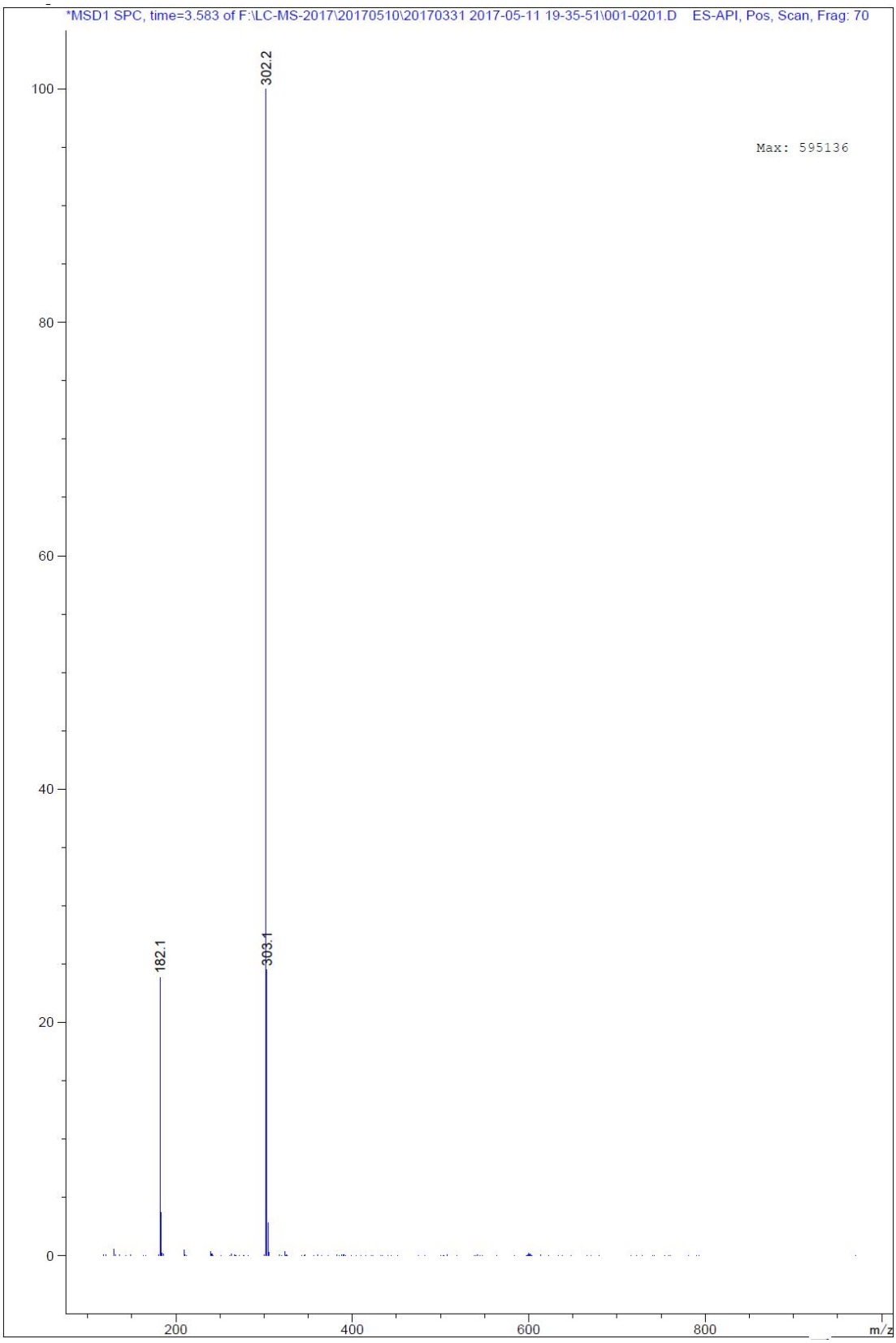
*MSD1 SPC, time=3.583 of F:\LC-MS-2017\20170510\20170331 2017-05-11 19-35-51\001-0201.D ES-API, Pos, Scan, Frag: 70
Max: 595136
302.2
182.1
303.1
100
80
60
40
20
0
200
400
600
800
m/z

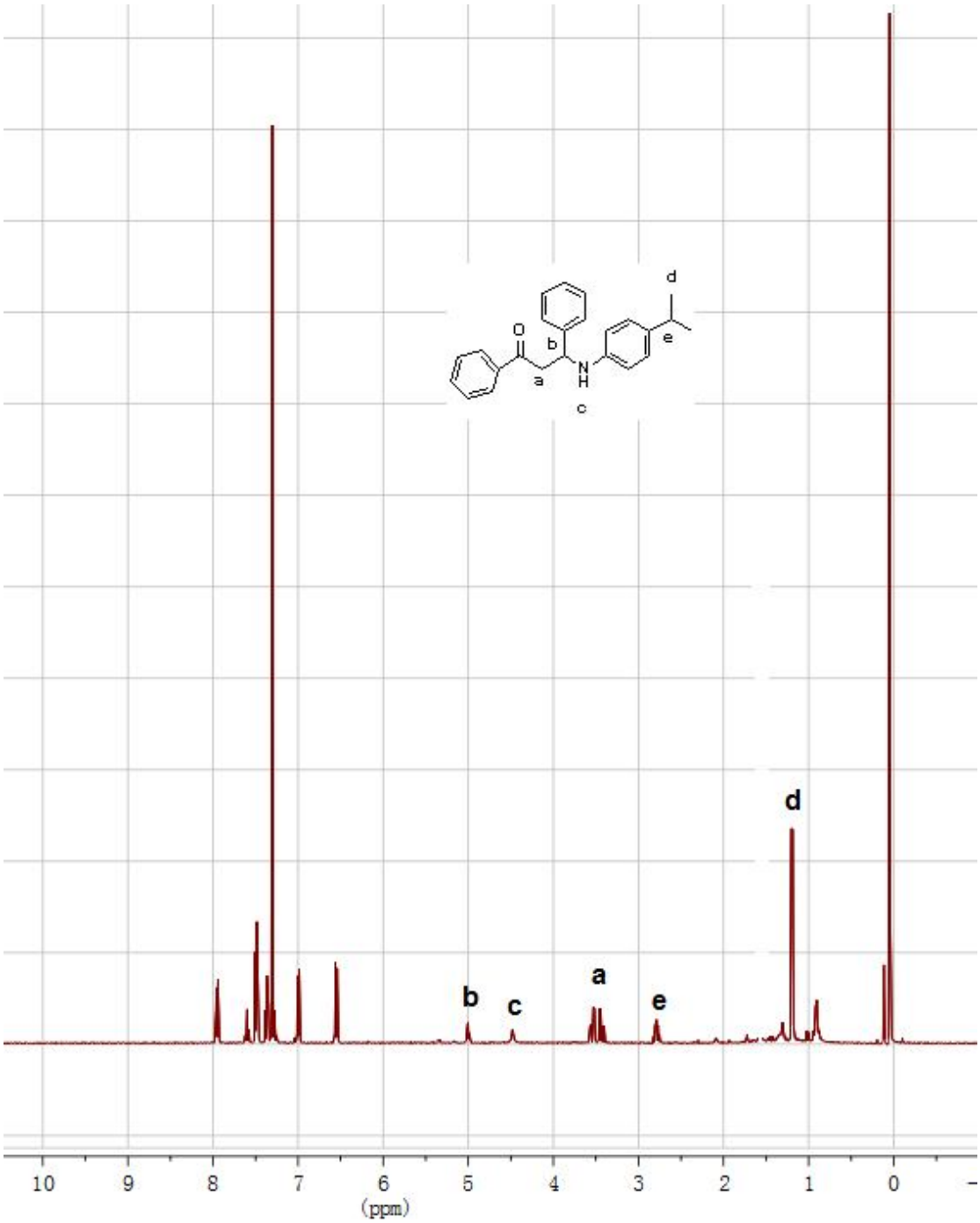
d
O
b
e
N
H
a
c
d
b
c
a
e
10
9
8
7
6
5
4
3
2
1
0
(ppm)

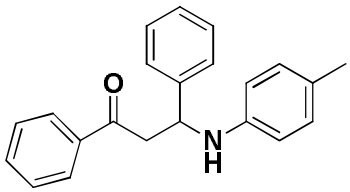

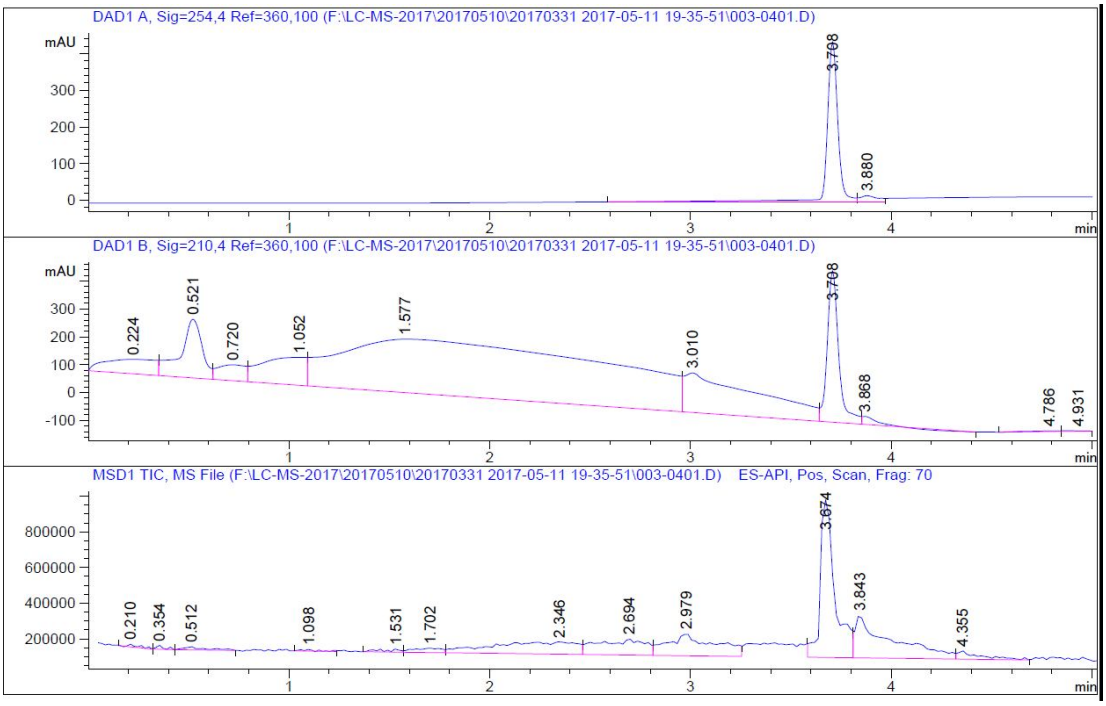

Signal 1: DAD1 A, Sig=254,4 Ref=360,100

#	Ret. [min]		Width [min]	Area [mAU*s]	Height [mAU]	Area %
1	3.708	BV	0.0605	1746.08337	438.46490	96.7860
2	3.880	VV	0.0852	115.69041	18.44072	3.2140

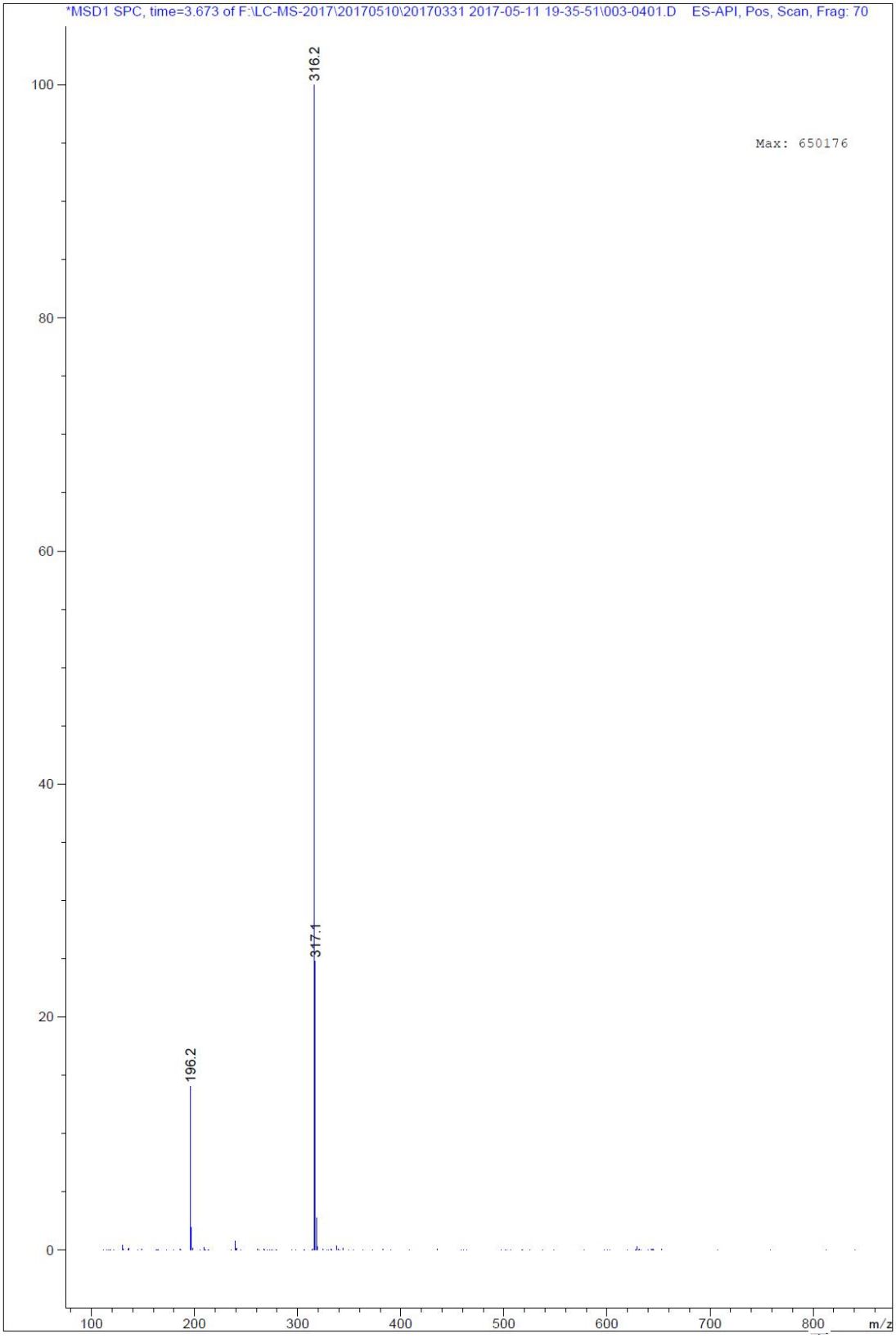
*MSD1 SPC, time=3.673 of F:\LC-MS-2017\20170510\20170331 2017-05-11 19-35-51\003-0401.D ES-API, Pos, Scan, Frag: 70
Max: 650176
316.2
317.1
196.2
100
80
60
40
20
0
100
200
300
400
500
600
700
800
m/z

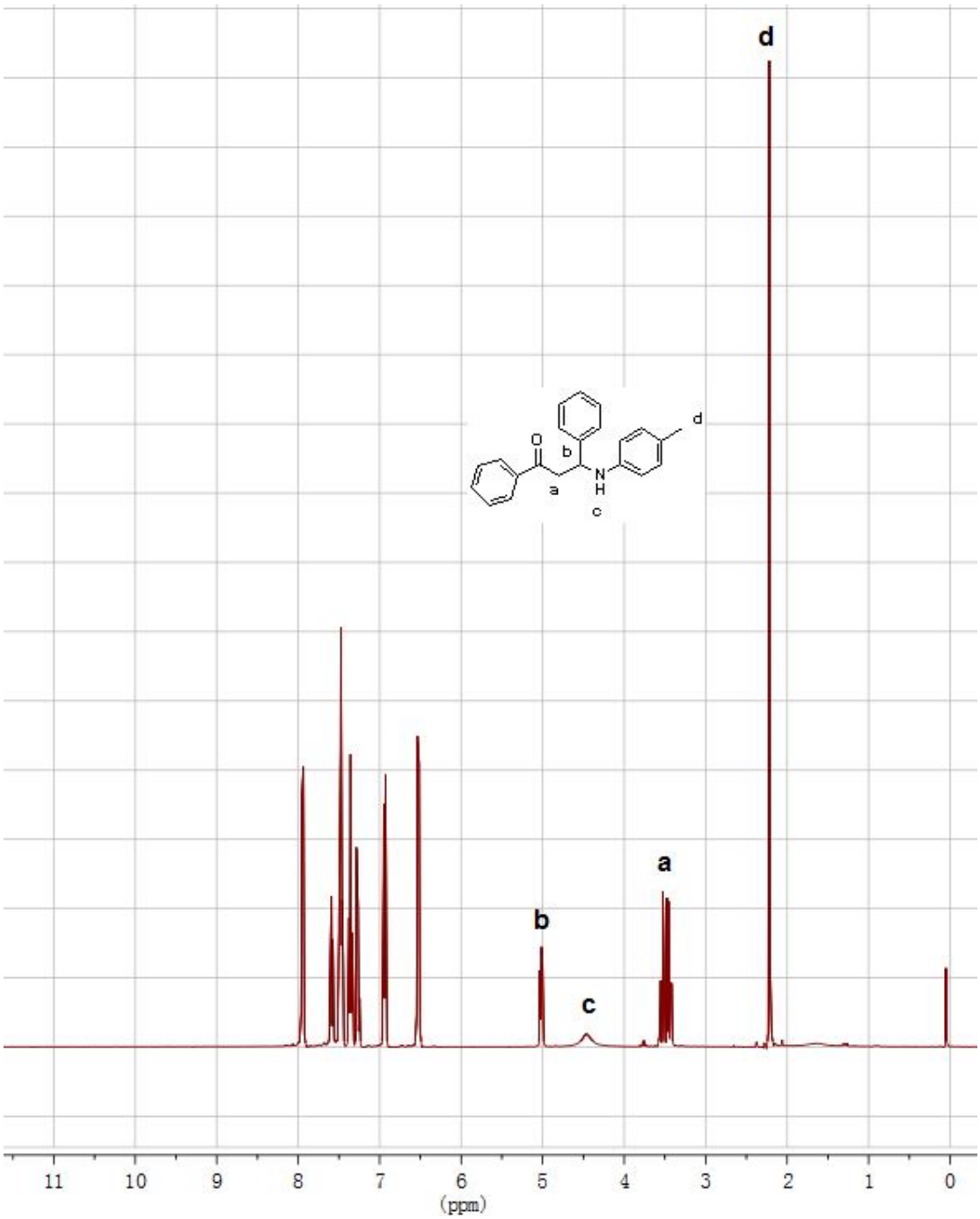
d
a
b
c
O
b
N
H
a
c
d
11
10
9
8
7
6
5
4
3
2
1
0
(ppm)

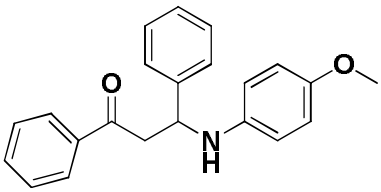

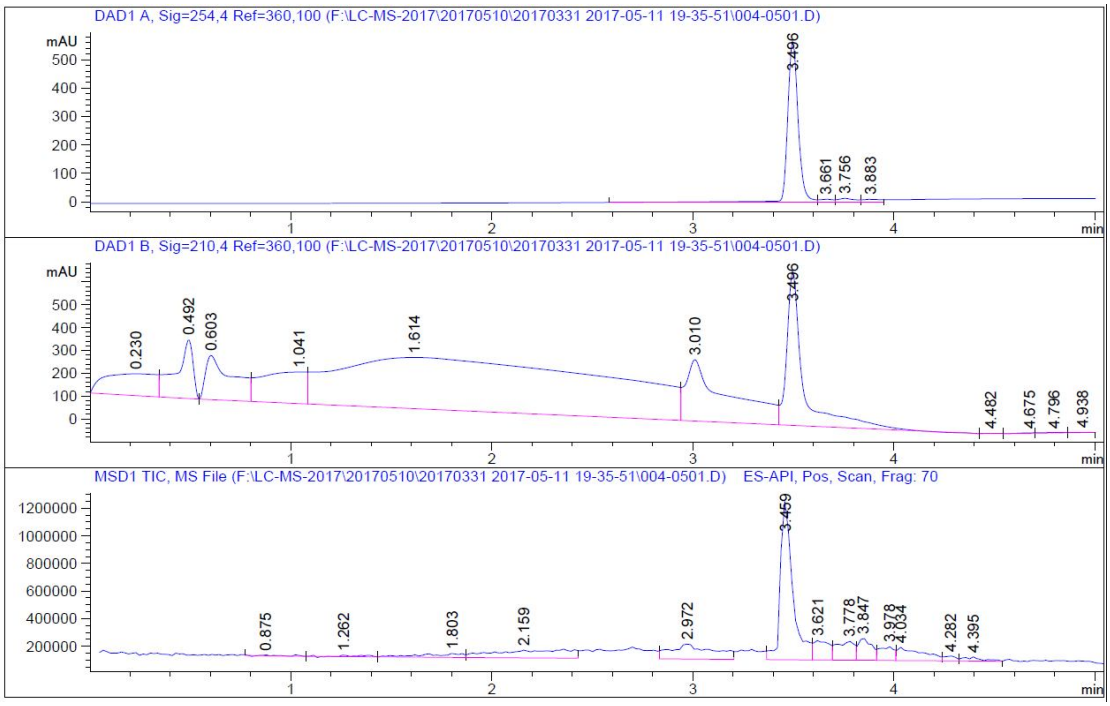

Signal 1: DAD1 A, Sig=254,4 Ref=360,100

#	Ret. [min]		Width [min]	Area [mAU*s]	Height [mAU]	Area %
1	3.496	BV	0.0579	2140.83325	569.24255	96.8294
2	3.661	VV	0.0705	54.41576	11.24067	1.0087
3	3.756	VV	0.0842	88.16521	14.65067	2.1406

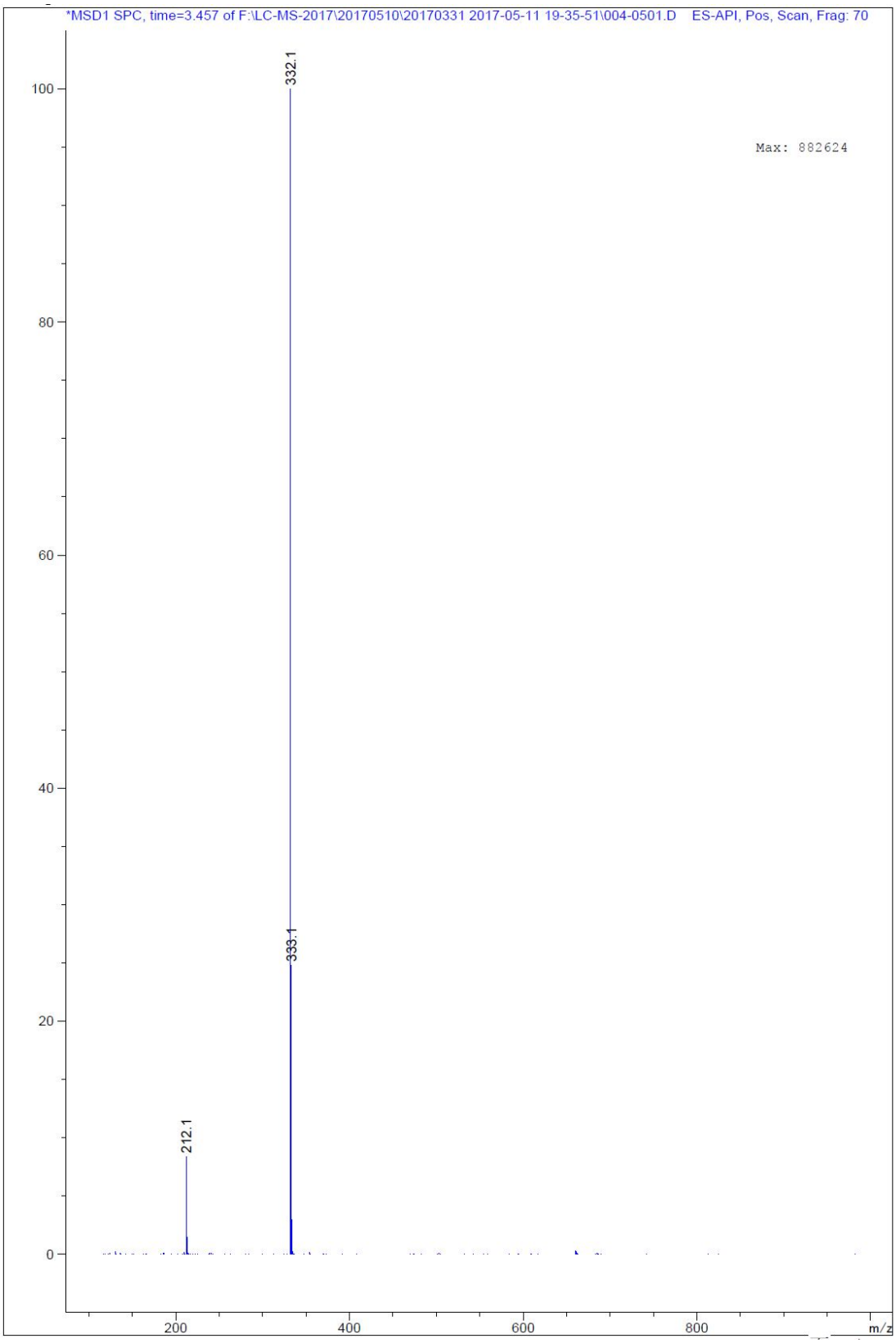
*MSD1 SPC, time=3.457 of F:\LC-MS-2017\20170510\20170331 2017-05-11 19-35-51\004-0501.D ES-API, Pos, Scan, Frag: 70
Max: 882624
332.1
333.1
212.1
100
80
60
40
20
0
200
400
600
800
m/z

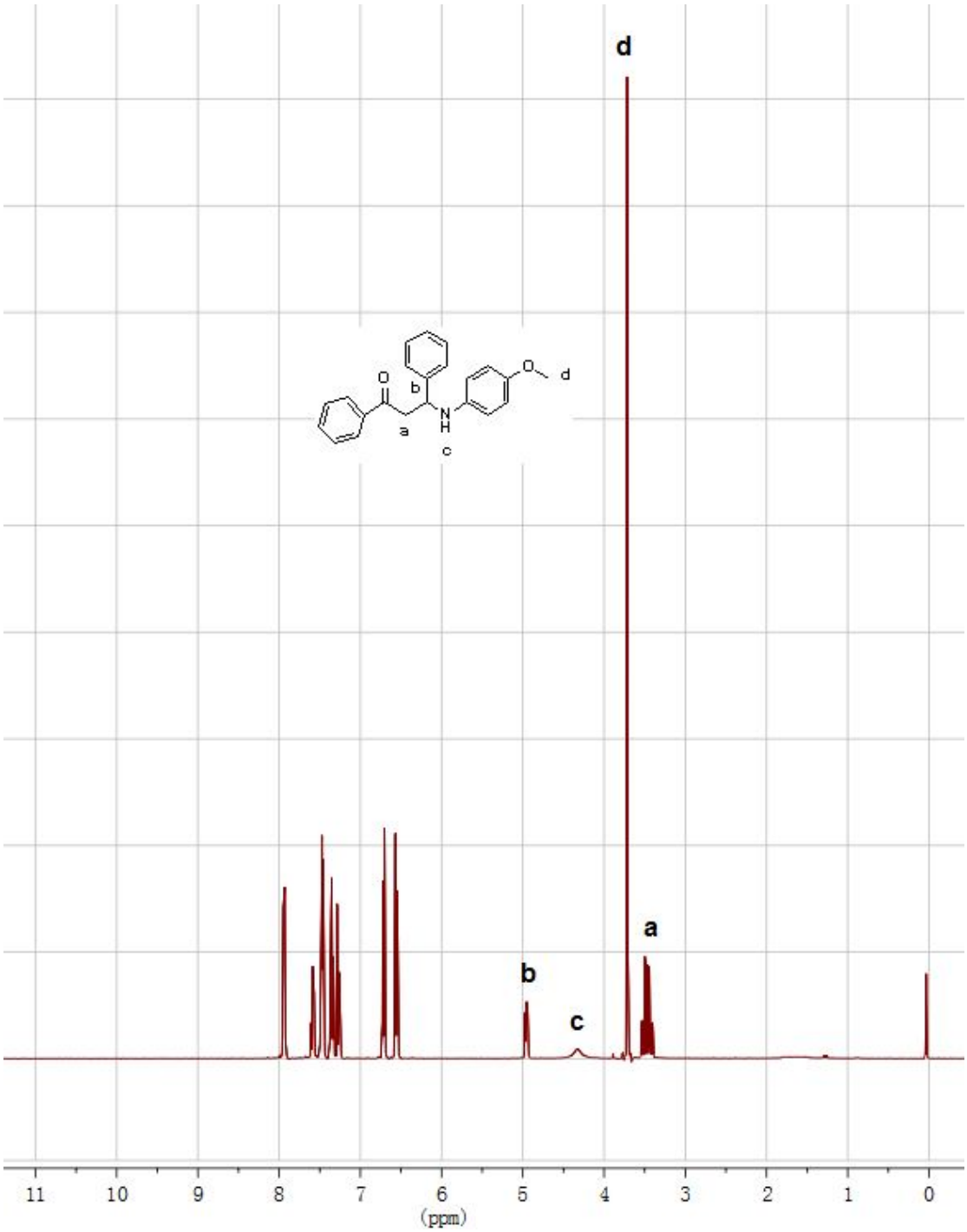
d
a
b
c
11
10
9
8
7
6
5
4
3
2
1
0
(ppm)

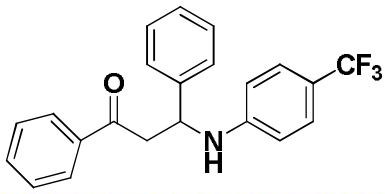

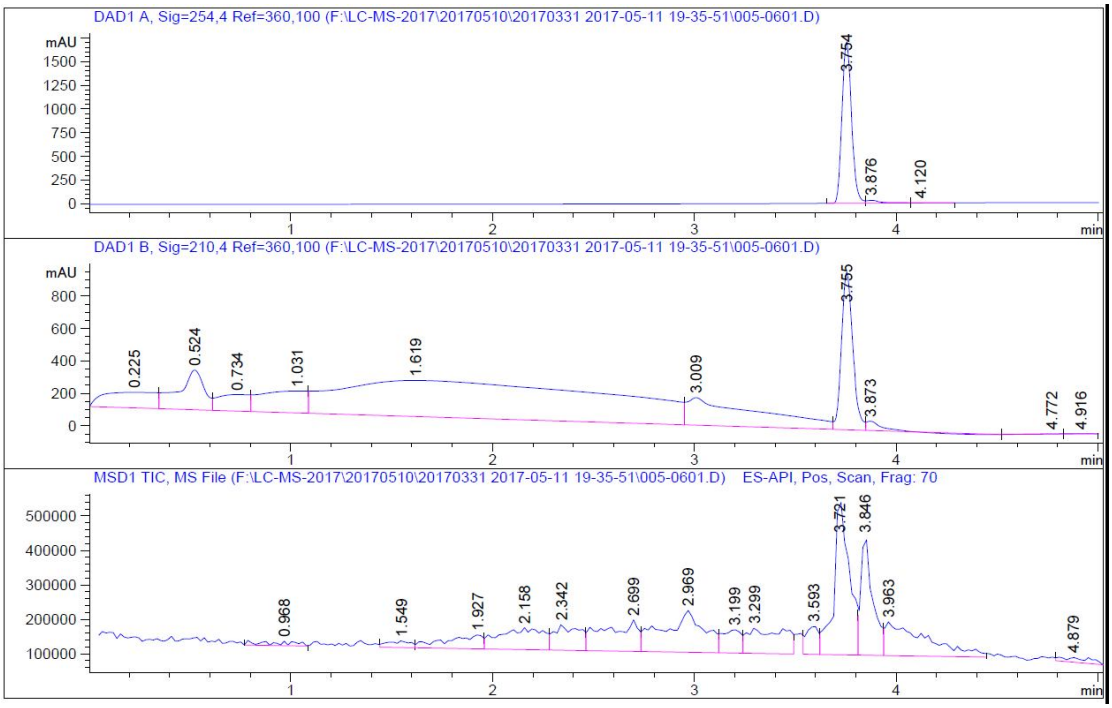

Signal 1: DAD1 A, Sig=254,4 Ref=360,100

#	Ret. [min]		Width [min]	Area [mAU*s]	Height [mAU]	Area %
1	3.754	VV	0.0502	5609.65039	1711.38232	96.9913
2	3.876	VV	0.0693	152.87480	31.14444	2.6432
3	4.120	VB	0.1216	21.13739	2.42801	0.3655

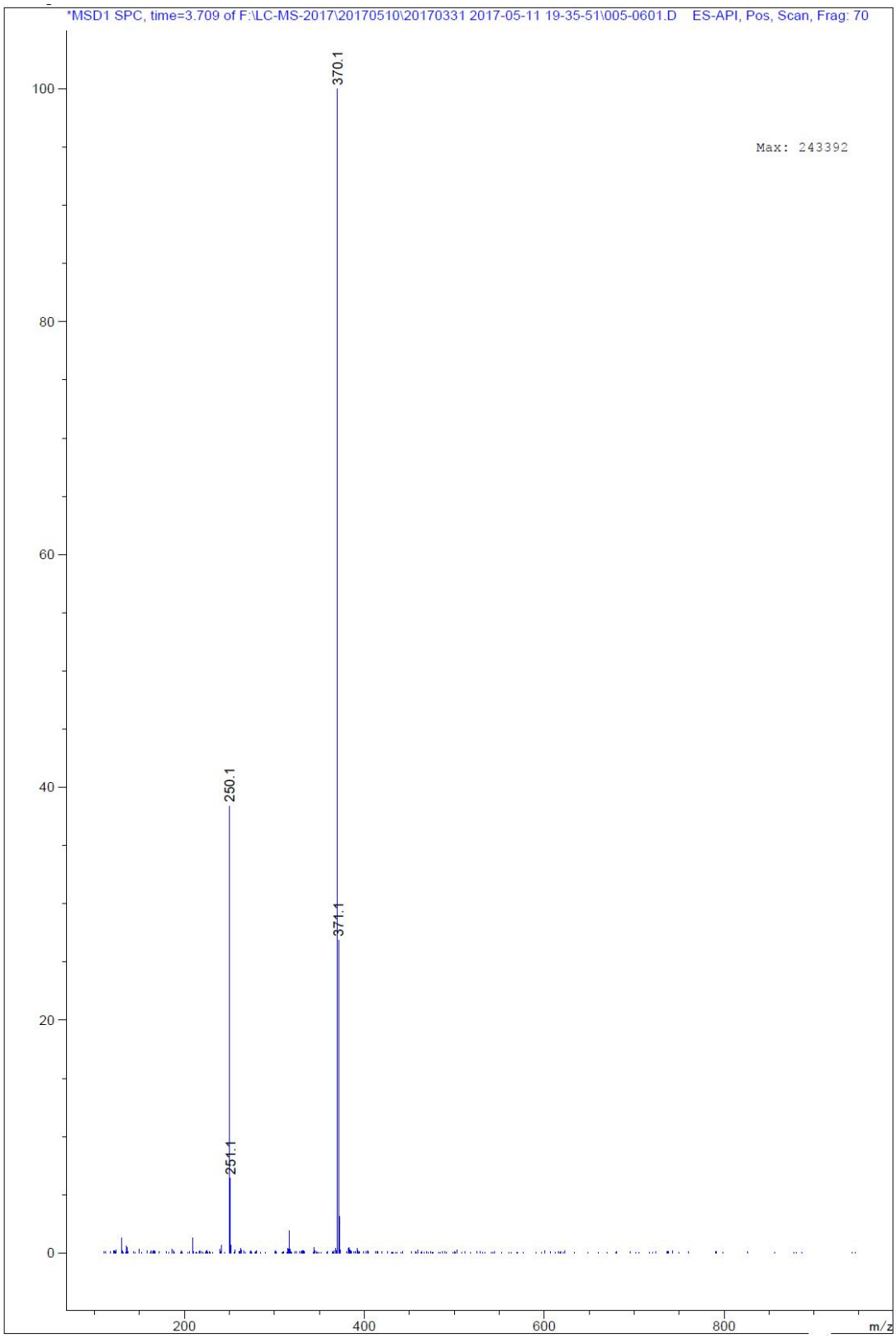
*MSD1 SPC, time=3.709 of F:\LC-MS-2017\20170510\20170331 2017-05-11 19-35-51\005-0601.D ES-API, Pos, Scan, Frag: 70
Max: 243392
370.1
371.1
250.1
251.1
100
80
60
40
20
0
200
400
600
800
m/z

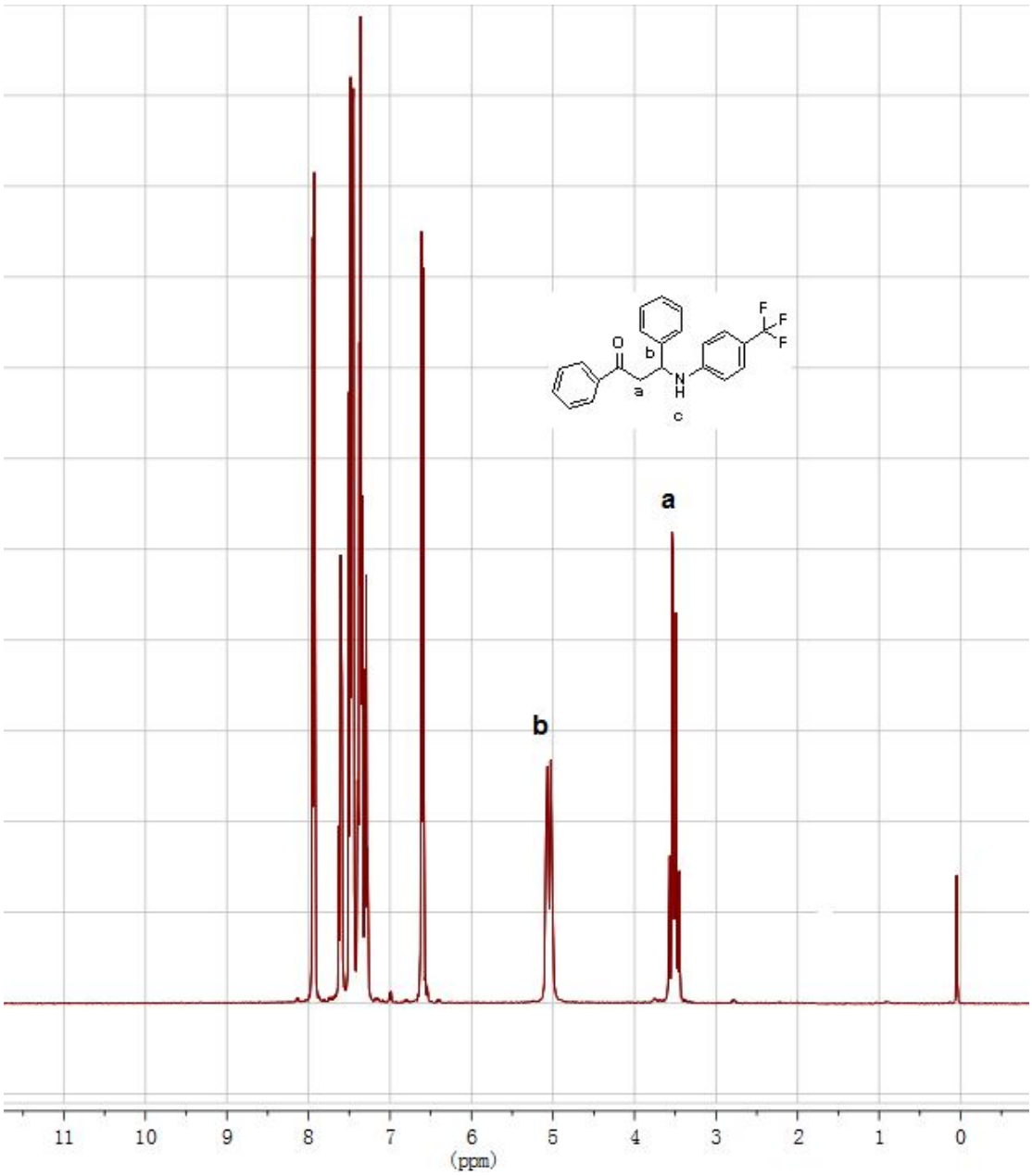
a
b
11
10
9
8
7
6
5
4
3
2
1
0
(ppm)

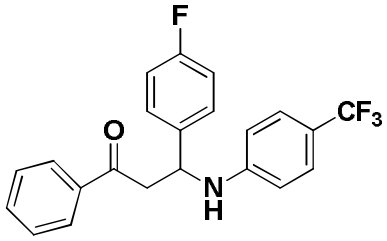

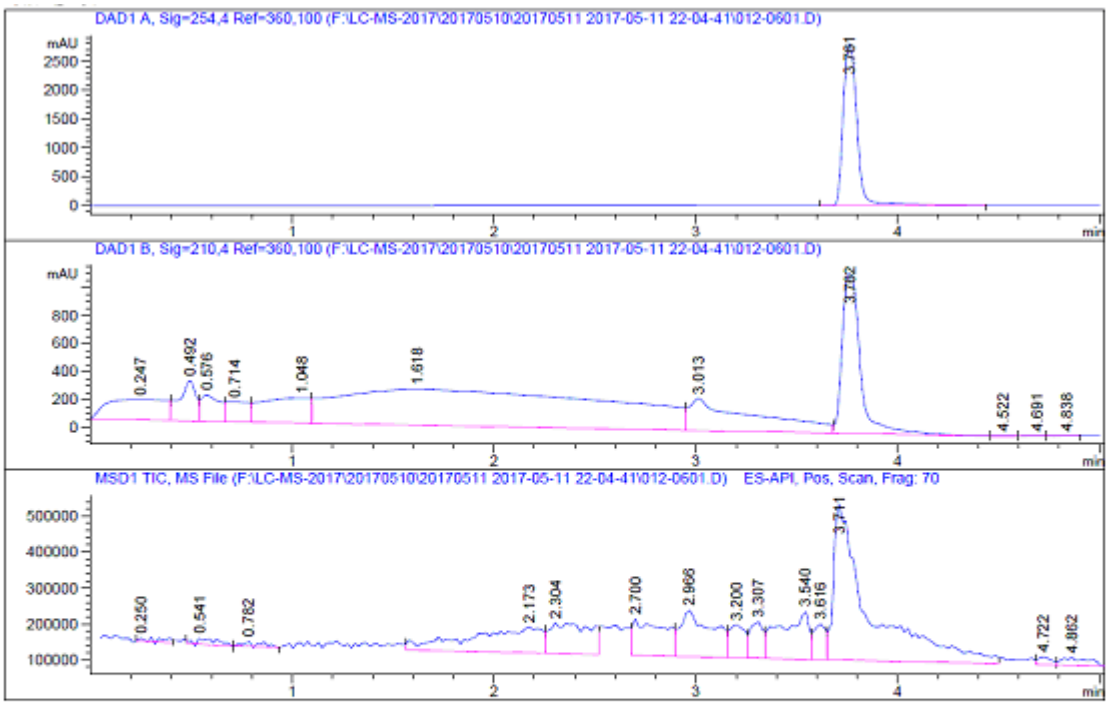

Signal 1: DAD1 A, Sig=254,4 Ref=360,100

#	Ret. [min]		Width [min]	Area [mAU*s]	Height [mAU]	Area %
1	3.761	VB	0.0771	1.32207e4	2799.46558	100.0000

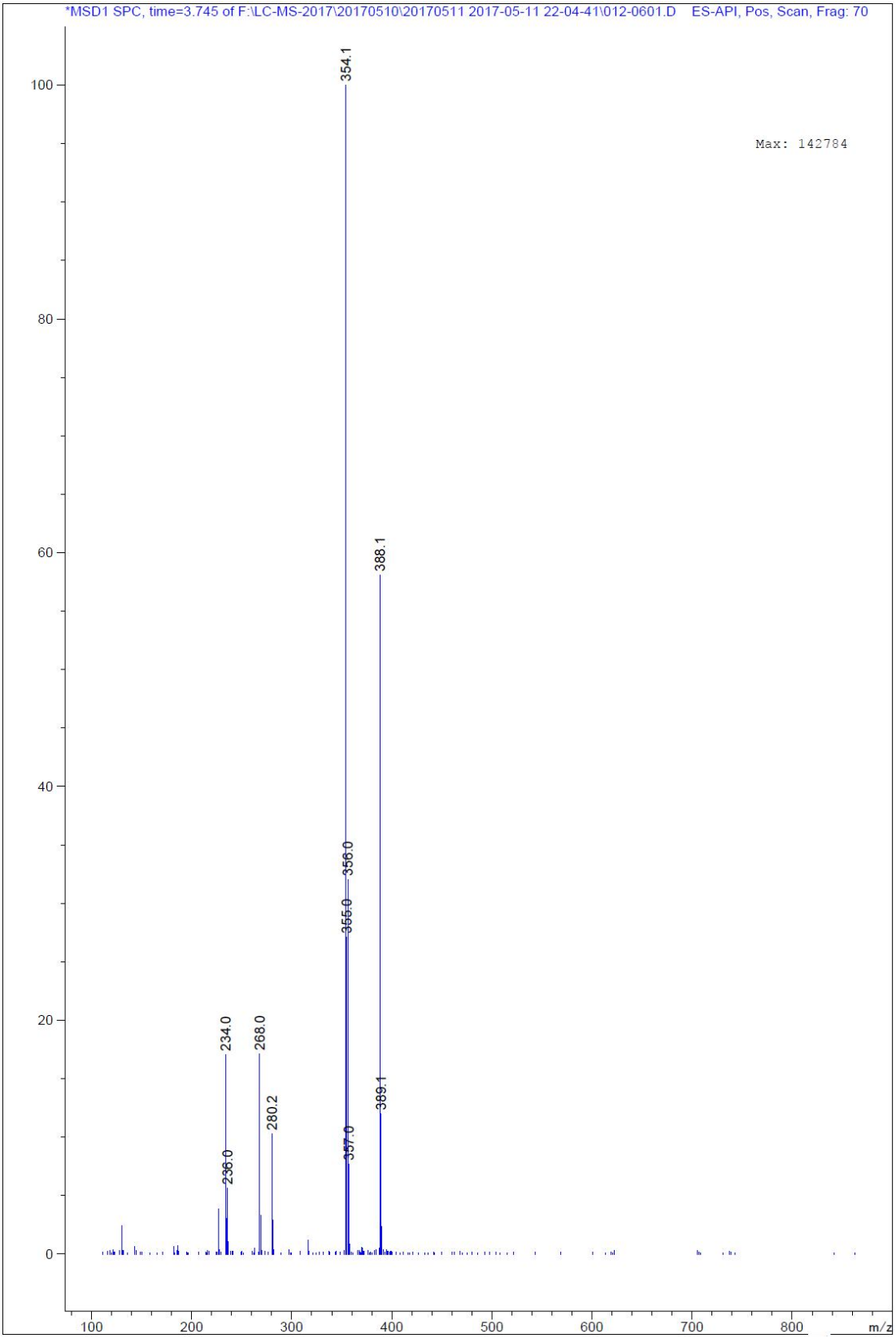
*MSD1 SPC, time=3.745 of F:\LC-MS-2017\20170510\20170511 2017-05-11 22-04-41\012-0601.D ES-API, Pos, Scan, Frag: 70
Max: 142784
354.1
388.1
356.0
355.0
234.0
268.0
280.2
389.1
357.0
236.0
100
80
60
40
20
0
100
200
300
400
500
600
700
800
m/z

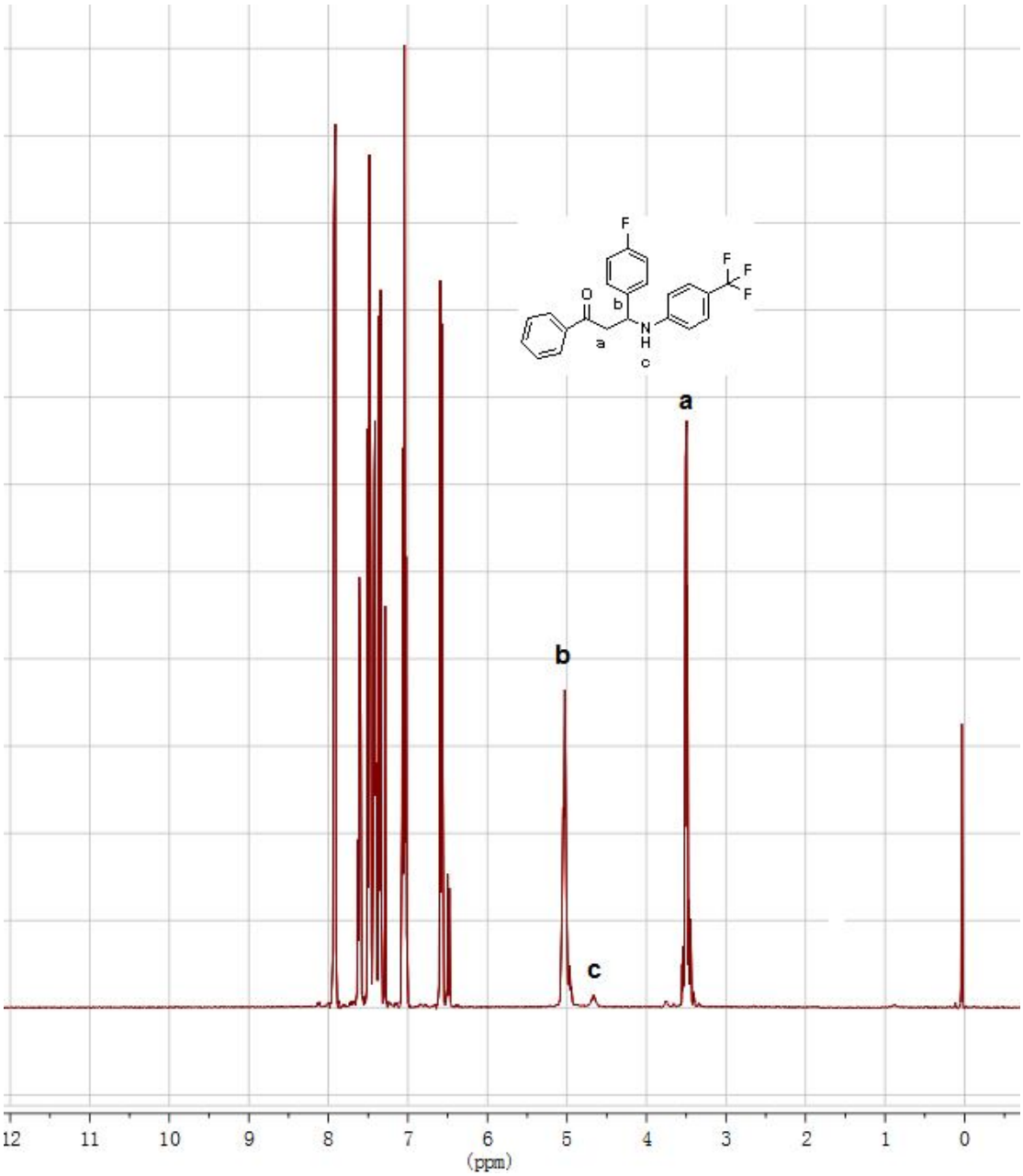
F
F
F
F
O
b
N
H
a
c
a
b
c
12
11
10
9
8
7
6
5
4
3
2
1
0
(ppm)

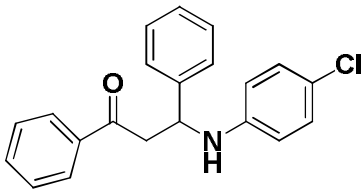

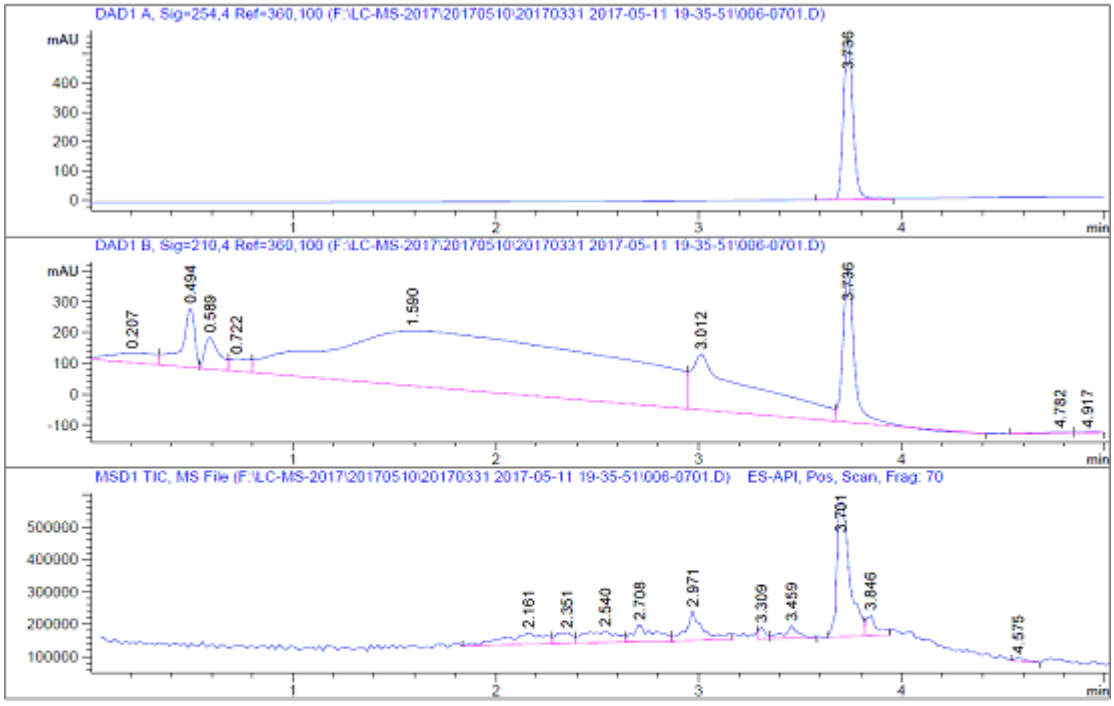

Signal 1: DAD1 A, Sig=254,4 Ref=360,100

#	Ret. [min]		Width [min]	Area [mAU*s]	Height [mAU]	Area %
1	3.736	VB	0.0504	1807.67908	549.19427	100.0000

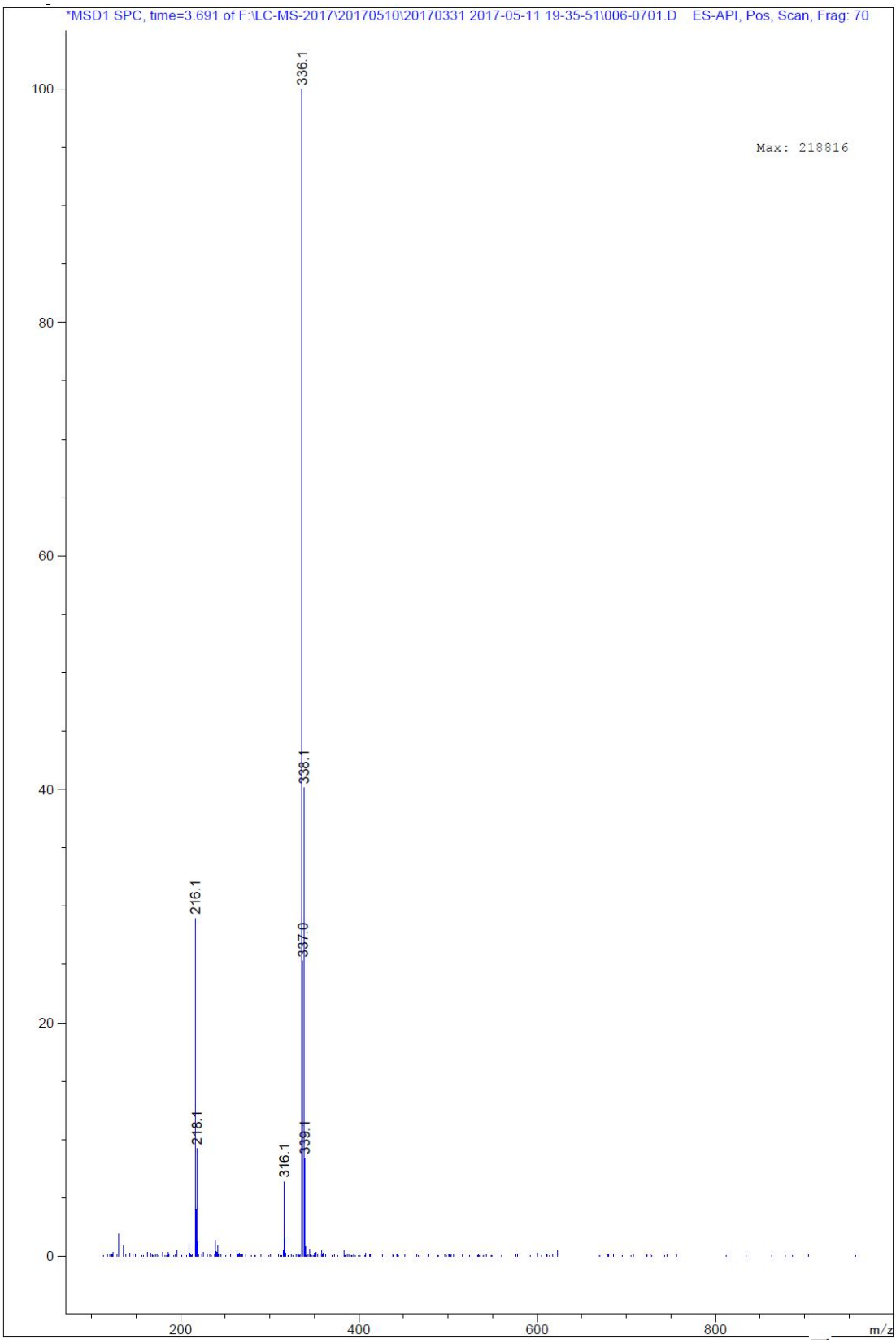
*MSD1 SPC, time=3.691 of F:\LC-MS-2017\20170510\20170331 2017-05-11 19-35-51\006-0701.D ES-API, Pos, Scan, Frag: 70
Max: 218816
336.1
338.1
337.0
339.1
216.1
218.1
316.1
100
80
60
40
20
0
200
400
600
800
m/z

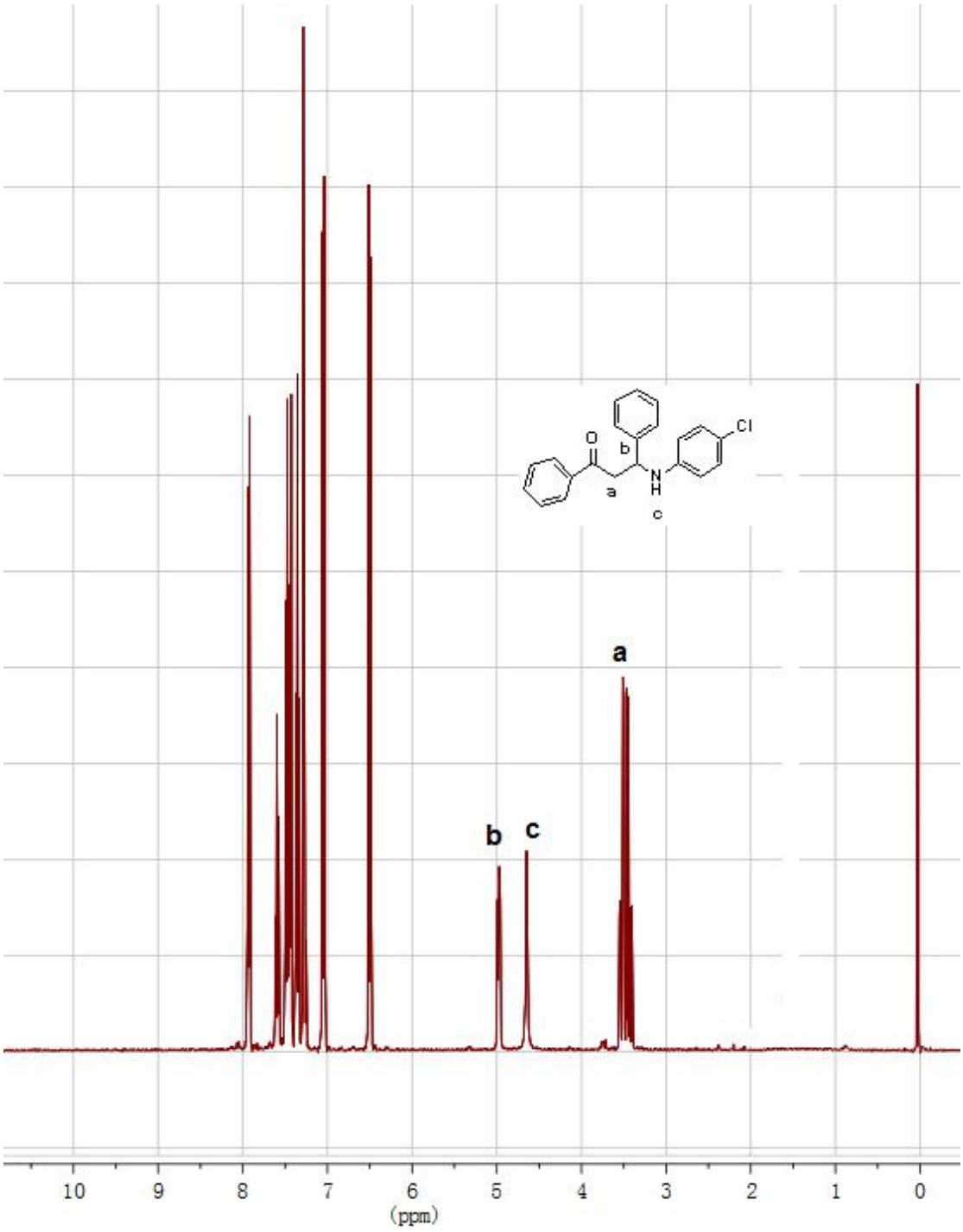
a
b
c
10
9
8
7
6
5
4
3
2
1
0
(ppm)

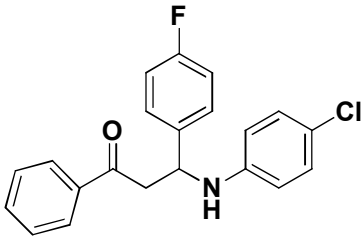

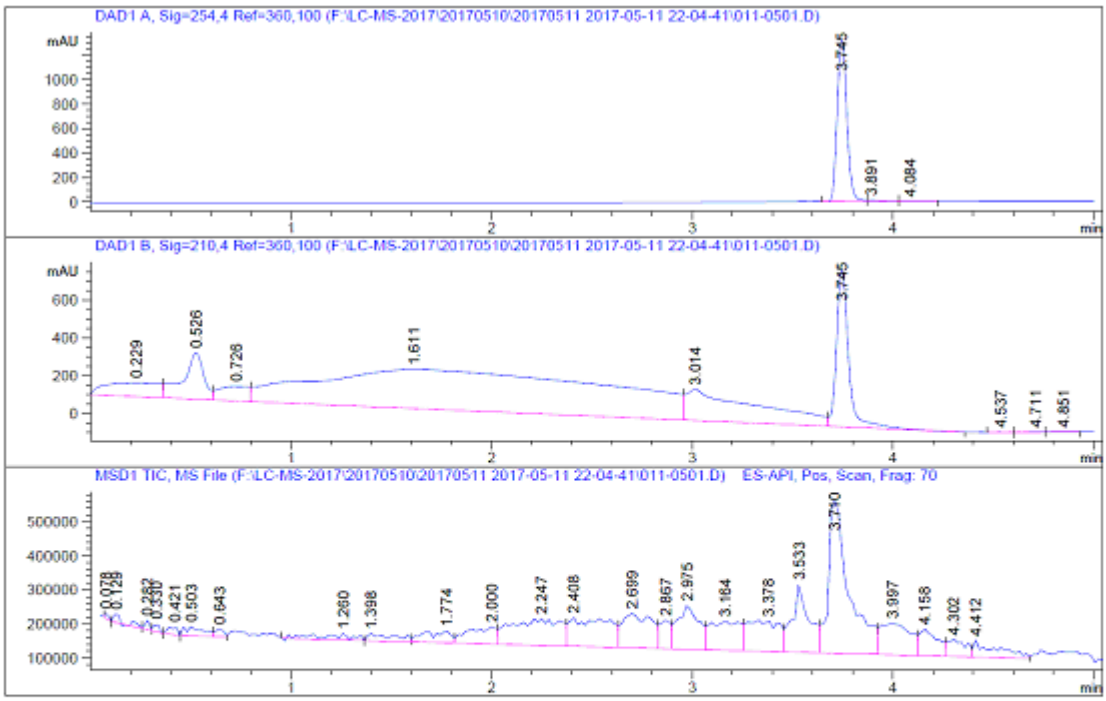

Signal 1: DAD1 A, Sig=254,4 Ref=360,100

#	Ret. [min]		Width [min]	Area [mAU*s]	Height [mAU]	Area %
1	3.745	VV	0.0508	4400.44434	1324.37939	98.4656
2	3.891	VV	0.0754	48.53432	8.65463	1.0860
3	4.084	VB	0.1201	20.03745	2.24639	0.4484

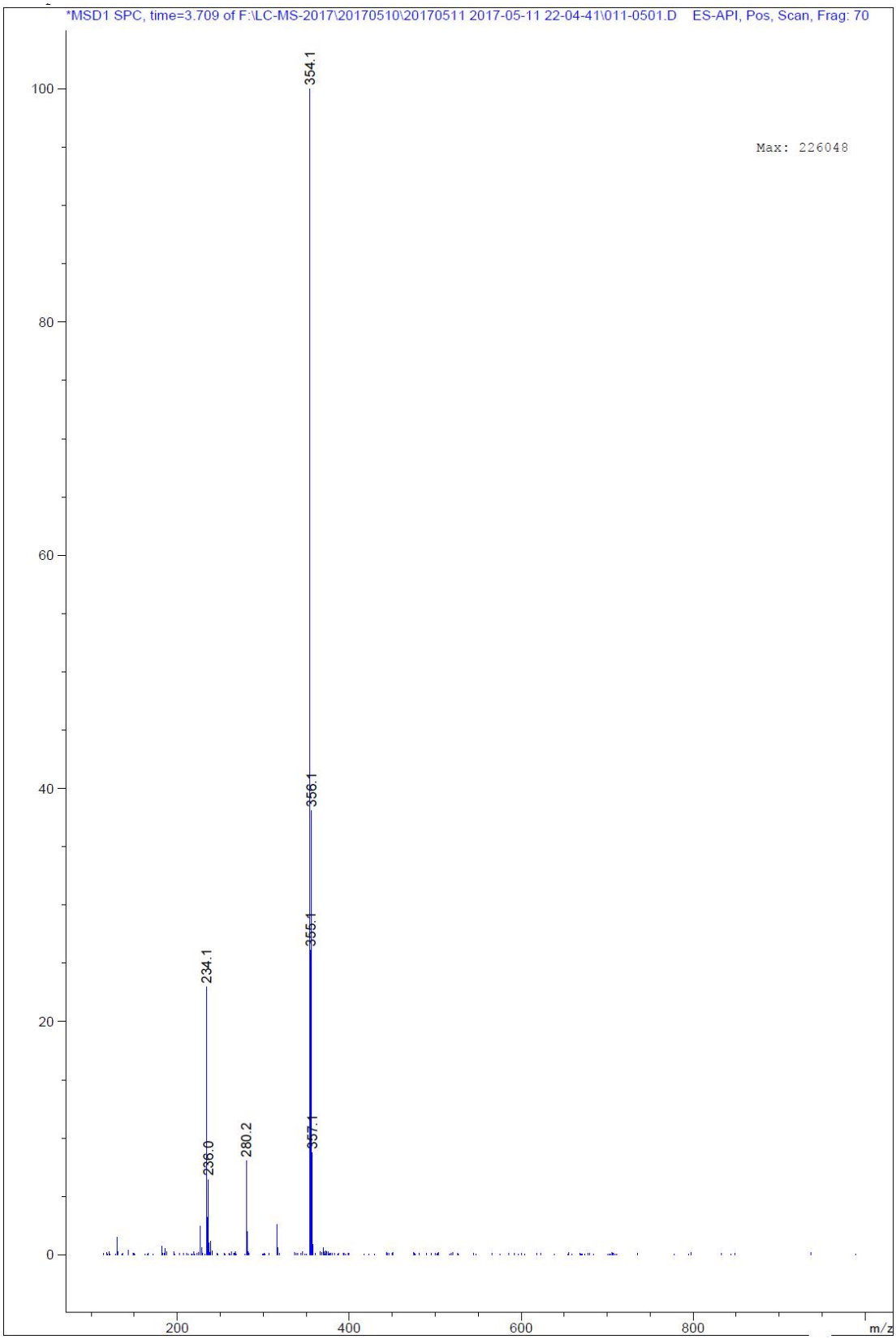
*MSD1 SPC, time=3.709 of F:\LC-MS-2017\20170510\20170511 2017-05-11 22-04-41\011-0501.D ES-API, Pos, Scan, Frag: 70
Max: 226048
354.1
356.1
355.1
357.1
234.1
236.0
280.2
100
80
60
40
20
0
200
400
600
800
m/z

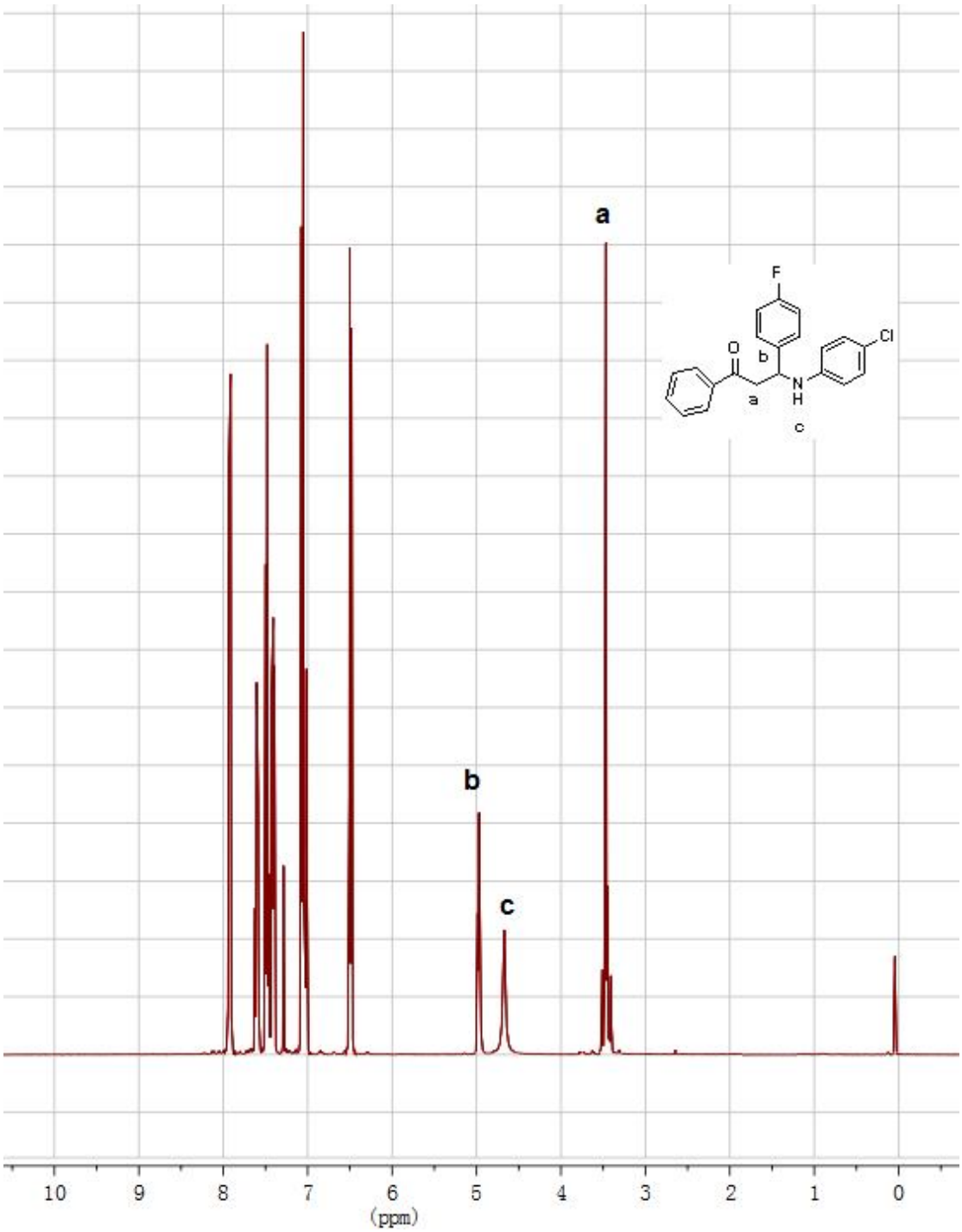
a
b
c
F
Cl
O
b
a
N
H
c
10
9
8
7
6
5
4
3
2
1
0
(ppm)

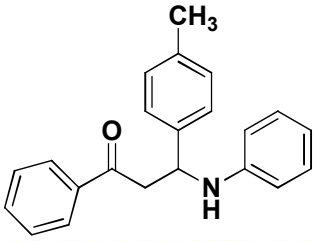

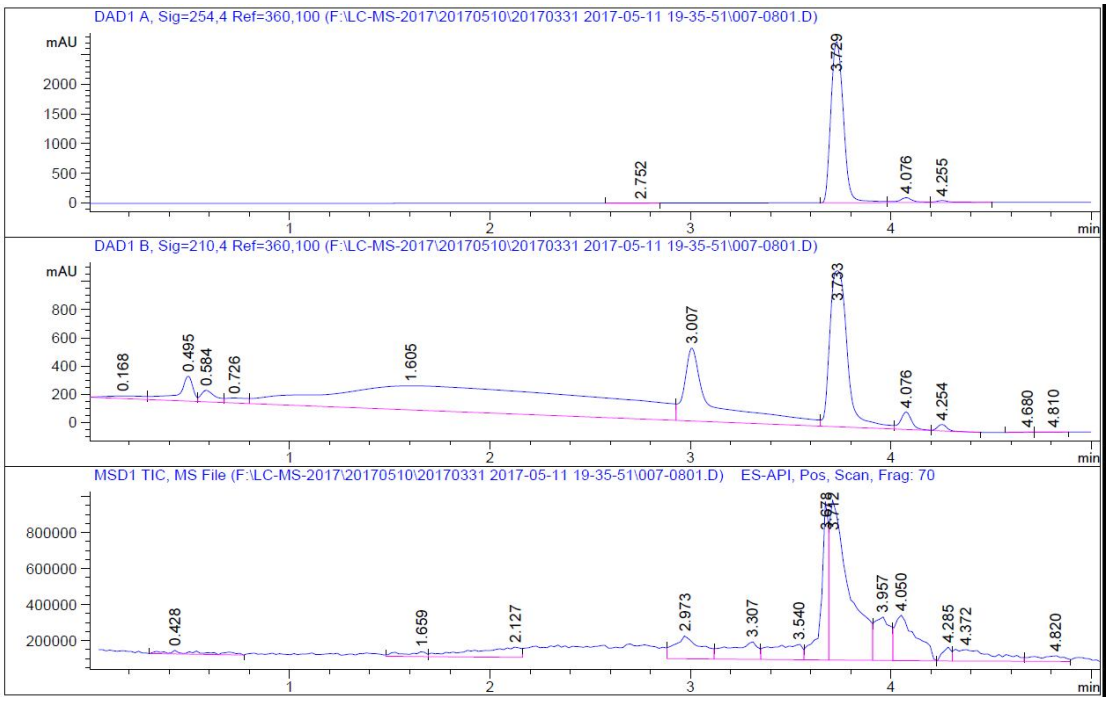

Signal 1: DAD1 A, Sig=254,4 Ref=360,100

#	Ret. [min]		Width [min]	Area [mAU*s]	Height [mAU]	Area %
1	2.752	BV	0.0715	7.97230	1.67573	0.0647
2	3.729	VV	0.0685	1.17573e4	2717.94751	96.6258
3	4.076	VV	0.0708	399.20911	81.97607	2.2401

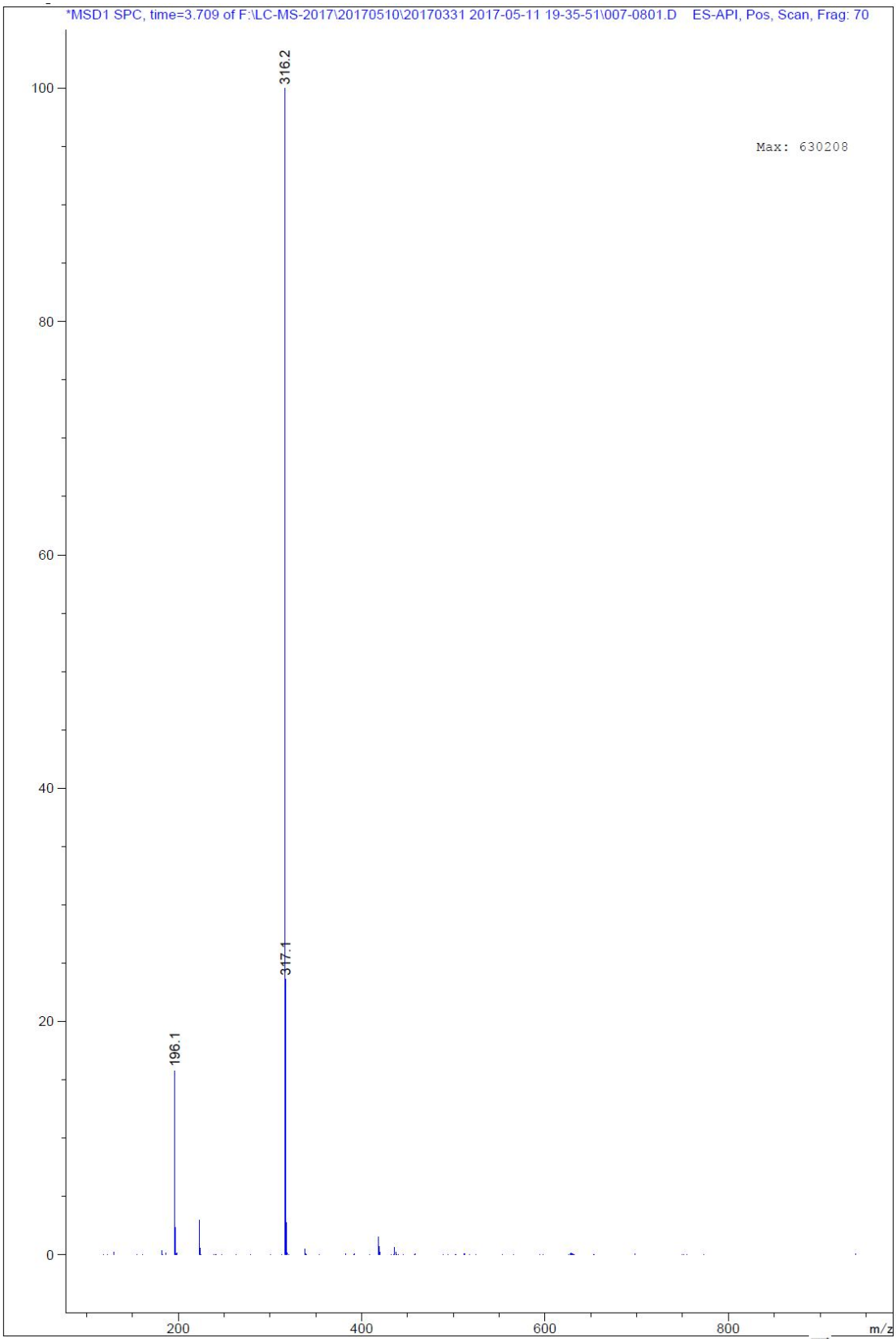
*MSD1 SPC, time=3.709 of F:\LC-MS-2017\20170510\20170331 2017-05-11 19-35-51\007-0801.D ES-API, Pos, Scan, Frag: 70
Max: 630208
316.2
317.1
196.1
100
80
60
40
20
0
200
400
600
800
m/z

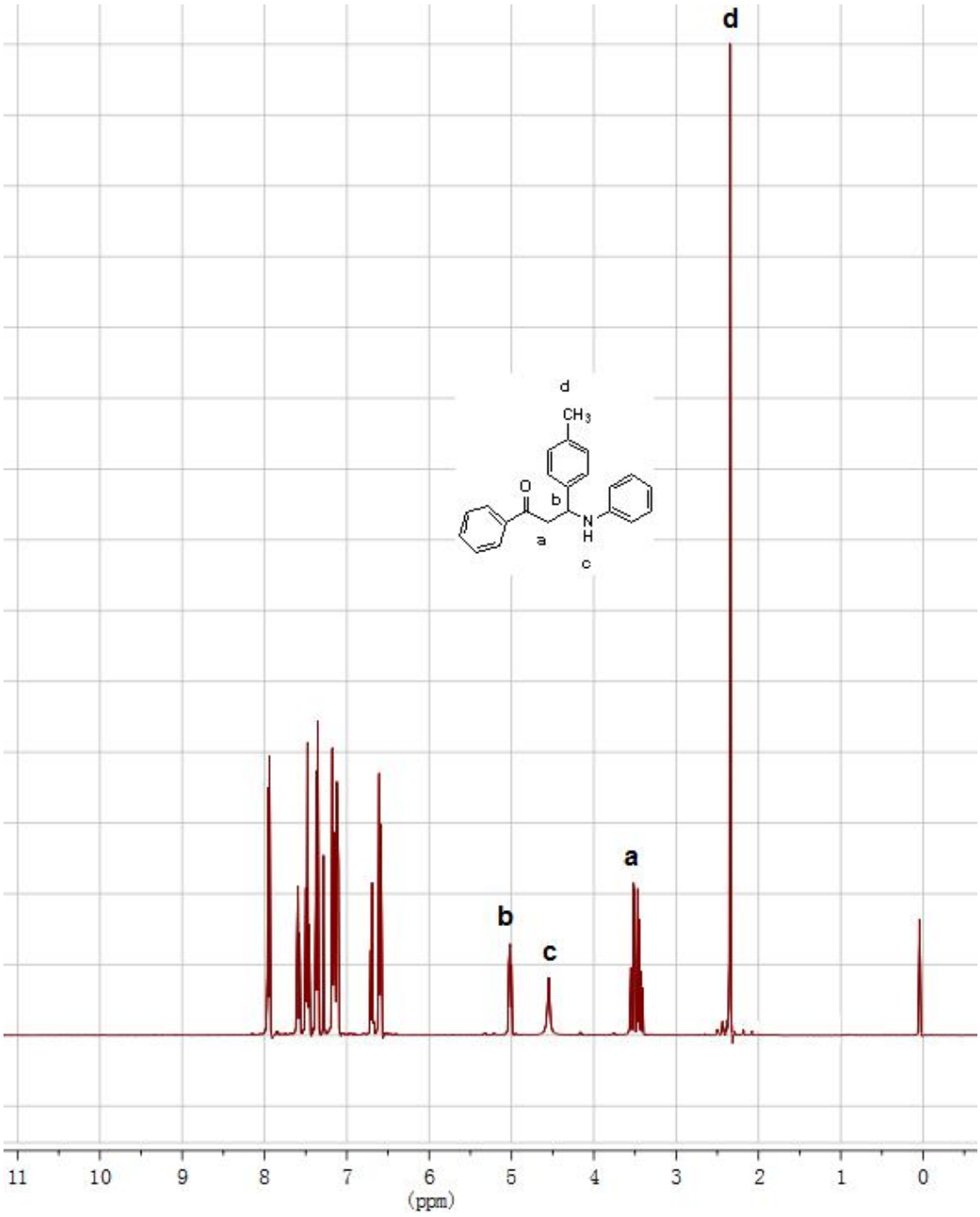
d
CH3
O
b
N
H
a
c
d
a
b
c
11
10
9
8
7
6
5
4
3
2
1
0
(ppm)

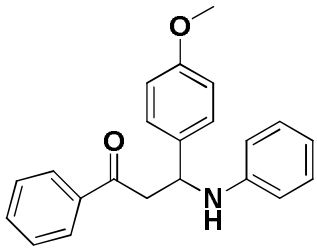

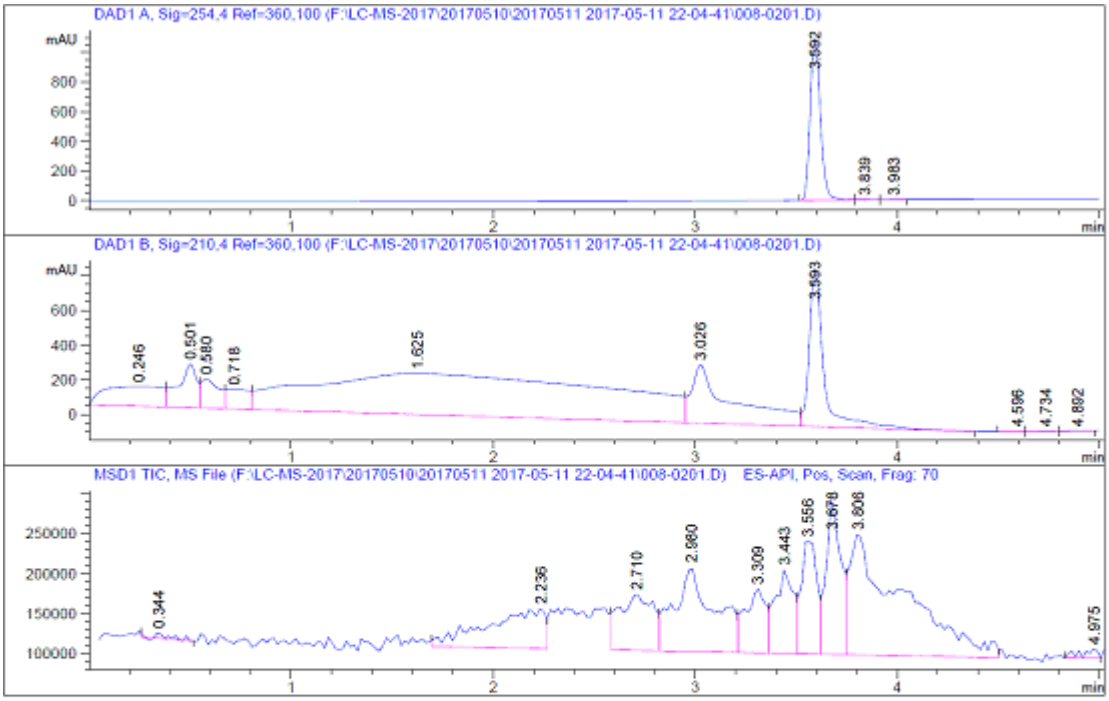

Signal 1: DAD1 A, Sig=254,4 Ref=360,100

#	Ret. [min]		Width [min]	Area [mAU*s]	Height [mAU]	Area %
1	3.592	VV	0.0551	3858.55542	1096.24524	98.9342
2	3.839	VV	0.0734	23.46119	4.60474	0.6015
3	3.983	VV	0.0704	18.10696	3.61616	0.4643

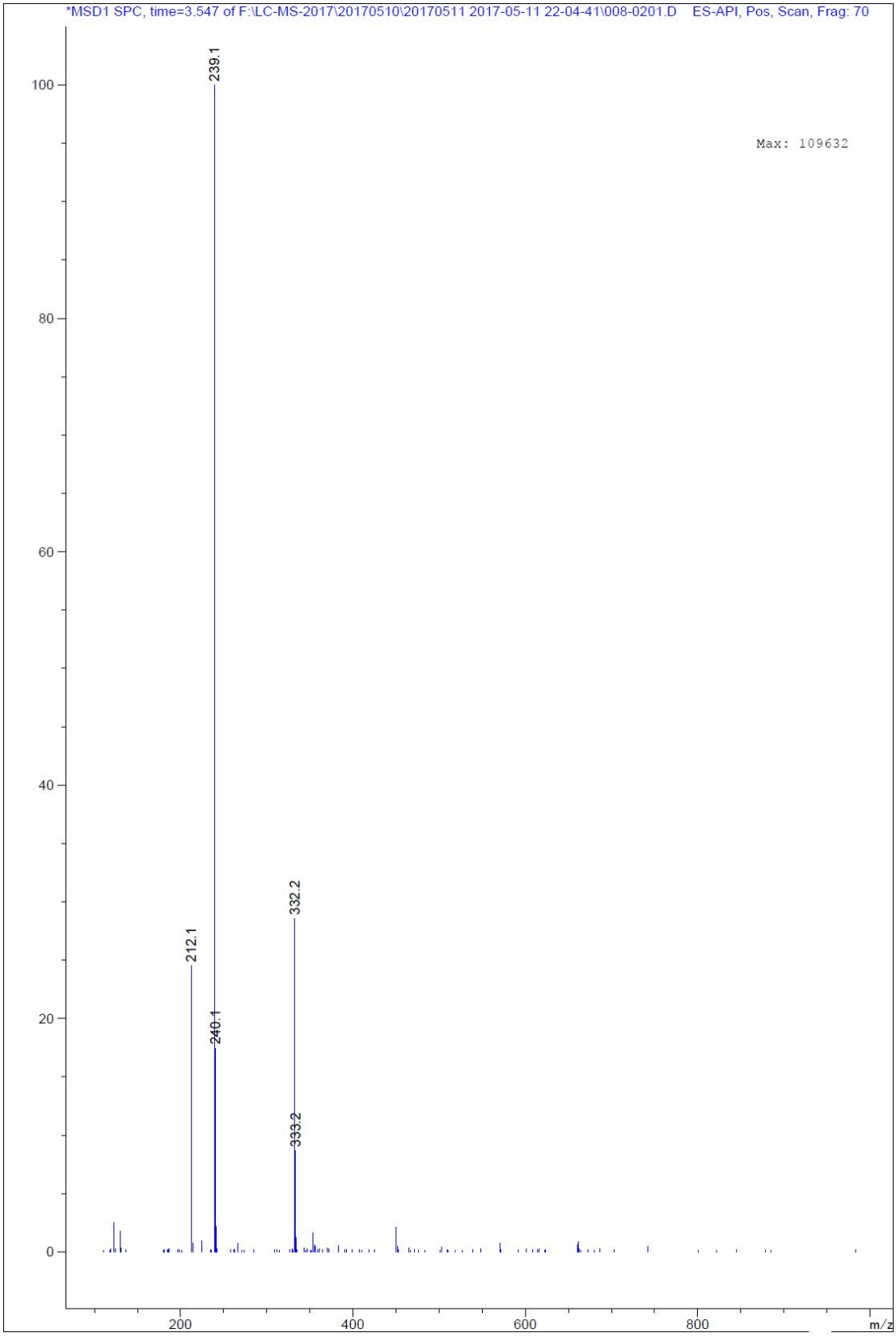
*MSD1 SPC, time=3.547 of F:\LC-MS-2017\20170510\20170511 2017-05-11 22-04-41\008-0201.D ES-API, Pos, Scan, Frag: 70
Max: 109632
239.1
212.1
240.1
332.2
333.2
100
80
60
40
20
0
200
400
600
800
m/z

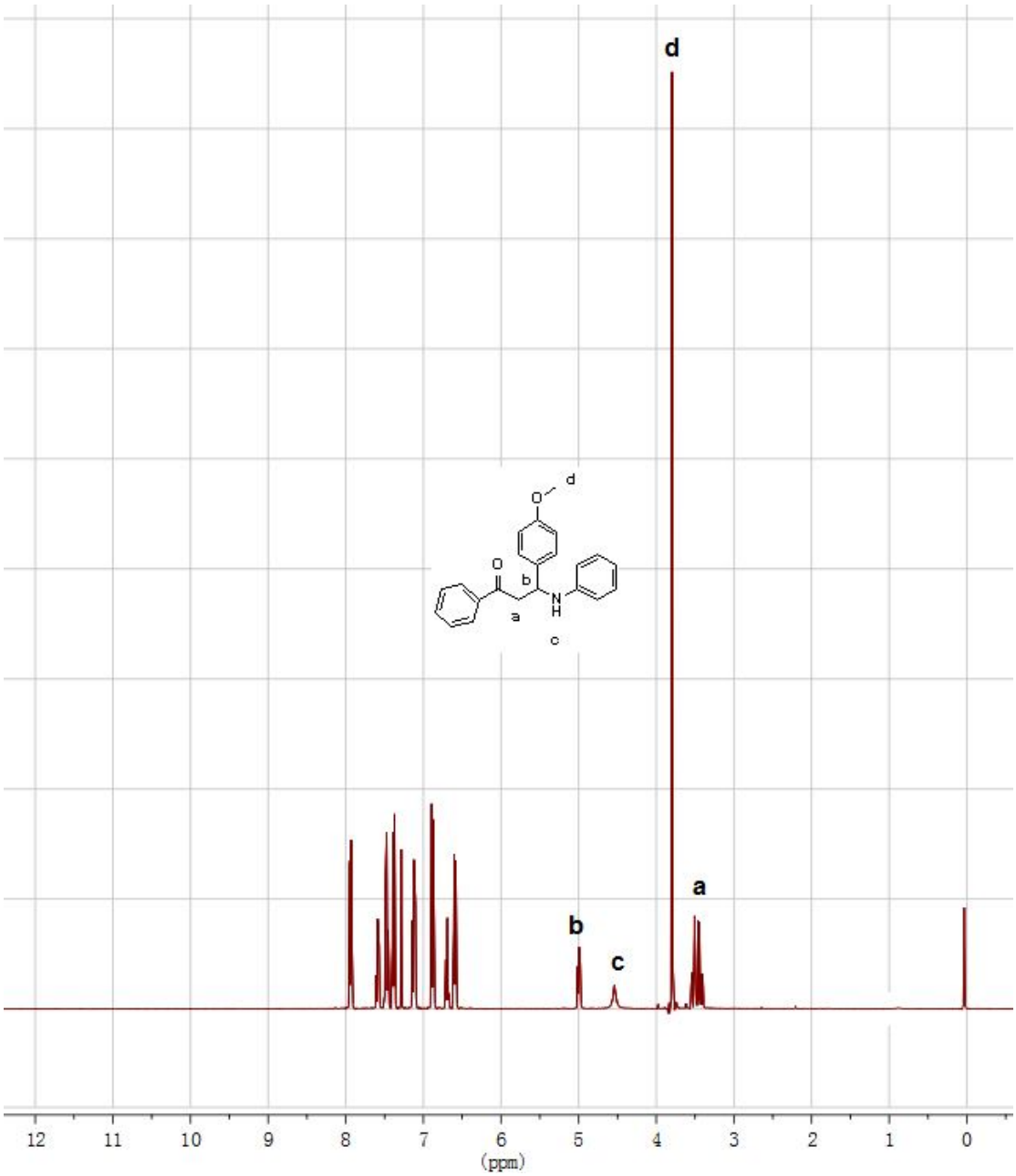
d
a
b
c
12
11
10
9
8
7
6
5
4
3
2
1
0
(ppm)

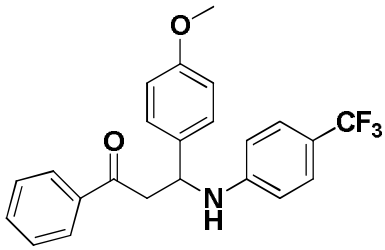

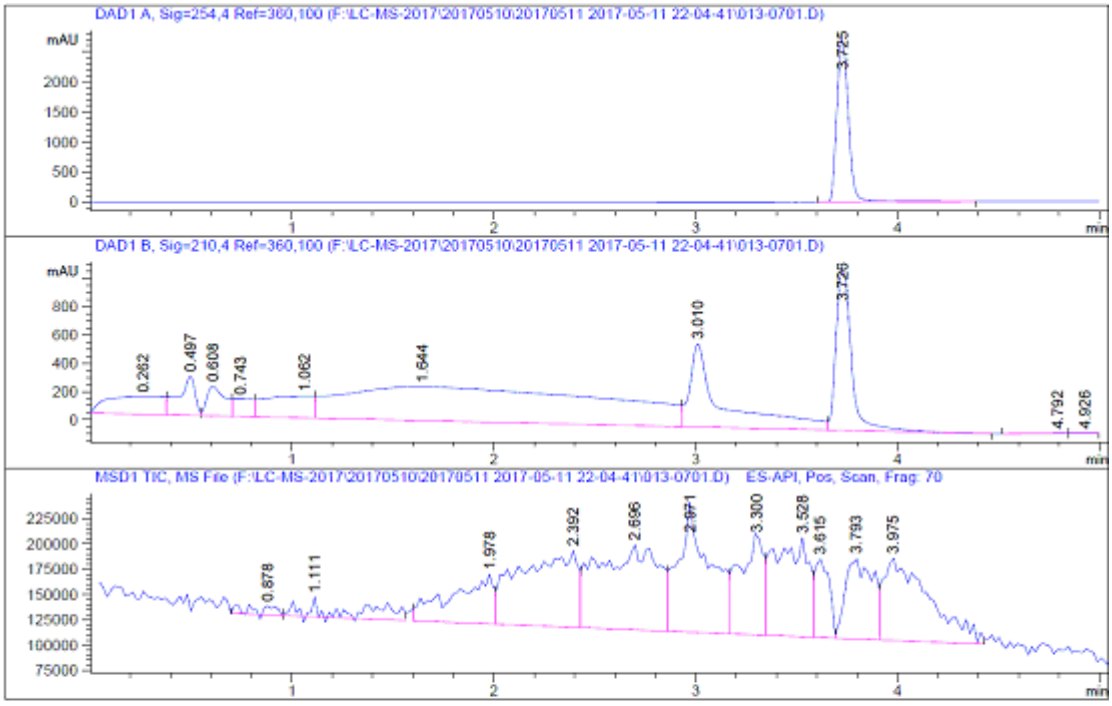

Signal 1: DAD1 A, Sig=254,4 Ref=360,100

#	Ret. [min]		Width [min]	Area [mAU*s]	Height [mAU]	Area %
1	3.725	VB	0.0647	1.08128e4	2703.03125	100.0000

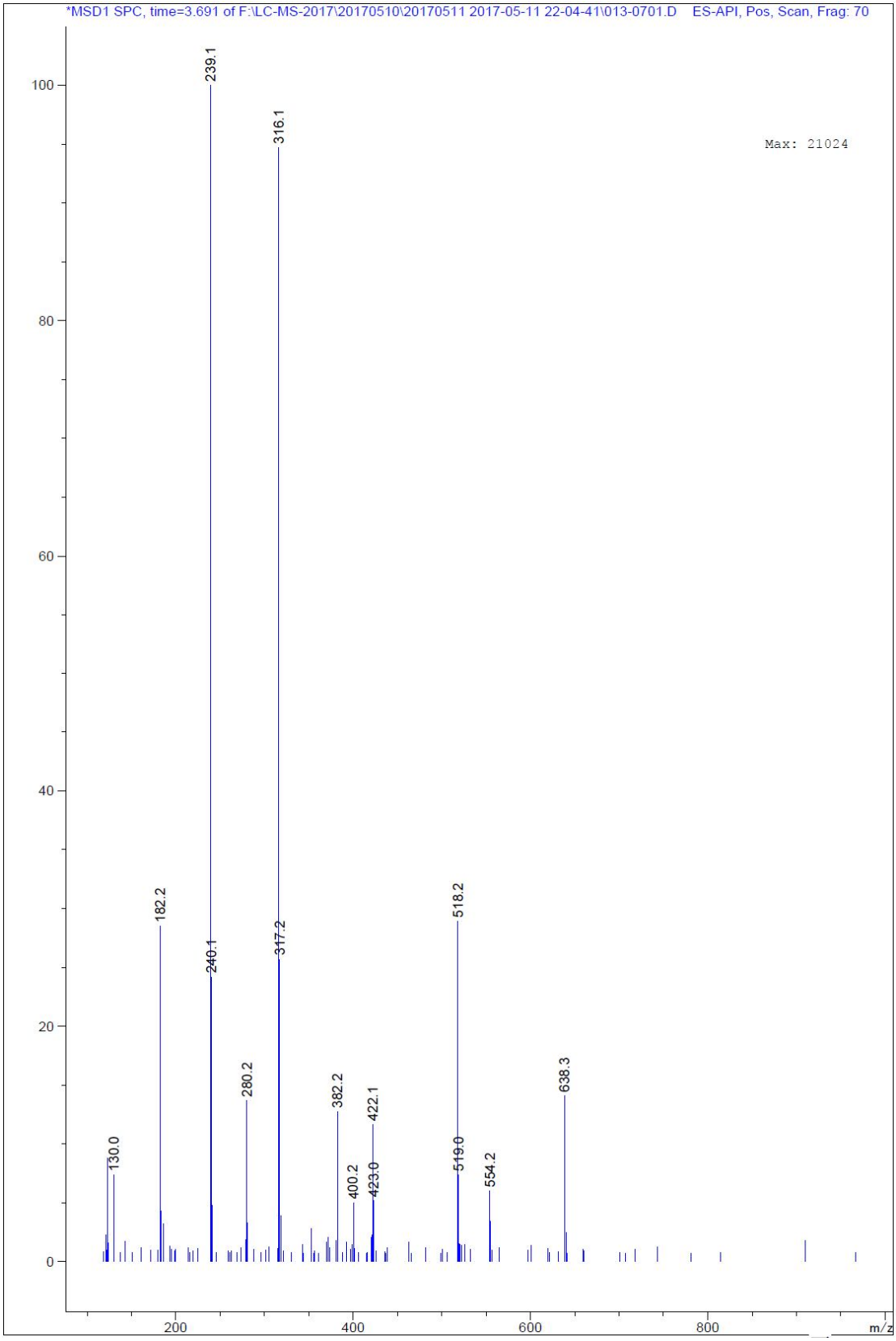
*MSD1 SPC, time=3.691 of F:\LC-MS-2017\20170510\20170511 2017-05-11 22-04-41\013-0701.D ES-API, Pos, Scan, Frag: 70
Max: 21024
239.1
316.1
182.2
240.1
317.2
518.2
280.2
382.2
422.1
638.3
130.0
400.2
423.0
519.0
554.2
100
80
60
40
20
0
200
400
600
800
m/z

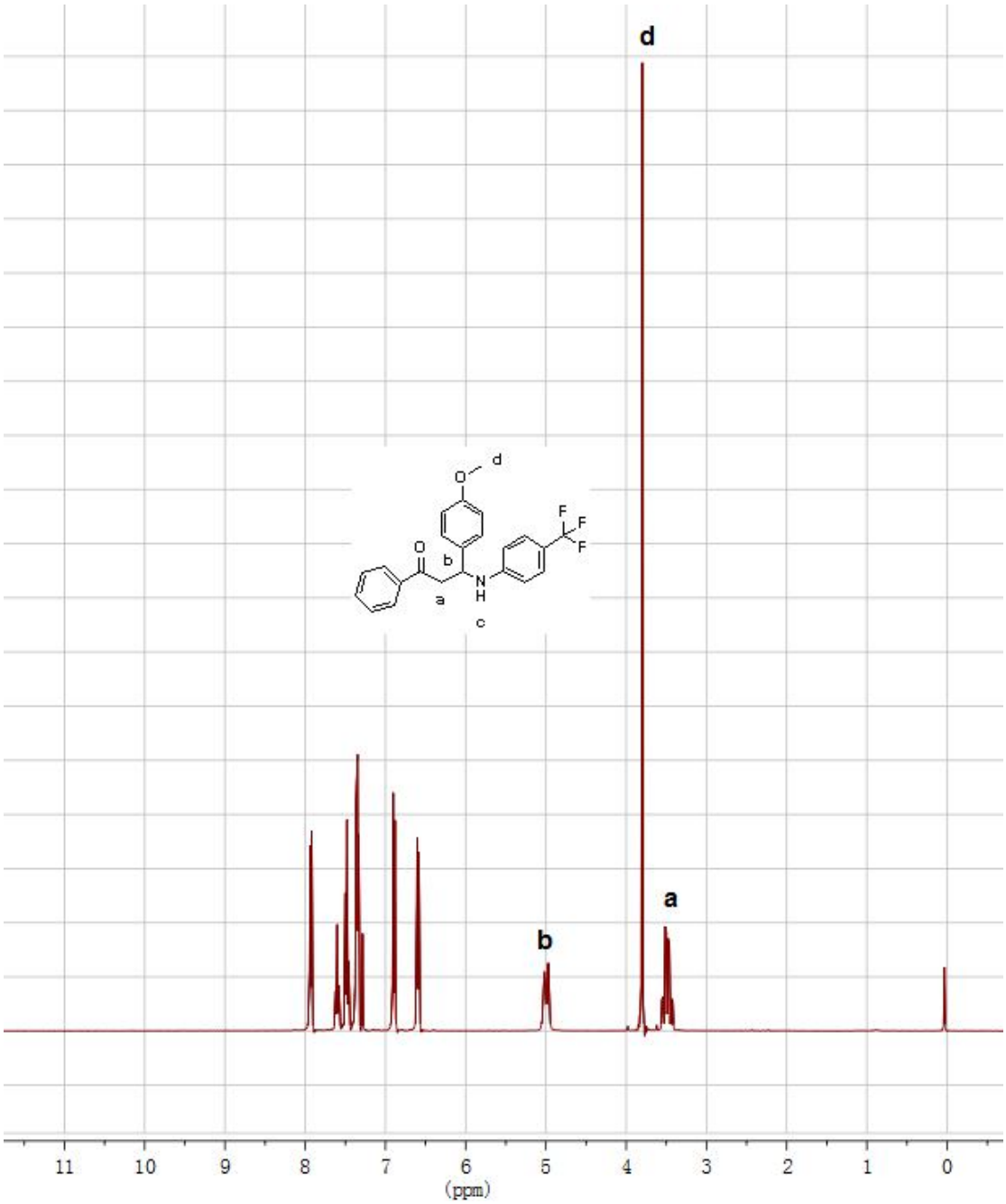
d
a
b
11
10
9
8
7
6
5
4
3
2
1
0
(ppm)

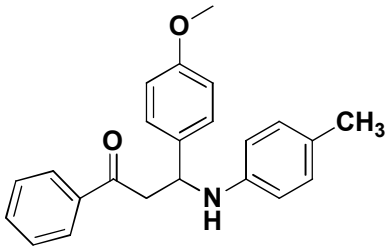

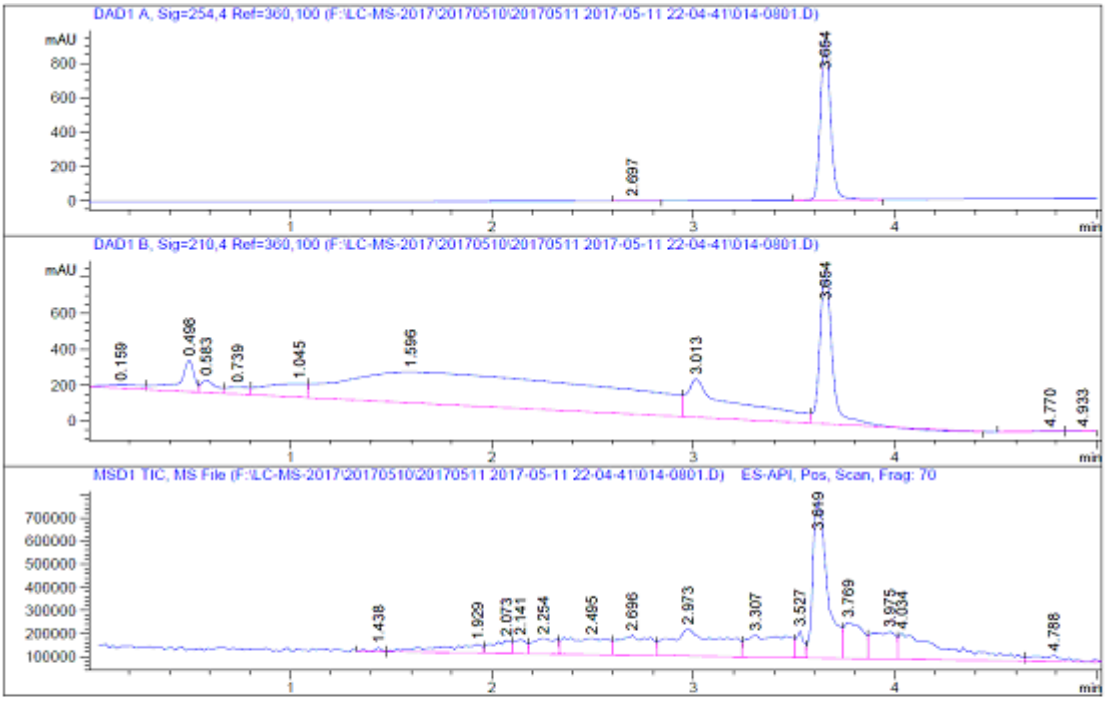

Signal 1: DAD1 A, Sig=254,4 Ref=360,100

#	Ret. [min]		Width [min]	Area [mAU*s]	Height [mAU]	Area %
1	2.697	BB	0.0852	7.53898	1.27161	0.2285
2	3.654	VB	0.0549	3291.33105	939.30597	99.7715

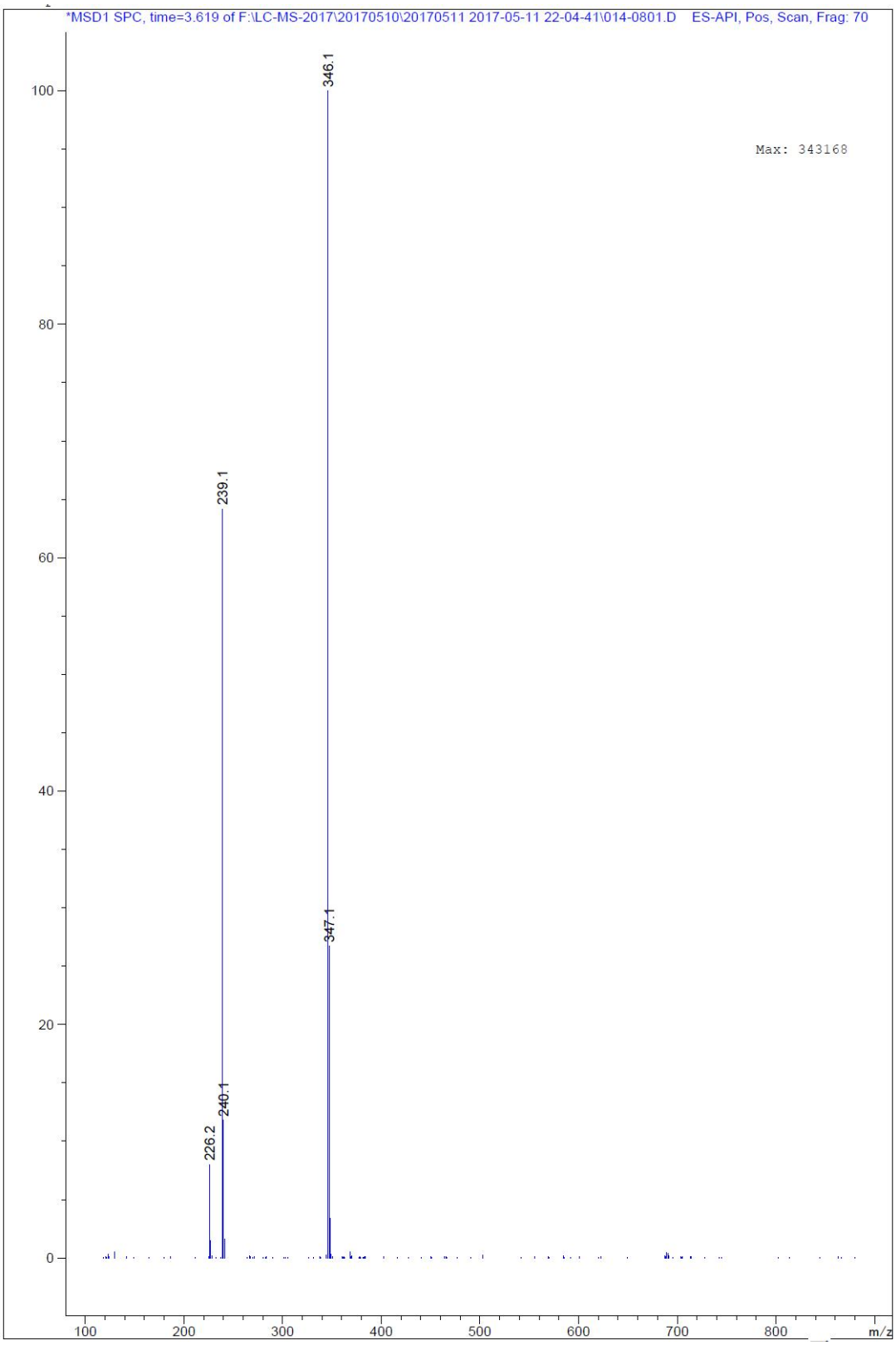
*MSD1 SPC, time=3.619 of F:\LC-MS-2017\20170510\20170511 2017-05-11 22-04-41\014-0801.D ES-API, Pos, Scan, Frag: 70
Max: 343168
346.1
239.1
347.1
240.1
226.2
100
80
60
40
20
0
100
200
300
400
500
600
700
800
m/z

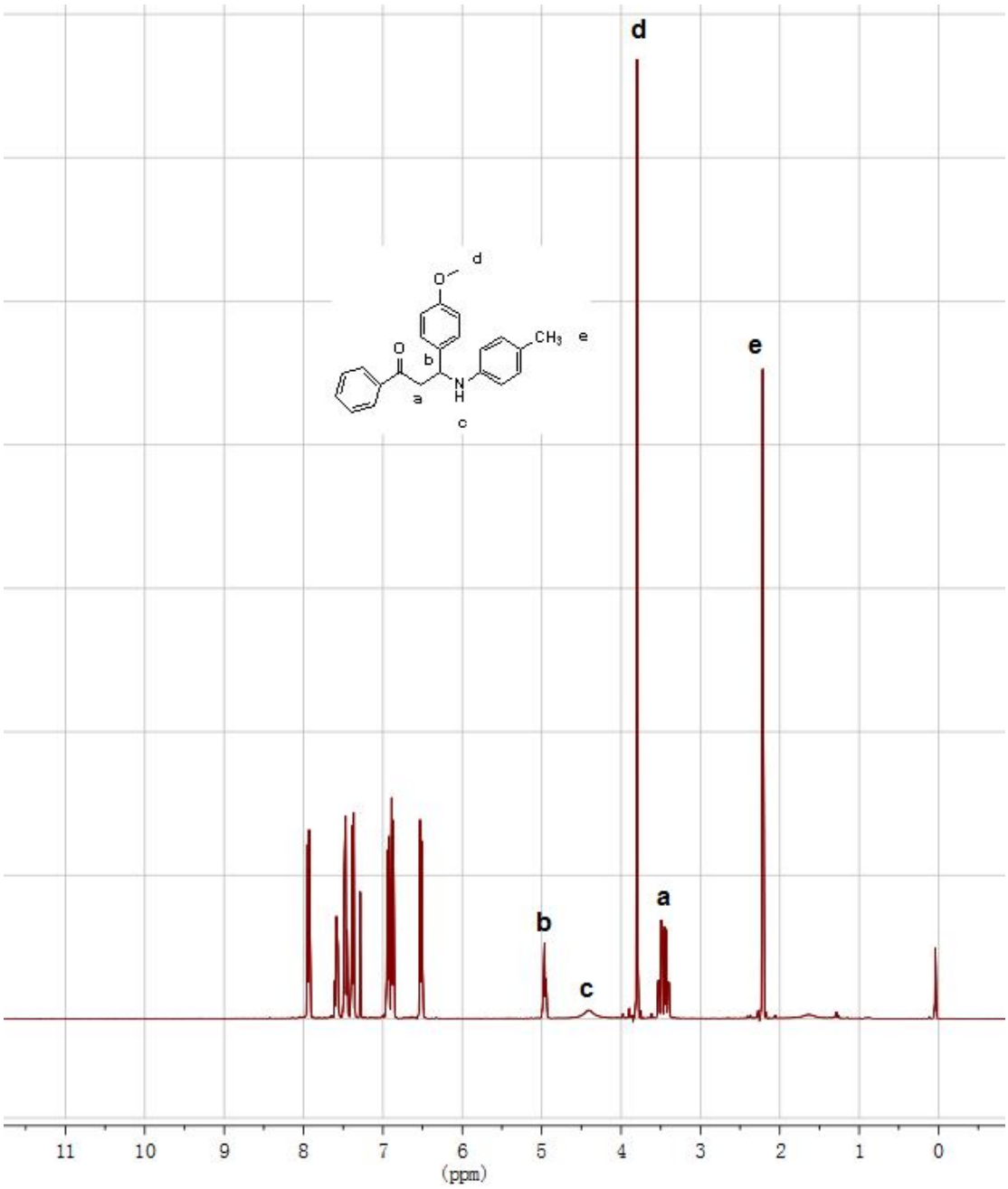
d
e
a
b
c
11
10
9
8
7
6
5
4
3
2
1
0
(ppm)

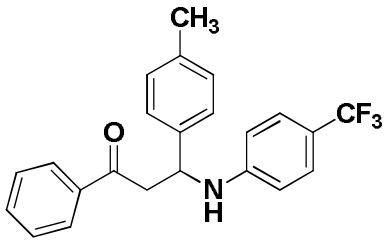

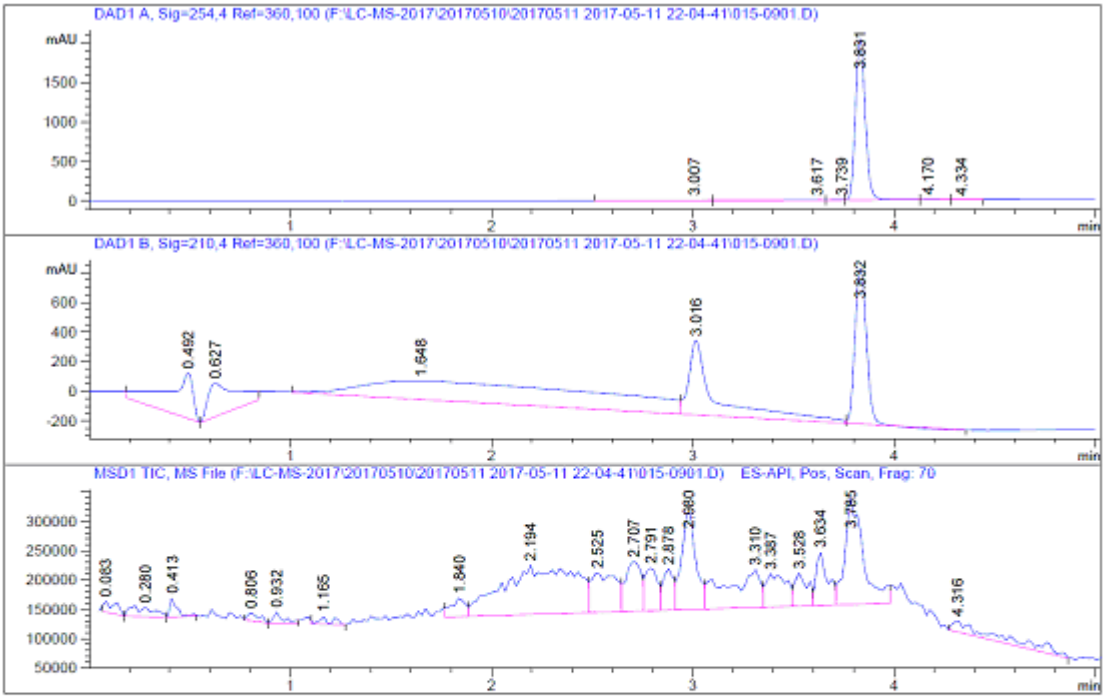

Signal 1: DAD1 A, Sig=254,4 Ref=360,100

#	Ret. [min]		Width [min]	Area [mAU*s]	Height [mAU]	Area %
1	3.007	BV	0.1090	13.05139	1.92734	0.1859
2	3.617	VV	0.0952	11.59978	1.58919	0.1652
3	3.739	VV	0.0574	15.15384	4.49562	0.2159
4	3.831	VV	0.0535	6935.52588	2048.71802	98.7974
5	4.170	VV	0.1060	30.70253	4.16616	0.4374

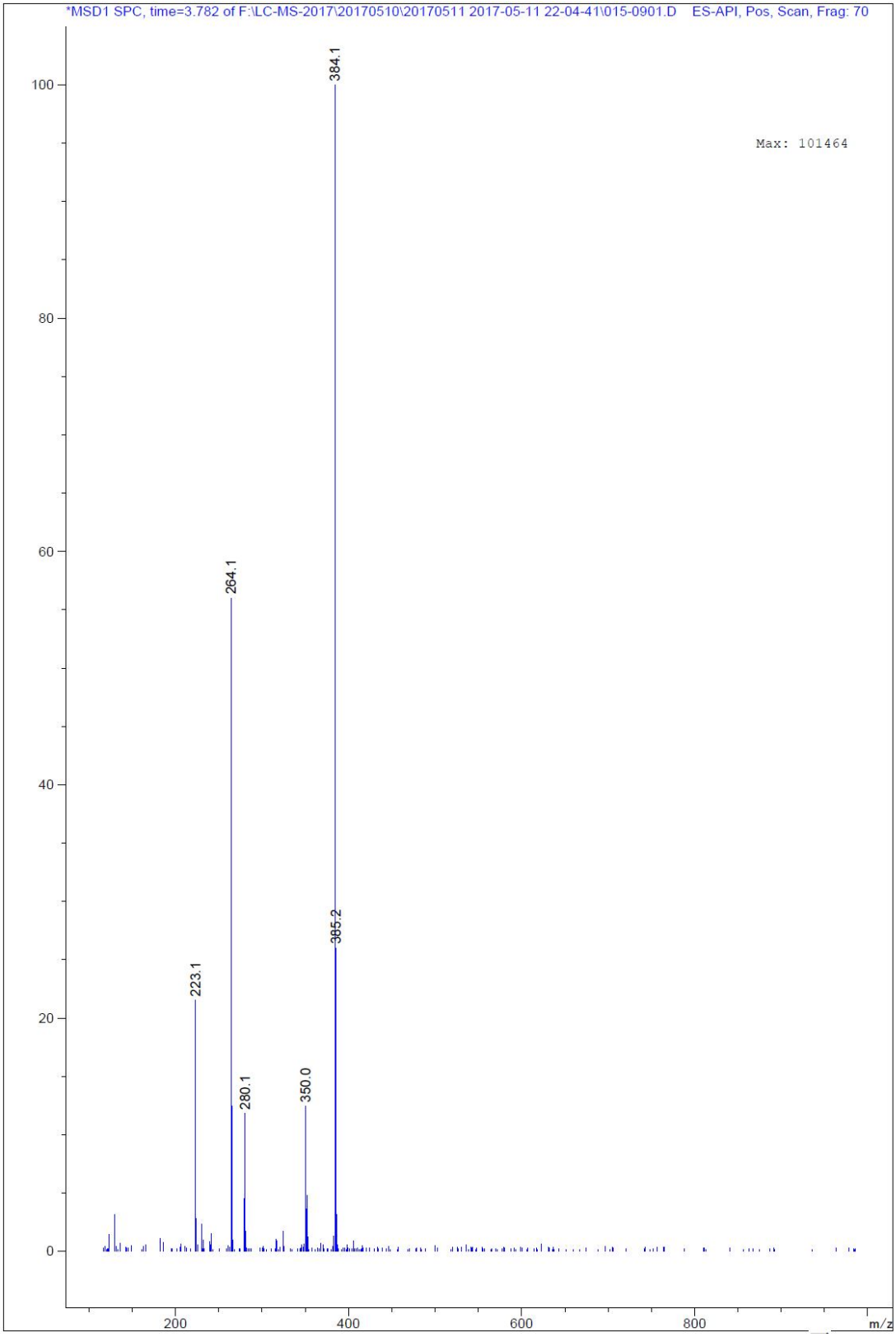
*MSD1 SPC, time=3.782 of F:\LC-MS-2017\20170510\20170511 2017-05-11 22-04-41\015-0901.D ES-API, Pos, Scan, Frag: 70
Max: 101464
384.1
264.1
385.2
223.1
280.1
350.0
100
80
60
40
20
0
200
400
600
800
m/z

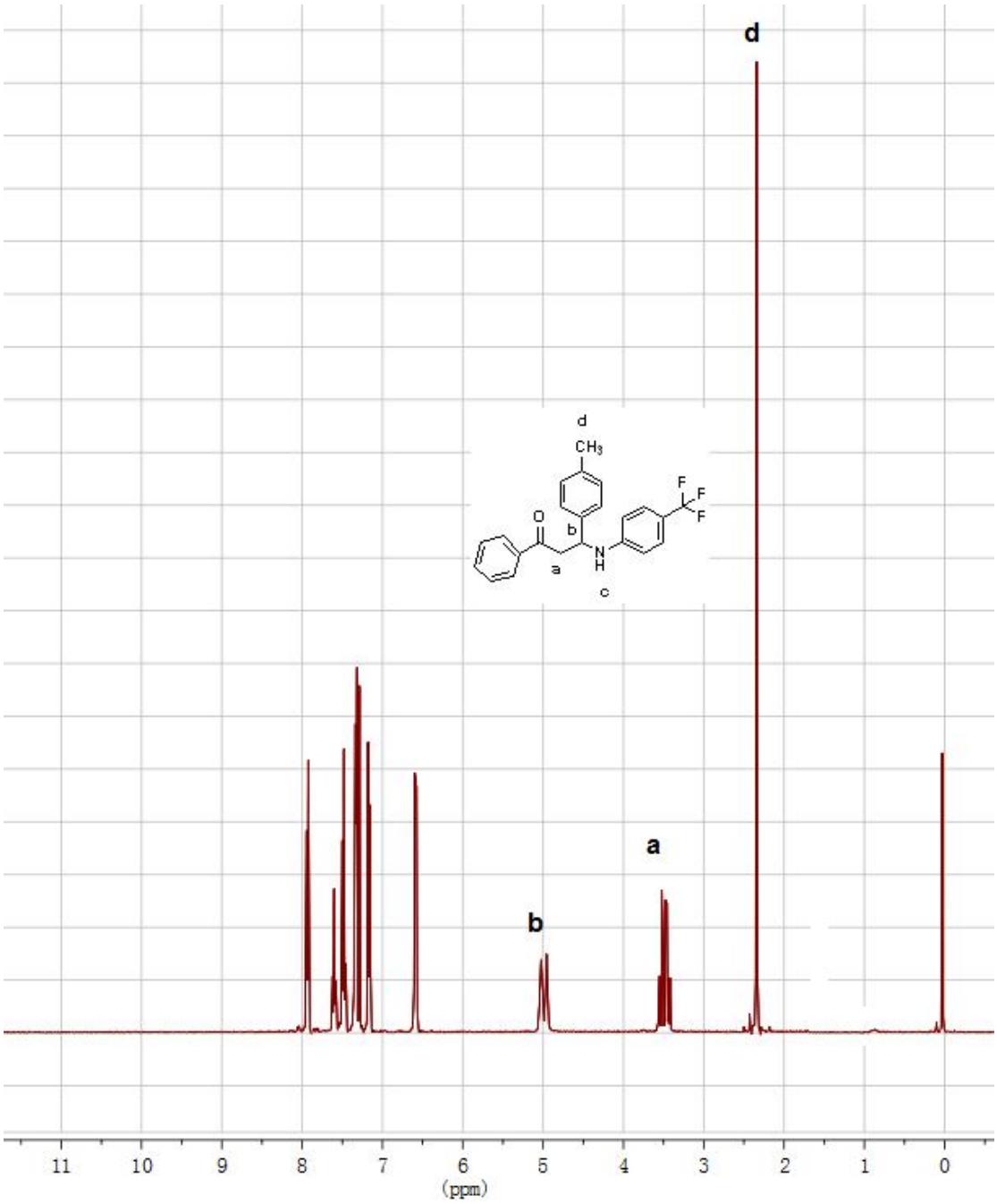
d
a
b
d
CH3
F
F
F
O
b
N
H
a
c
11
10
9
8
7
6
5
4
3
2
1
0
(ppm)

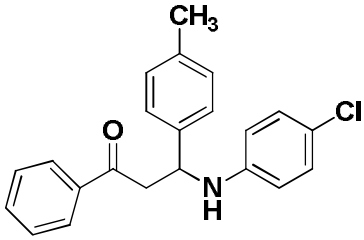

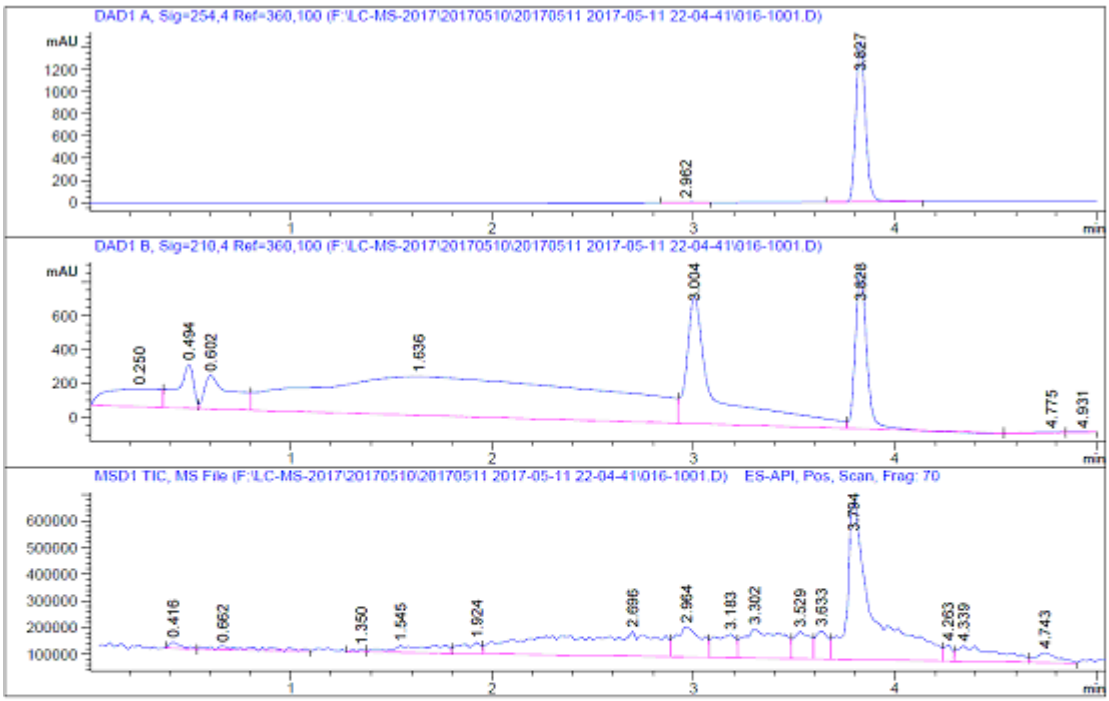

Signal 1: DAD1 A, Sig=254,4 Ref=360,100

#	Ret. [min]		Width [min]	Area [mAU*s]	Height [mAU]	Area %
1	2.962	VV	0.0711	9.79821	2.07324	0.2014
2	3.827	VB	0.0528	4855.04590	1458.35632	99.7986

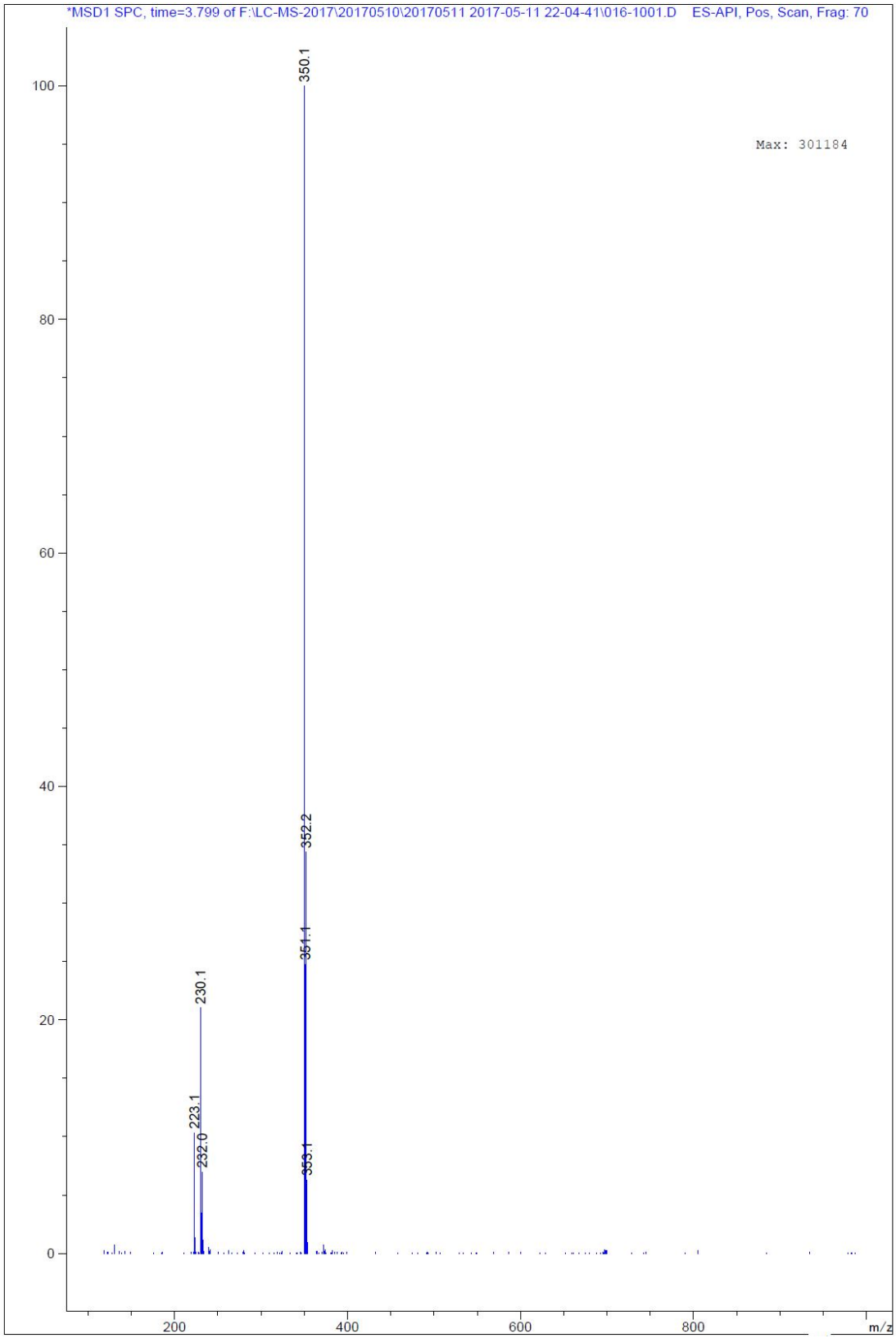
*MSD1 SPC, time=3.799 of F:\LC-MS-2017\20170510\20170511 2017-05-11 22-04-41\016-1001.D ES-API, Pos, Scan, Frag: 70
Max: 301184
350.1
352.2
351.1
353.1
230.1
223.1
232.0
100
80
60
40
20
0
200
400
600
800
m/z

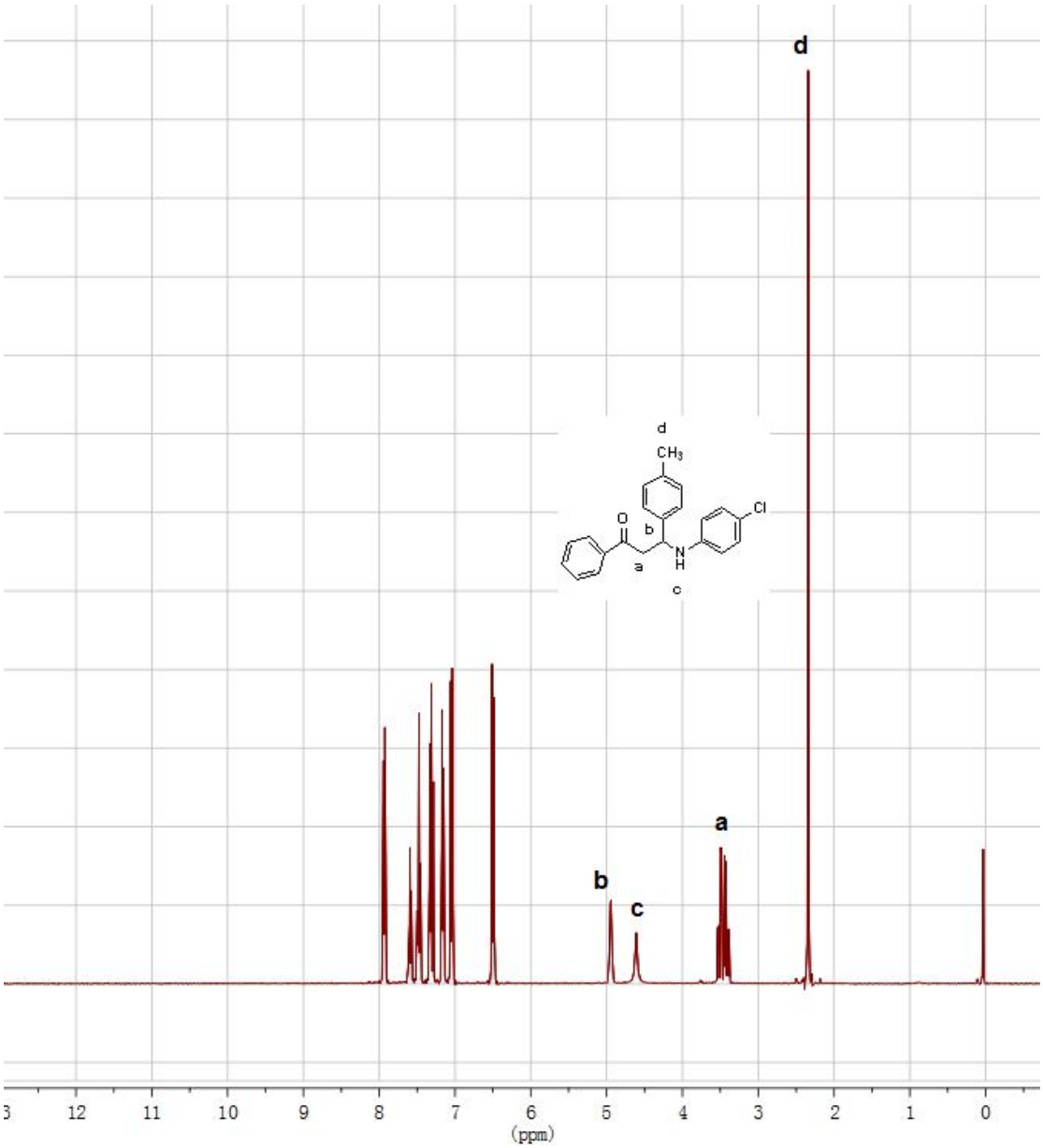
d
CH3
Cl
O
b
N
H
a
c
d
a
b
c
3
12
11
10
9
8
7
6
5
4
3
2
1
0
(ppm)

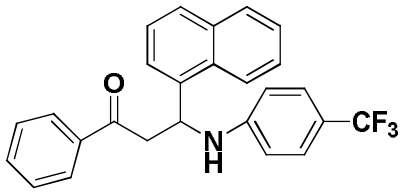

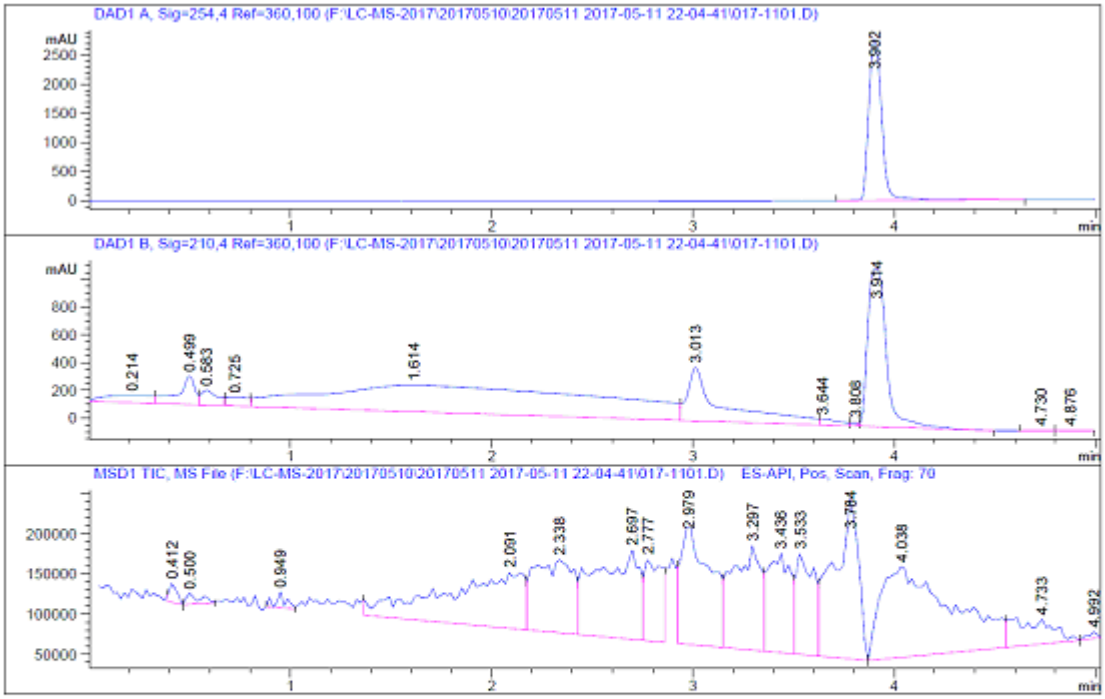

Signal 1: DAD1 A, Sig=254,4 Ref=360,100

#	Ret. [min]		Width [min]	Area [mAU*s]	Height [mAU]	Area %
1	3.902	VB	0.0723	1.24385e4	2776.58813	100.0000

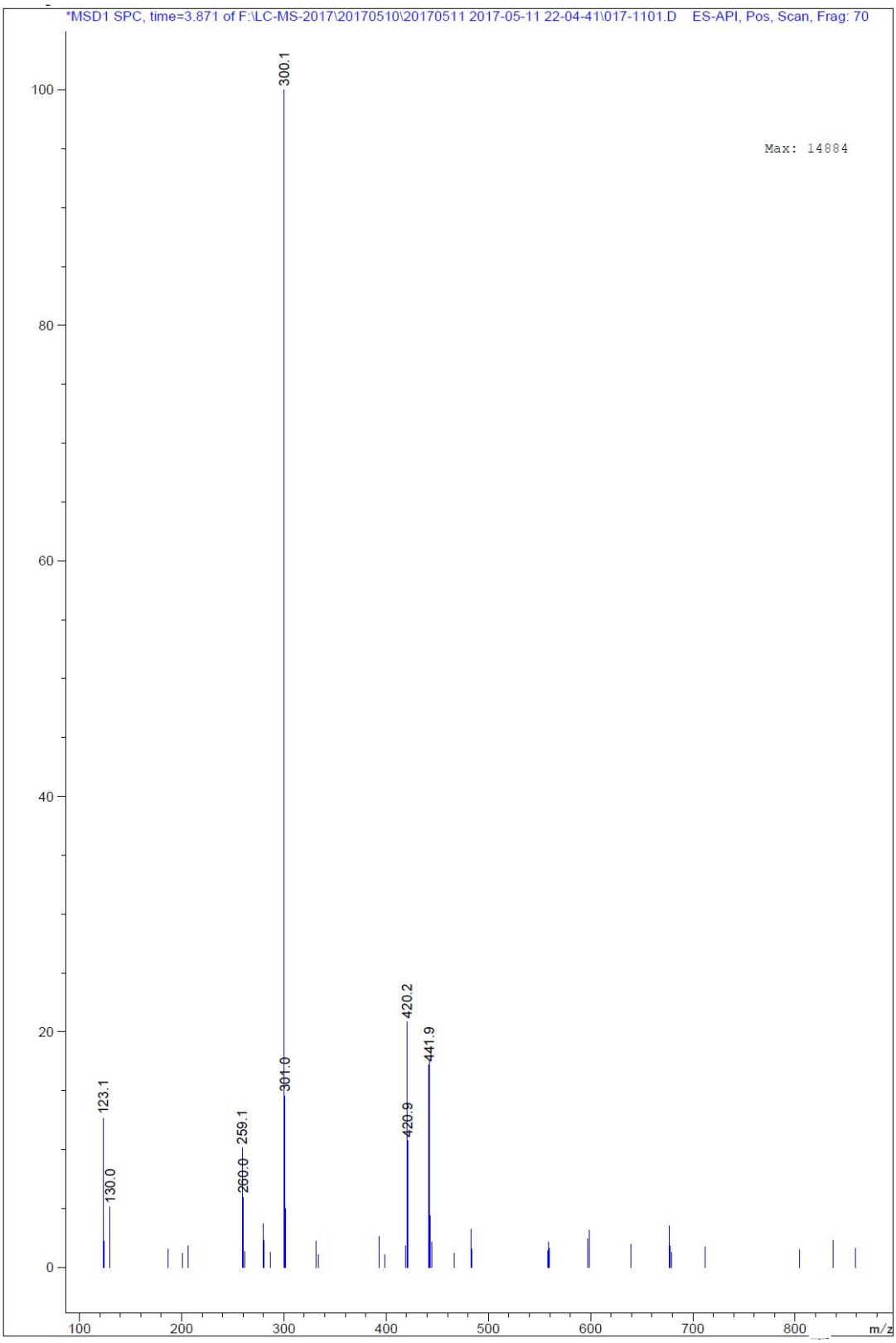
*MSD1 SPC, time=3.871 of F:\LC-MS-2017\20170510\20170511 2017-05-11 22-04-41\017-1101.D ES-API, Pos, Scan, Frag: 70
Max: 14884
300.1
301.0
123.1
130.0
259.1
260.0
420.2
420.9
441.9
100
80
60
40
20
0
100
200
300
400
500
600
700
800
m/z

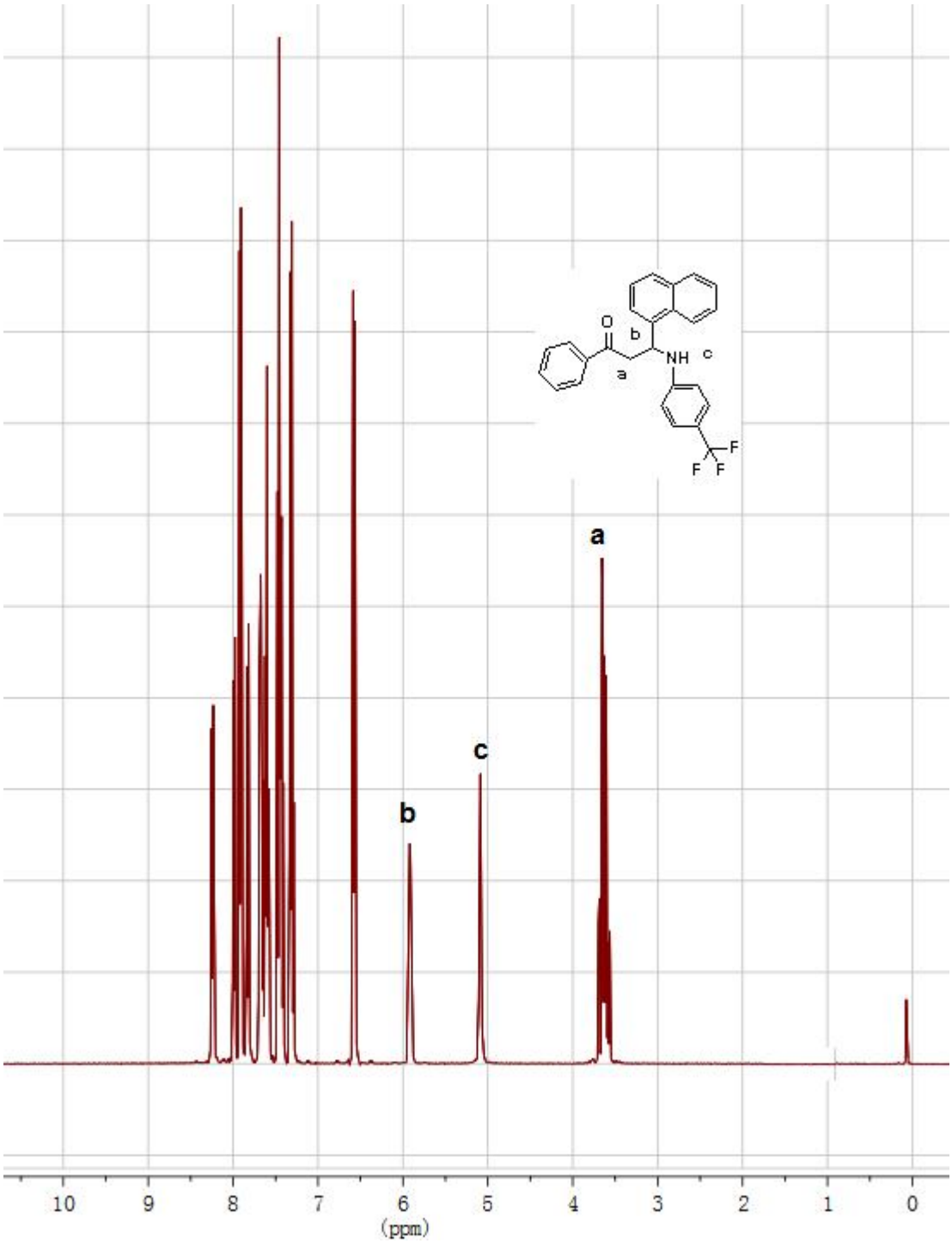
a
b
c
O
b
NH
c
a
F
F
F
10
9
8
7
6
5
4
3
2
1
0
(ppm)

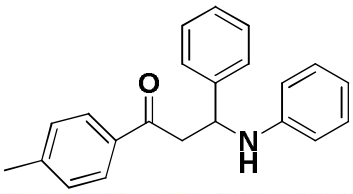

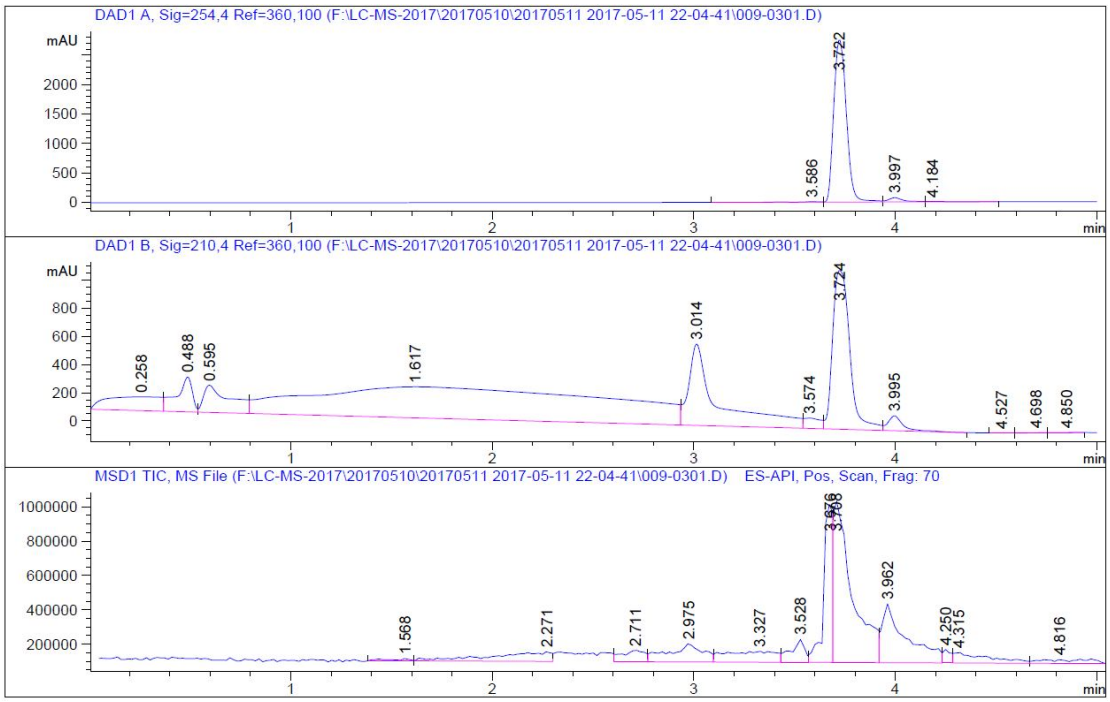

Signal 1: DAD1 A, Sig=254,4 Ref=360,100

#	Ret. [min]		Width [min]	Area [mAU*s]	Height [mAU]	Area %
1	3.586	VV	0.0330	13.03133	7.98408	0.1045
2	3.722	VV	0.0706	1.20100e4	2767.75464	96.9922
3	3.997	VV	0.0759	368.40842	71.71082	2.9538

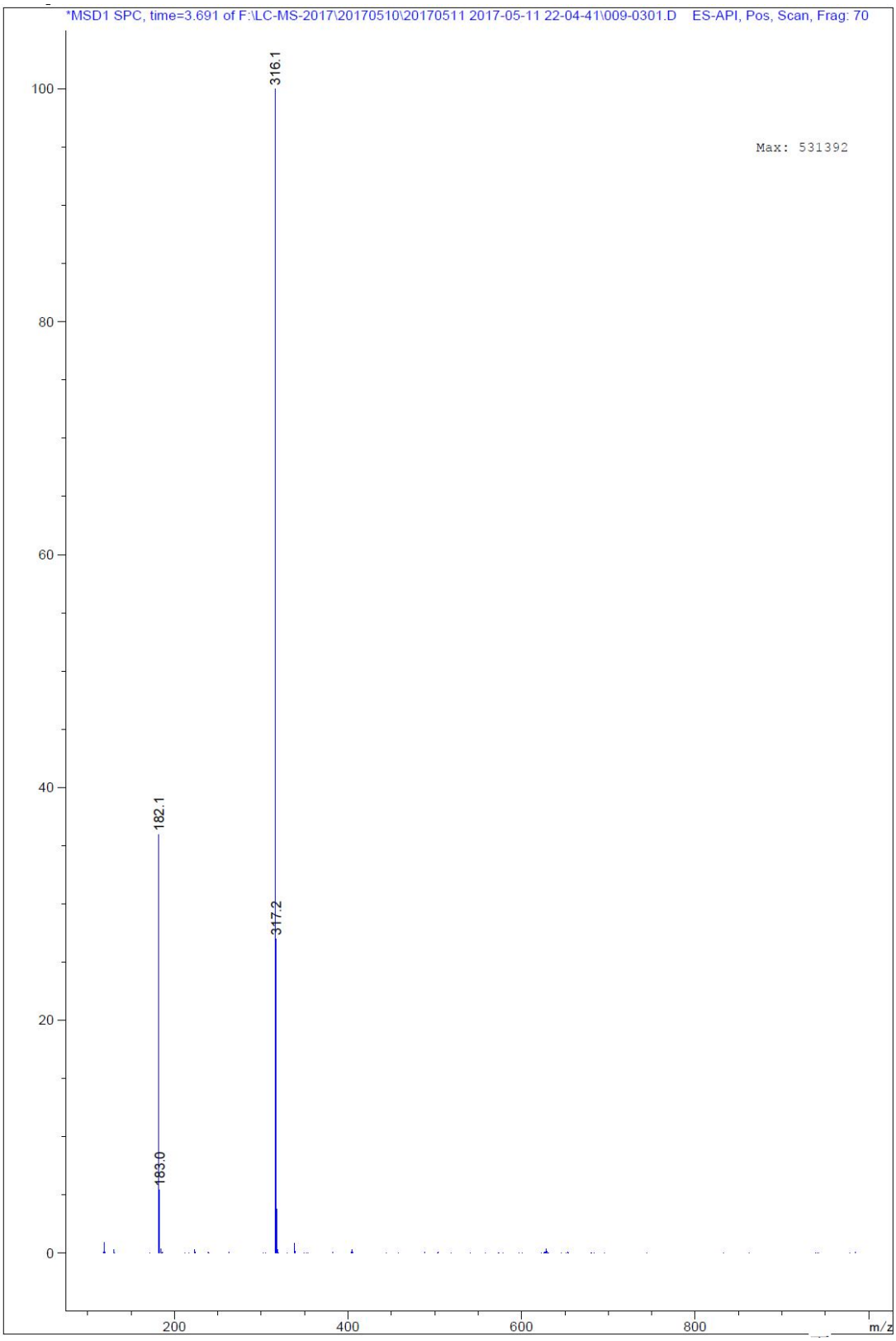
*MSD1 SPC, time=3.691 of F:\LC-MS-2017\20170510\20170511 2017-05-11 22-04-41\009-0301.D ES-API, Pos, Scan, Frag: 70
Max: 531392
316.1
317.2
182.1
183.0
100
80
60
40
20
0
200
400
600
800
m/z

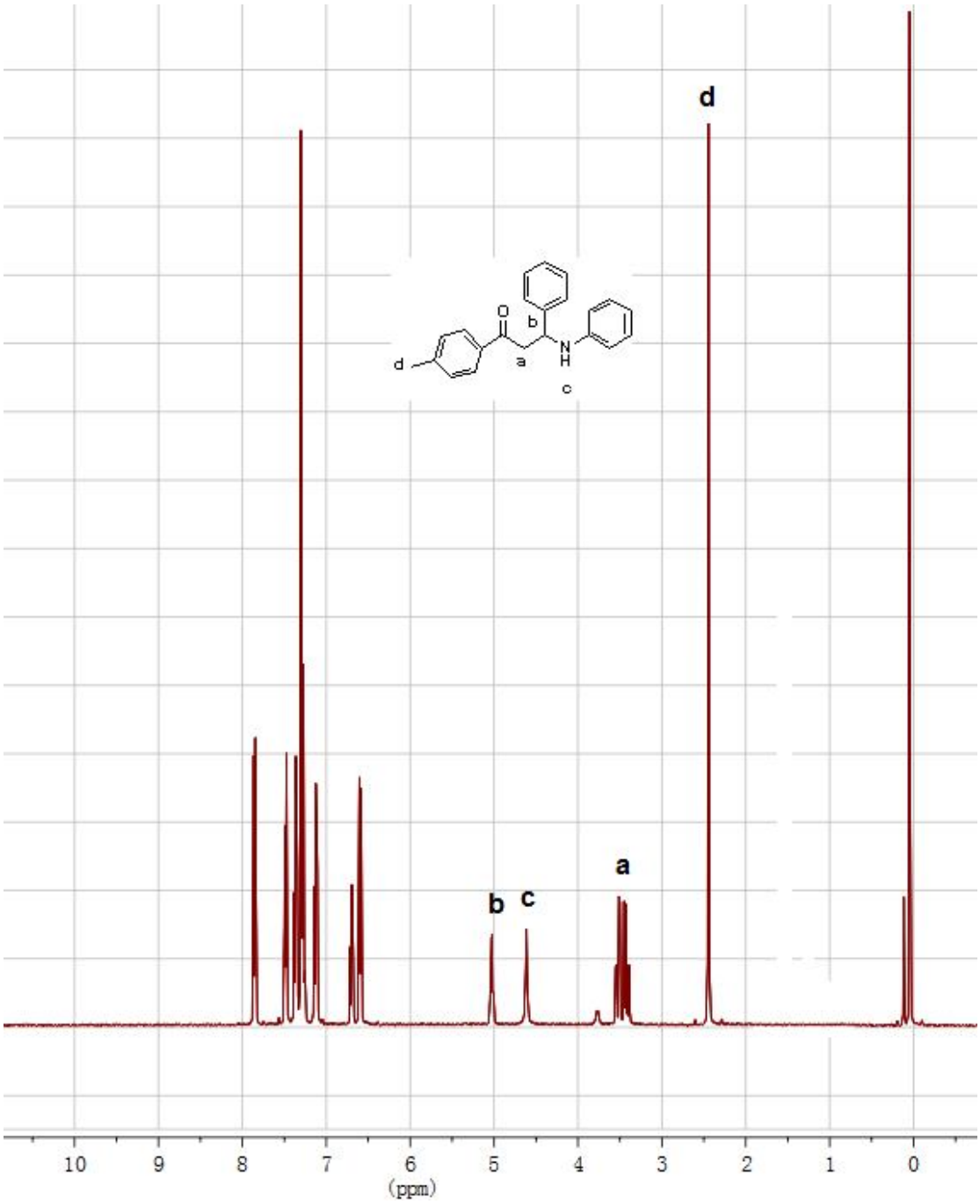
d
a
b
c
10
9
8
7
6
5
4
3
2
1
0
(ppm)

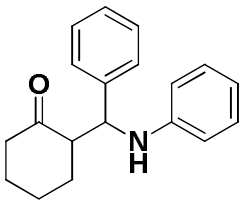

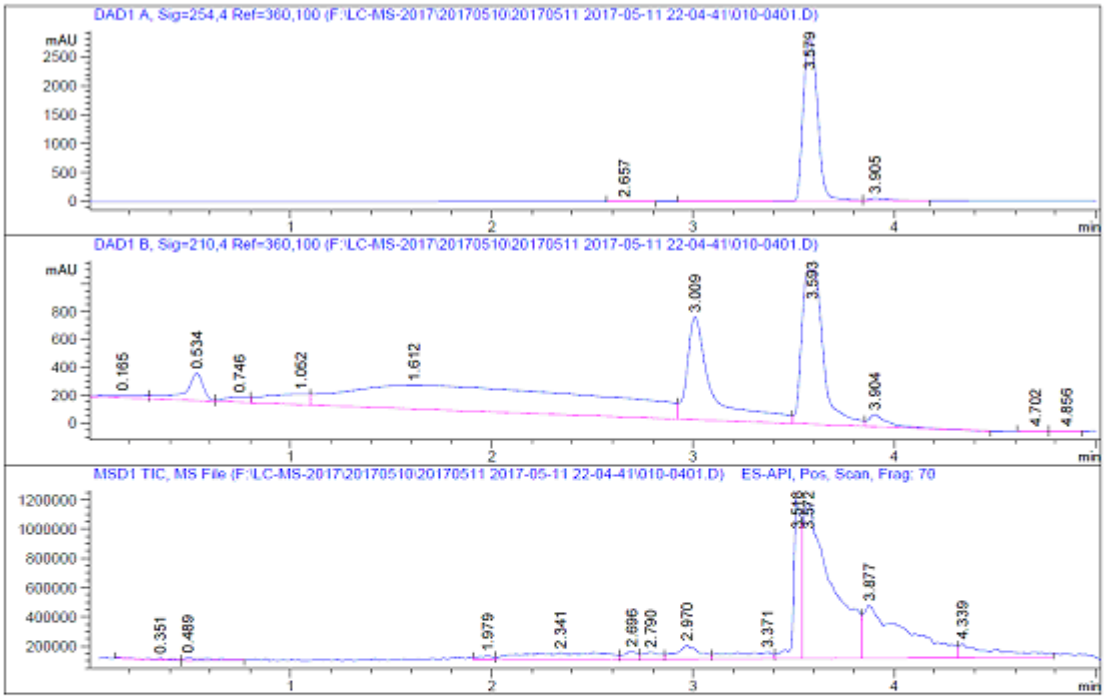

Signal 1: DAD1 A, Sig=254,4 Ref=360,100

#	Ret. [min]		Width [min]	Area [mAU*s]	Height [mAU]	Area %
1	2.657	BB	0.0799	23.17871	4.36533	0.1638
2	3.579	BV	0.0797	1.38250e4	2795.21606	97.6704
3	3.905	VB	0.0933	306.56445	45.10844	2.1658

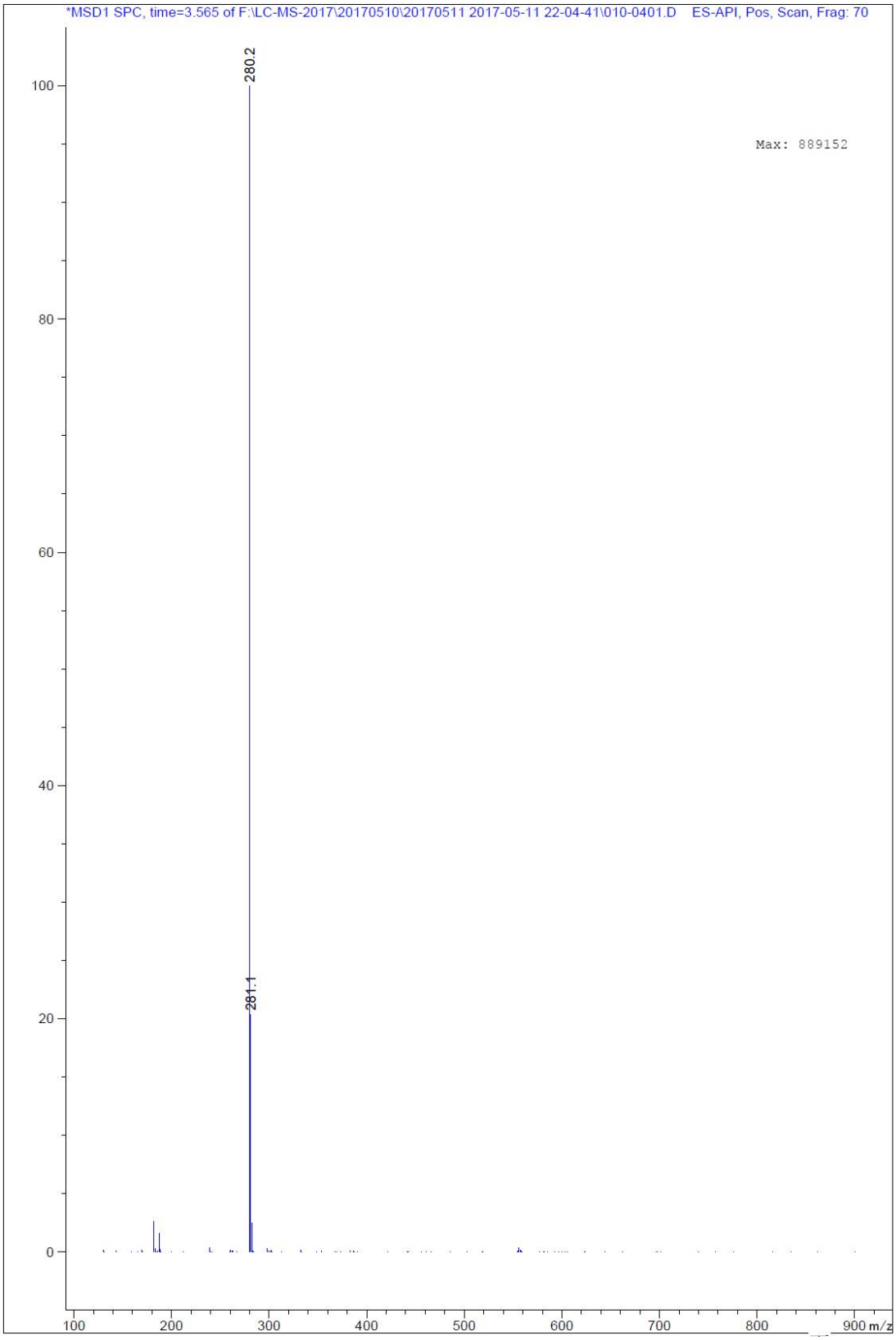
*MSD1 SPC, time=3.565 of F:\LC-MS-2017\20170510\20170511 2017-05-11 22-04-41\010-0401.D ES-API, Pos, Scan, Frag: 70
280.2
281.1
Max: 889152
100
80
60
40
20
0
100
200
300
400
500
600
700
800
900 m/z

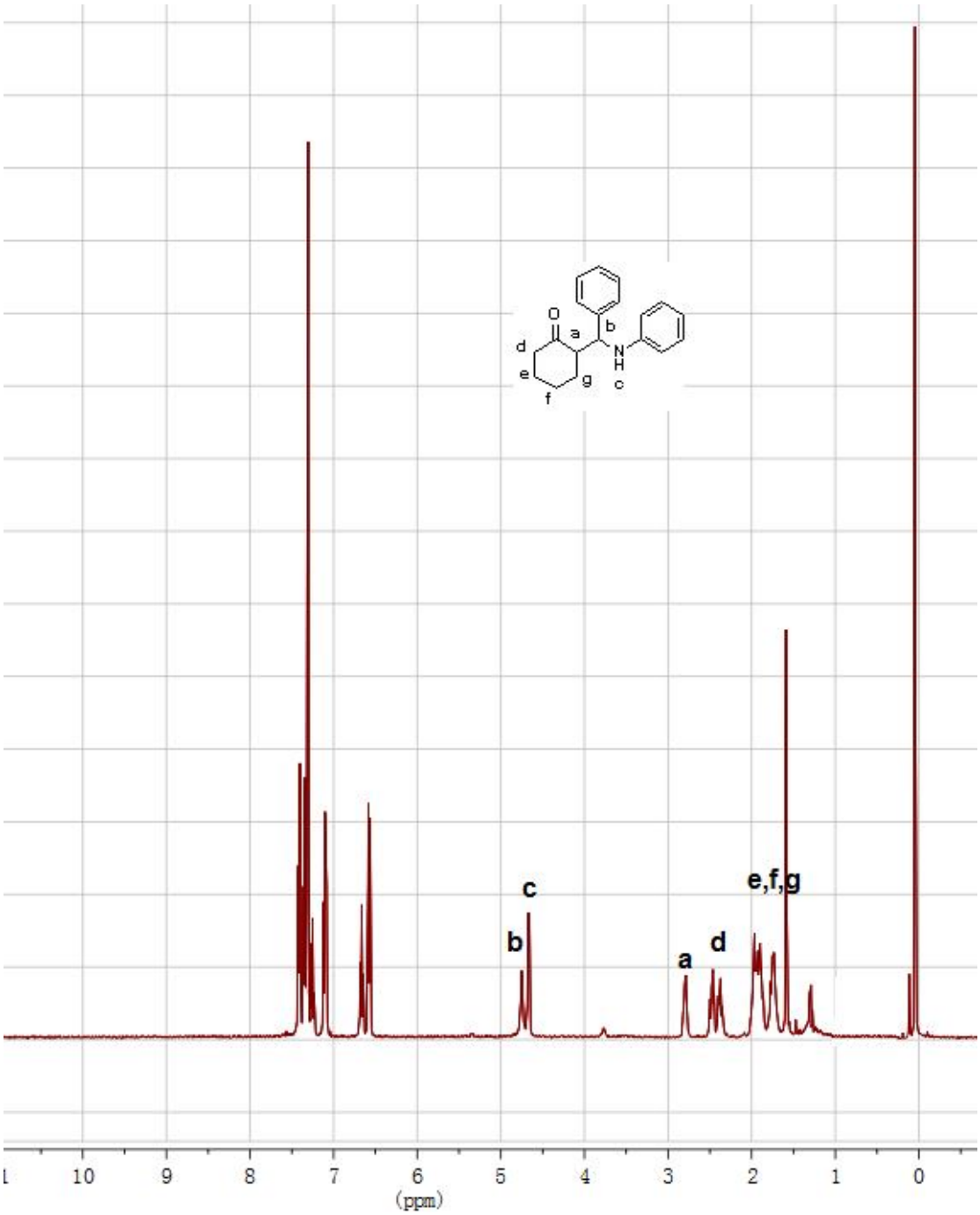
O
a
b
d
N
H
e
g
c
f
c
b
a
d
e,f,g
10
9
8
7
6
5
4
3
2
1
0
(ppm)

References

1 M. M. Ambursa, P. Sudarsanamc, L. H. Voon, S. B. A. Hamid and S. K. Bhargava, *Fuel Process. Technol.*, 2017, **162**, 87.

2 S. B. Abd Hamid, M. M. Ambursa, P. Sudarsanam, L. H. Voon and S. K. Bhargava, *Catal. Commun.*, 2017, **94**, 18.

3 E. A. Alarcón, A. L. Villa and C. M. de Correa, *Micropor. Mesopor. Mat.*, 2009, **122**, 208.

4 Z. Jeirani and J. Soltan, *Chem. Eng. J.*, 2017, **307**, 756.

5 A. K. Tripathi, Y. L. Verma and R. K. Singh, *J. Mater. Chem. A*, 2015, **3**, 23809.

6 T. Cheng, Q. Zhao, D. Zhang and G. Liu, *Green Chem.*, 2015, **17**, 2100.

7 S. Rostamizadeh, M. Nojavan, R. Aryan, E. Isapoor and M. Azad, *J. Mol. Catal. A: Chem.*, 2013, **374–375**, 102.

8 J. Yang, L. Zhou, X. Guo, L. Li, P. Zhang, R. Hong and T. Qiu, *Chem. Eng. J.*, 2015, **280**, 147.

9 S. J. Zhang and X. M. Lu, Ionic liquids: from fundamental research to industrial applications, Science Press, Beijing, 2006.

10 C. Xing, R. Tan, P. Hao, M. Gao, D. Yin and D. Yin, *Mol. Catal.*, 2017, **433**, 37.

11 C. Cai, H. Wang and J. Han, *Appl. Surf. Sci.*, 2011, **257**, 9802.

12 X. Chen, D. Song, C. Asumana and G. Yu, *J. Mol. Catal. A: Chem.*, 2012, **359**, 8; S. Hu, Z. Zhang, J. Song, Y. Zhou and B. Han, *Green Chem.*, 2009, **11**, 1746; Y. Jiang, H. Zang, S. Han, B. Yan, S. Yu and B. Cheng, *RSC Adv.*, 2016, **6**, 103774; M. Currie, J. Estager, P. Licence, S. Men, P. Nockemann, K. R. Seddon, M. Swadźba-Kwaśny and C. Terrade, *Inorg. Chem.* 2013, **52**, 1710; A. S. Amarasekara, *Chem. Rev.*, 2016, **116**, 6133.